DAMPING ESTIMATION OF PLATES FOR STATISTICAL ENERGY ANALYSIS

by

KRANTHI KUMAR VATTI

Submitted to the graduate degree program in Aerospace Engineering and the Graduate Faculty of the University of Kansas in partial fulfillment of the requirements for the degree of Master of Science.

_____

Chairperson Dr. Mark S. Ewing

_____

Dr. Rick Hale

_____

Dr. Saeed Farokhi

Date Defended: 9th March, 2011

The Thesis Committee for Kranthi Kumar Vatti

certifies that this is the approved version of the following thesis:

DAMPING ESTIMATION OF PLATES FOR STATISTICAL ENERGY ANALYSIS

_____

Chairperson Dr. Mark S. Ewing

Date Approved: 11th March, 2011

ABSTRACT

The Power Input Method (P.I.M.) and the Impulse Response Decay Method (I.R.D.M.) are used to evaluate how the accuracy of damping loss factor estimation for plates is affected with respect to various processing parameters, such as the frequency resolution, the frequency bandwidth, the number of measurement locations, and the signal to noise ratio. In several computational experiments, accuracy is assessed for a wide range of damping loss factors from low (0.1%) to moderate (1%) to high (10%). A wide range of frequency is considered, including "low frequencies" for which modal density is less than one per band.

The Power Input Method (P.I.M.) is first validated with computational studies of an analytical single degree of freedom oscillator. Experimental loss factor estimates for plates (multiple degree of freedom systems) are also computed using the P.I.M. algorithm. The P.I.M. is shown to estimate loss factors with reasonable accuracy for highly damped plates in the 300 Hz – 4000 Hz, wherein modal density exceeds unit value. In this case "reasonable accuracy" means the estimated loss factors are within 10% of those predicted by the impulse response decay method. For lower damping levels the method fails.

The analytical Impulse Response Decay Method (I.R.D.M.) is validated by the use of two computational models: a single degree of freedom oscillator and a uniform rectangular panel. The panel computational model is a finite element model of a rectangular plate mechanically excited at a single point. The computational model is used to systematically evaluate the effect of frequency resolution, frequency bandwidth, the number of measurement points used in the computations, and noise level for all the three levels of damping. The "optimized" I.R.D.M. is shown to accurately estimate damping in plate simulations with low to moderate levels of

damping with a deviation of no more than 2% from the known damping value. For highly damped plates the I.R.D.M. tends to under-estimate loss factors at high frequency. Experimental loss factor estimation for an aluminum plate with full constrained layer damping treatment, classified as a highly damped plate, and an undamped steel plate, classified as a lightly damped plate are computed using the "optimized" I.R.D.M. algorithm.

Statistical Energy Analysis (S.E.A.), which is a natural extension of the Power Input Method, is used to evaluate coupling loss factors for two sets of plates, one set joined along a line and the other set joined at a point. Two alternative coupling loss factor estimation algorithms are studied, one using individual plate loss factor estimations, and the other using the loss factors of the plates estimated when the plates are coupled. The modal parameters (modal density and coupling loss factors) for both sets of plates are estimated experimentally and are compared with theoretical results. The estimations show reasonable agreement between agreement and theory that is, within 5 % for the damped system of plates. For the undamped system of plates the results are less accurate with deviations of more than 100% at low modal density and approximately 30% variation at higher frequencies.

ACKNOWLEDGEMENTS

I want to express my gratitude to those individuals who, during the past three and half years, have supported me in some way or another. To my advisor, Professor Dr. Mark S. Ewing, a special thanks for giving me the opportunity to work with him and for his patience, tolerance, understanding, and encouragement. I am truly grateful.

Further encouragement came from my committee members Dr. Rick Hale, and Dr. Saeed Farokhi to whom I am indebted for their patience. I really appreciate their time and effort for being part of my committee. Additional thanks are extended to Dr. Richard Colgren and Dr. Shariar Keshmiri for their advice during the course of my study.

I want to thank Spirit Aerosystems, particularly Dr. Mark Moeller and Mr. Albert Allen for the support of this work and for technical assistance. Thanks are extended to Wanbo Liu who constructed many of the specimens that are used for various experiments and providing the analytical Nastran data. I also want to thank Ignatius Vaz at ESI group who helped me in learning the statistical energy analysis simulation software.

I would also like to thank all the faculty and staff of the Department of Aerospace Engineering, particularly Amy Borton, as a whole for their support.

Special thanks go to friends Himanshu Dande, Akhilesh Katipally, Kolapan Jayachandran Saiarun, Vamshi Zillepalli, Jayasimha Tutika, Pradeep Attalury, Ranganathan Parthasarathy, and Viraj Singh. They were encouraging me during my whole research.

Finally, without the support and encouragement of my parents, Vatti Venkat Reddy and Vatti Vanitha Vani, I could not have made it this far. Thank you.

TABLE OF CONTENTS

LIST OF FIGURES

LIST OF TABLES

1 OVERVIEW OF THE DAMPING ESTIMATION TECHNIQUES

1.1 INTRODUCTION

Vibrating structures accumulate the energy of vibration in the form of kinetic energy (stored by mass) and potential energy (stored by elasticity). Each real, vibrating structure dissipates and radiates energy. In all materials, internal dissipation leads to conversion of mechanical energy into thermal energy [1]. There are also many engineered damping mechanisms [2] which are used to transform the mechanical energy into heat. Mechanisms of energy dissipation include sliding friction, liquid viscosity, and both magnetic and mechanical hysteresis [3].

Dissipation of mechanical energy from a vibrating system is usually by conversion of the mechanical energy into heat. Damping serves to limit the steady-state resonant response and to attenuate traveling waves in the structure. There are two types of damping: material damping and system damping. Material damping is the damping that is inherent in the material while system damping includes the damping due to engineered devices as well as damping mechanisms at the supports, boundaries, joints, interfaces, etc. Since utilizing engineered damping materials is the most common way to reduce resonance responses, accurate measurements of both material and system damping are crucial to the proper design and modeling of systems from a vibration reduction standpoint [4].

A variety of nomenclature exists to denote damping. These include: damping ratio(ζ), log decrement(δ), loss factor (η), specific damping capacity (ψ), quality factor (Q), etc., There are

also many different test methods for predicting damping in structures. The various damping test methods can broadly be classified into three groups [5]:

a) Frequency-domain modal analysis curve-fitting methods,

b) Time domain decay-rate methods, and

c) Other methods based on energy and wave propagation.

In this thesis, the damping loss factor estimations by the Impulse Response Decay Method (I.R.D.M.) and the Power Injection Method (P.I.M.) are investigated. The I.R.D.M. and P.I.M. are validated by a single degree of freedom oscillator for various types of excitation signals. The I.R.D.M. is validated using a computationally-modeled plate element with varying levels of damping loss factor specifically 0.001, 0.01, and 0.1. The experimental validations of both the P.I.M. and the I.R.D.M. are shown with two plates, one an aluminum panel with full covering constrained layer damping treatment, and the second an undamped steel plate. Statistical Energy Analysis (S.E.A.) is used to study the coupling loss factors between two sets of coupled plate elements, one set joined at a point and the other set joined along a line.

1.2 DAMPING IN STRUCTURES

1.2.1 FREE VIBRATIONS OF A SINGLE DEGREE OF FREEDOM (SDOF) SYSTEM

Consider the single degree of freedom system shown in Figure 1-1. The general form of the differential equation describing the response is

$$m\ddot{x} + c\dot{x} + kx = f(t), \qquad x(0) = x_0, \quad \dot{x}(0) = \upsilon_0 \tag{1.1}$$

where $x(t)$ is the position of the mass, m is the mass, c is the damping rate, k is the stiffness, and $f(t)$ is the external dynamic load. The initial displacement of the system is x_0 and the initial velocity is υ_0. Let us consider the case with no external applied load i.e., $f(t) = 0$.

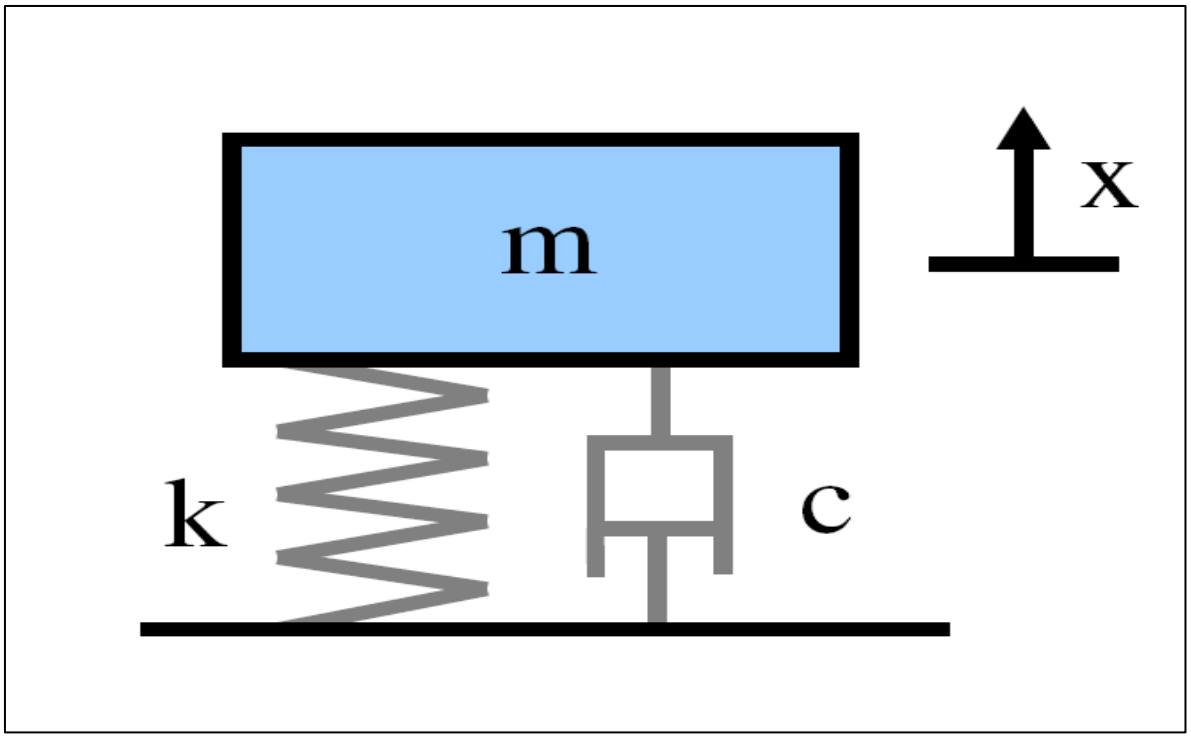

FIGURE 1-1 SINGLE DEGREE OF FREEDOM SYSTEM

A unique solution of Equation (1.1) for $f(t) = 0$ can be found for specified initial conditions assuming that $x(t)$ is of the form

$$x(t) = Ae^{\lambda t} \tag{1.2}$$

substituting Equation (1.2) into Equation (1.1) yields

$$A(\lambda^2 + \frac{c}{m}\lambda + \frac{k}{m})e^{\lambda t} = 0 \tag{1.3}$$

Since the trivial solution is not desired $A \neq 0,$ and $e^{\lambda t}$ is never zero. Equation (1.3) yields

$$\lambda^2 + \frac{c}{m}\lambda + \frac{k}{m} = 0 \tag{1.4}$$

Equation (1.4) is called the *characteristic equation* of Equation (1.1). Using simple algebra, the two solutions for λ are

$$\lambda_{1.2} = -\frac{c}{2m} \pm \frac{1}{2}\sqrt{\frac{c^2}{m^2} - 4\frac{k}{m}} \tag{1.5}$$

The quantity under the radical is called the *discriminant* and, together with the signs of m, c and $k,$ determines whether the roots are complex or real. Physically, $m, c,$ and k are all positive for this case, so the determinant of Equation (1.5) determines the nature of the roots of Equation (1.4).

The dimensionless *damping ratio,* ζ is defined as

$$\zeta = \frac{c}{2\sqrt{km}} \tag{1.6}$$

In addition the *damped natural frequency* is defined (for $0 < \zeta < 1$) by

$$\omega_d = \omega_n\sqrt{1-\zeta^2} \tag{1.7}$$

substituting Equation (1.6) and Equation (1.7) into Equation (1.1) we now have,

$$\ddot{x} + 2\zeta\omega_n \dot{x} + \omega_n^2 x = 0 \tag{1.8}$$

and Equation (1.5) becomes

$$\lambda_{1,2} = -\zeta\omega_n \pm \omega_n\sqrt{\zeta^2 - 1} = -\zeta\omega_n \pm \omega_d j, \qquad 0 < \zeta < 1 \tag{1.9}$$

The value of the damping ratio, ζ determines the nature of the solution of Equation (1.1).

There are three cases of interest.

Under-damped. This case occurs if the parameters of the system are such that

$$0 < \zeta < 1$$

so the discriminant given by Equation (1.9) is negative and the roots form a complex conjugate pair of values. The solution of Equation (1.8) then becomes

$$\begin{aligned} &x(t) = e^{-\zeta\omega_n t}(A\cos\omega_d t + B\sin\omega_d t) \\ &\textit{or} \\ &x(t) = Ce^{-\zeta\omega_n t}\sin(\omega_d t + \phi) \end{aligned} \tag{1.10}$$

where A, B, C, and ϕ are constants determined by the specified initial velocity, υ_o and the initial position, x_o :

$$A = x_0, \qquad C = \frac{\sqrt{(\upsilon_o + \zeta\omega_n x_o)^2 + (x_o\omega_d)^2}}{\omega_d}$$

$$B = \frac{\upsilon_o + \zeta\omega_n x_o}{\omega_d}, \qquad \phi = \tan^{-1}\left(\frac{x_o\omega_d}{\upsilon_o + \zeta\omega_n x_o}\right) \tag{1.11}$$

The response of the underdamped system has the form given in Figure 1-2

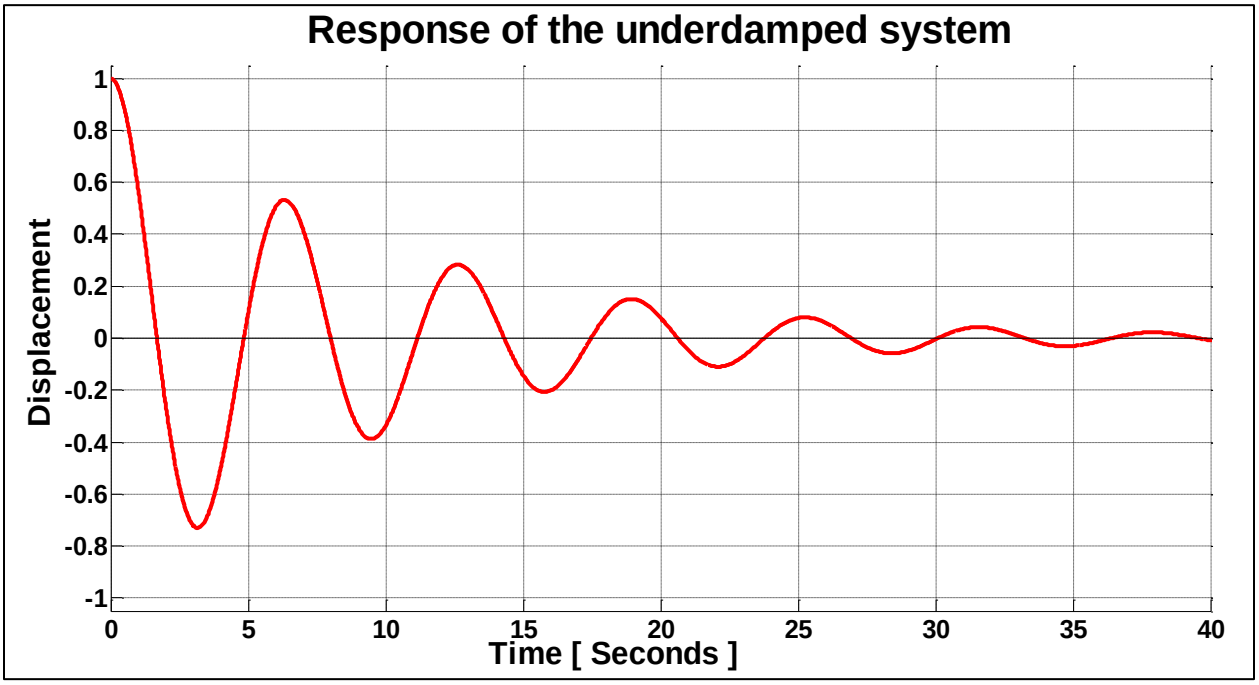

FIGURE 1-2 RESPONSE OF THE UNDERDAMPED SYSTEM

Over-damped. This case occurs if the parameters of the system are such that

$$\zeta > 1$$

so that the discriminant given by Equation (1.9) is positive and the roots are a pair of negative real numbers. The solution of Equation (1.8) then becomes

$$x(t) = Ae^{(-\zeta+\sqrt{\zeta^2-1})\omega_n t} + Be^{(-\zeta-\sqrt{\zeta^2-1})\omega_n t} \tag{1.12}$$

where A and B are again constants determined by υ_0 and x_0. They are

$$A = \frac{\upsilon_o + (\zeta + \sqrt{\zeta^2-1})\omega_n x_0}{2\omega_n(\sqrt{\zeta^2-1})}, B = \frac{\upsilon_o + (\zeta - \sqrt{\zeta^2-1})\omega_n x_0}{2\omega_n(\sqrt{\zeta^2-1})}$$

The response of an overdamped system has the form given in Figure 1-3. An overdamped system does not oscillate, but rather returns to its rest position exponentially.

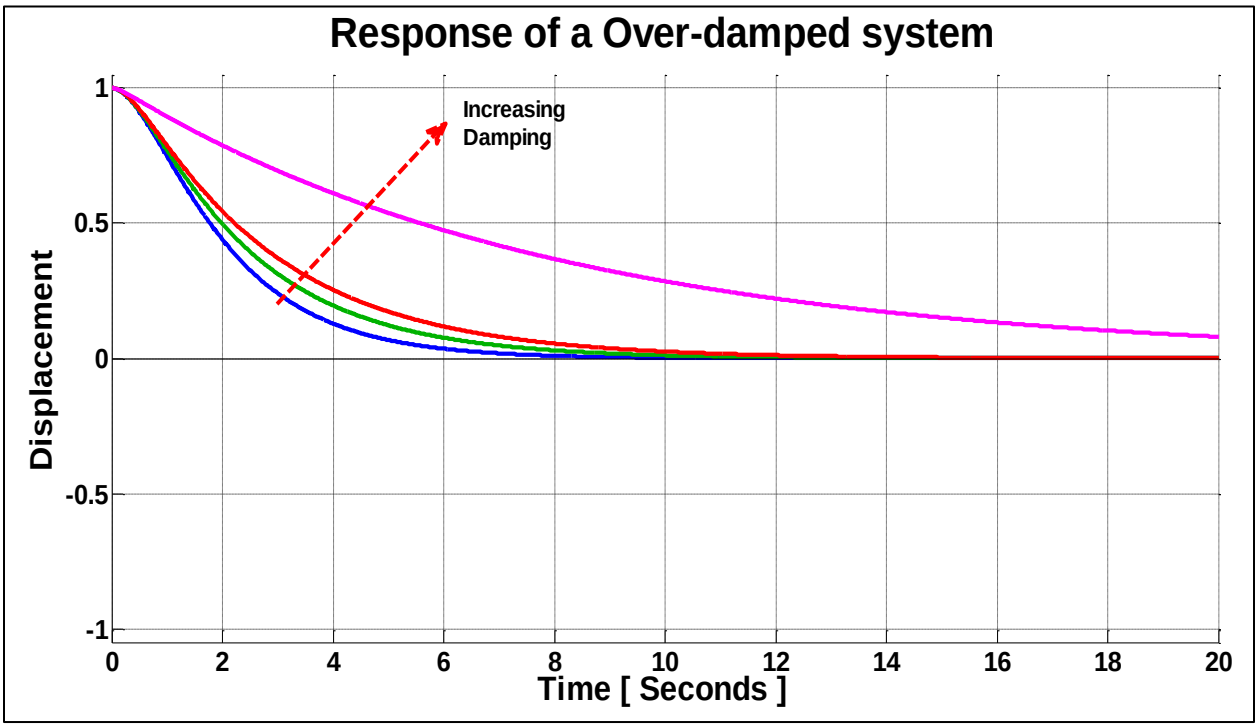

FIGURE 1-3 RESPONSE OF AN OVERDAMPED SYSTEM

Critically-damped. This case occurs if the parameters of the system are such that

$$\zeta = 1$$

so that the discriminant given by Equation (1.9) is zero and the roots are a pair of negative real repeated numbers. The solution of Equation (1.8) then becomes

$$x(t) = e^{-\omega_n t[(\upsilon_o + \omega_n x_o)t + x_o]} \tag{1.13}$$

The critically damped response is plotted in Figure 1-4.

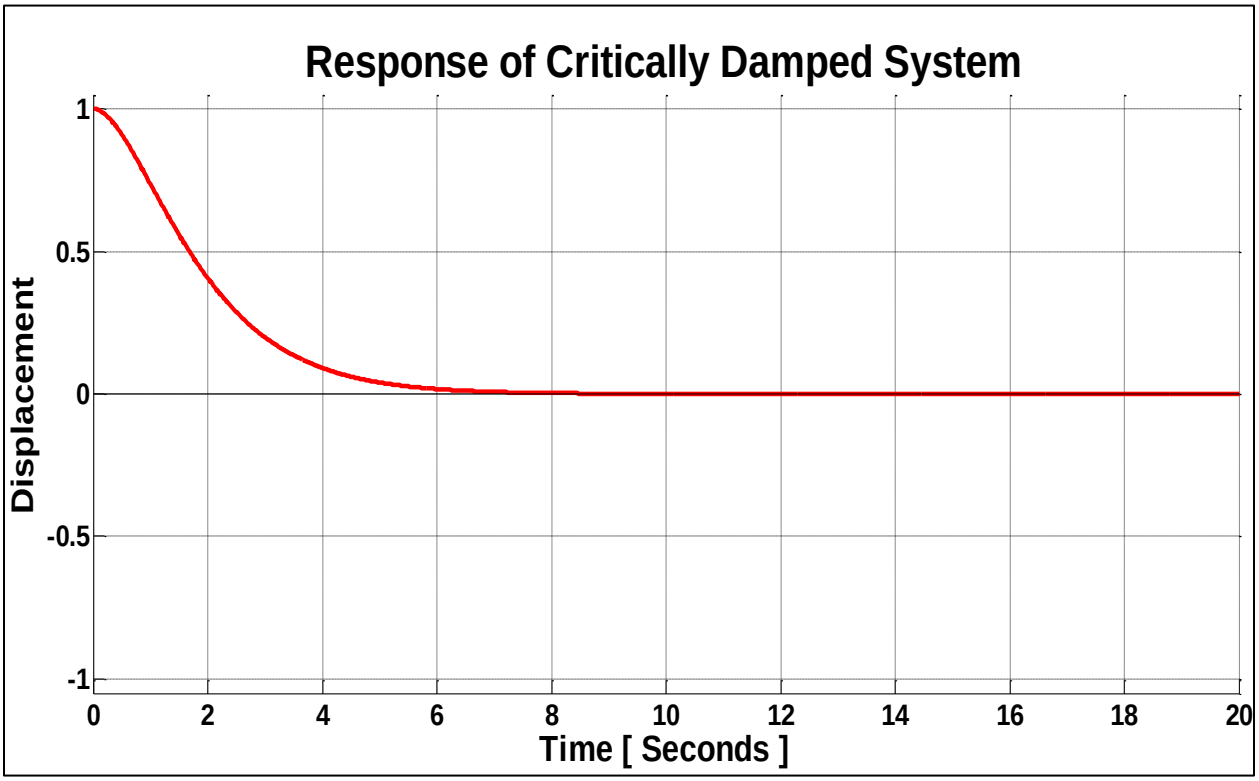

FIGURE 1-4 RESPONSE OF A CRITICALLY DAMPED SYSTEM

Critically damped systems are systems with the minimum value of damping that yields a non-oscillating system.

1.2.2 FORCED VIBRATIONS OF A SDOF SYSTEM

The preceding analysis considers the vibration of structure as a result of some initial disturbance i.e., $f(t) \neq 0$. The equation of motion for the forced vibration of the system becomes,

$$m\ddot{x} + c\dot{x} + kx = f(t) \tag{1.14}$$

Equation (1.14) is a linear, time variant, second order differential equation. The total solution to this problem involves two parts as follows:

$$x(t) = x_c(t) + x_p(t)$$

where:

- $x_c(t) =$ Transient portion
- $x_p(t) =$ Steady state portion

By setting $f(t)$=0, the homogeneous (transient) form of Equation (1.14) can be solved.

The homogeneous solution of the Equation (1.14) is:

$$x_c(t) = X_1 e^{\lambda_1 t} + X_2 e^{\lambda_2 t}$$

where X_1 and X_2 are constants determined from the initial conditions imposed on the system at $t = 0$.

1.2.2.1 HARMONIC EXCITATION

In many environments, rotating machinery, motors, and other mechanical systems cause periodic motions of structures to induce vibrations into other nearby mechanical devices and structures nearby. It is common practice to approximate the driving forces, $f(t)$ as periodic of the form

$$f(t) = F \sin \omega t$$

The equation for the forced vibration of the system becomes

$$m\ddot{x} + c\dot{x} + kx = F \sin(\omega t) \tag{1.15}$$

The particular solution (steady state) is a function of the form of the forcing function. If the forcing function is a pure sine wave of a single frequency, the response will also be a sine wave of the same frequency. If the forcing function is random in form, the response is also random. The particular solution has the form

$$x_p(t) = X \sin(\omega t - \theta) \tag{1.16}$$

where X is the steady state amplitude and θ is the phase shift at steady state. Substitution of Equation (1.16) into Equation (1.15) yields

$$X = \frac{F/k}{\sqrt{(1 - m\omega^2/k)^2 + (c\omega/k)^2}} \tag{1.17}$$

Equation (1.17) can be rewritten as

$$\frac{Xk}{F} = \frac{1}{\sqrt{(1 - m\omega^2 / k)^2 + (c\omega / k)^2}}$$

$$\frac{X}{F} = \frac{1}{\sqrt{(1 - m\omega^2)^2 + (c\omega)^2}}$$

and we have

$$\tan\theta = \frac{(c\omega / k)}{1 - m\omega^2 / k} = \frac{2\zeta(\omega / \omega_n)}{1 - (\omega / \omega_n)^2} \tag{1.18}$$

where $\omega_n = \sqrt{k / m}$ as mentioned before. Since the system is linear, the sum of the two solutions is a solution, and the total time response for the system for the case $0 < \zeta < 1$ becomes

$$x(t) = e^{-\zeta\omega_n t}(A\sin\omega_d t + B\cos\omega_d t) + X\sin(\omega t - \theta) \tag{1.19}$$

Here, A and B are constants of integration determined by the initial conditions and the forcing function (and in general will be different from the values of A and B determined for the free response).

From Equation (1.19) the following conclusions can be drawn.

1. As t becomes larger, the transient response (the first term) becomes very small, and hence the steady state response term is assigned to the particular solution (the second term).
2. The coefficient of the steady state response, or particular solution, becomes large when the excitation frequency is close to the undamped natural frequency, i.e., $\omega \approx \omega_n$. This

phenomenon is known as *resonance* and is extremely important in vibration analysis and testing.

Alternatively the equation of motion for damped free vibrations of a system can also be obtained from energy concepts by incorporating an energy dissipation function into the energy balance equation. Hence,

$$d(T+U)/dt = -\Pi \tag{1.20}$$

where Π is the power (the negative sign indicates that the power is removed from the system). Power is *force* $\times$ *velocity*, and the power dissipated from a system with viscous damping is,

$$\Pi = F_v\dot{x} = c_v\dot{x}^2 = 2\zeta m\omega_n \tag{1.21}$$

From Equation (1.21) we have the damping loss factor $\eta(\eta = 2\zeta)$ as

$$\eta = \frac{\Pi}{\omega_n m\dot{x}^2} \tag{1.22}$$

Equation (1.22) is the basis for the Power Input Method (PIM) which is discussed in Chapter 2.

1.2.2.2 IMPULSE RESPONSE

Impulse response, namely the response of the spring-mass-damper system given by Equation (1.1) to an impulse, is established in terms of a fictitious function called the *unit impulse function*, or the *Dirac delta function.*

This delta function is defined by the two properties

$$\delta(t-a)=0, \quad t\neq a$$
$$\int_{-\infty}^{\infty}\delta(t-a)dt=1 \tag{1.23}$$

where a is the instant of time at which the impulse is applied. The response of the system for the underdamped case (with $a=x_o=\upsilon_o=0$) can be given by

$$x(t)=\begin{cases}0, & t<a\\ \dfrac{e^{-\zeta\omega t}\sin\omega_d t}{m\omega_d}, & t>a\end{cases} \tag{1.24}$$

The response of a system to an impulse may be used to determine the response of an underdamped system to any input $F(t)$ by defining the *impulse response function* as

$$h(t)=\frac{1}{m\omega_d}e^{-\zeta\omega_n t}\sin\omega_d t \tag{1.25}$$

Then the solution of

$$m\ddot{x}(t)+c\dot{x}(t)+kx(t)=F(t)$$

for the case of zero initial conditions is given by

$$x(t)=\int_0^t F(\tau)h(t-\tau)d\tau=\frac{1}{m\omega_d}e^{-\zeta\omega_n t}\int_0^t F(\tau)e^{\zeta\omega_n t}\sin\omega_d(t-\tau)d\tau \tag{1.26}$$

This last expression gives an analytical representation for the response to any driving force that has an integral [5]. Equation (1.26) is called the convolution integral.

Consider the response of the system given by Equation (1.25). The system's response amplitude when plotted versus time will have a slope proportional to $e^{(-\pi f \eta t)}$, where f is the frequency, η is the loss factor, and t is time [6]. A typical transient response of a S.D.O.F. system is shown in Figure 1-5.

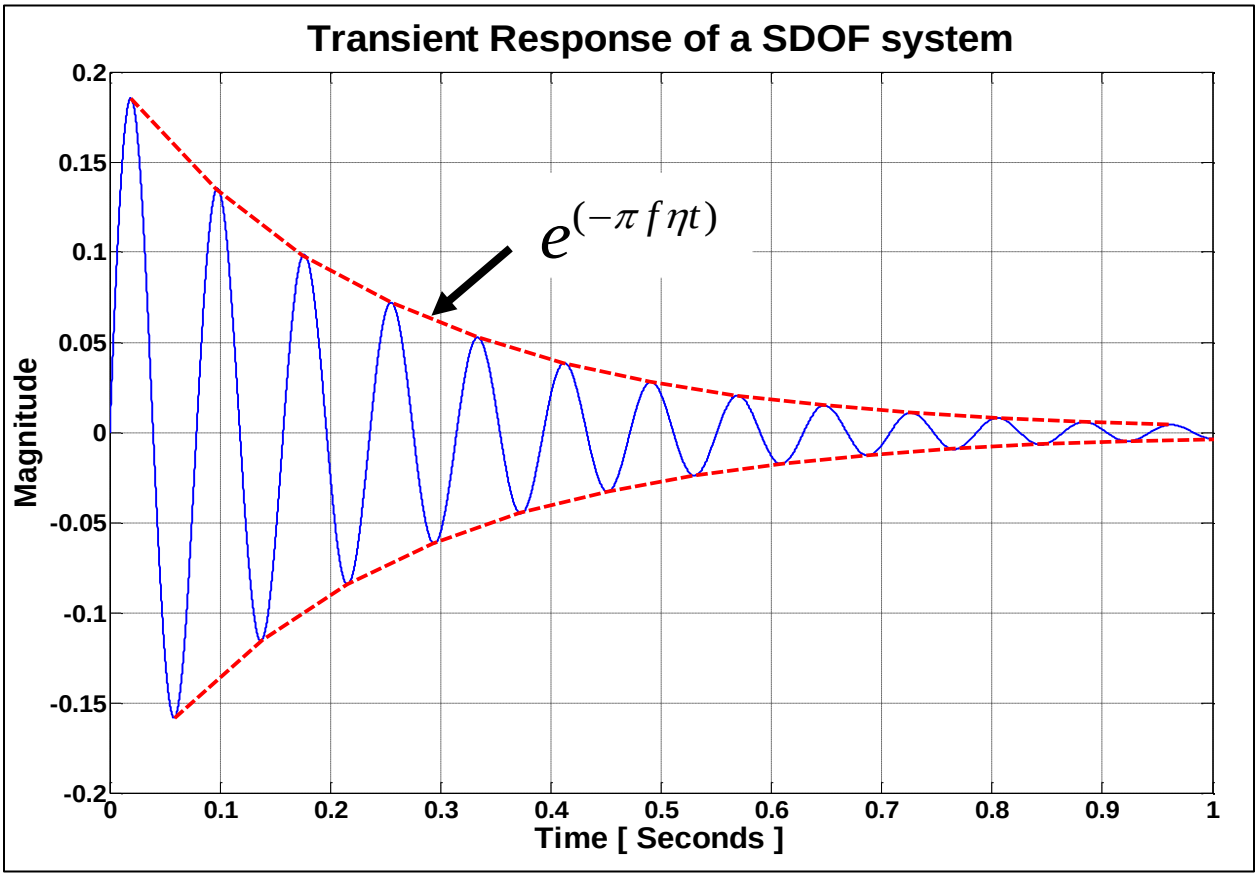

FIGURE 1-5 TRANSIENT RESPONSE OF A SINGLE DEGREE OF FREEDOM SYSTEM

The energy of the system is proportional to the peak amplitude squared; therefore, the system response will decay at a rate equal to $Ge^{(-\pi f \eta t)}$ where G is related to the peak response amplitude of the system. The peak amplitude and the slope are shown in Figure 1-6.

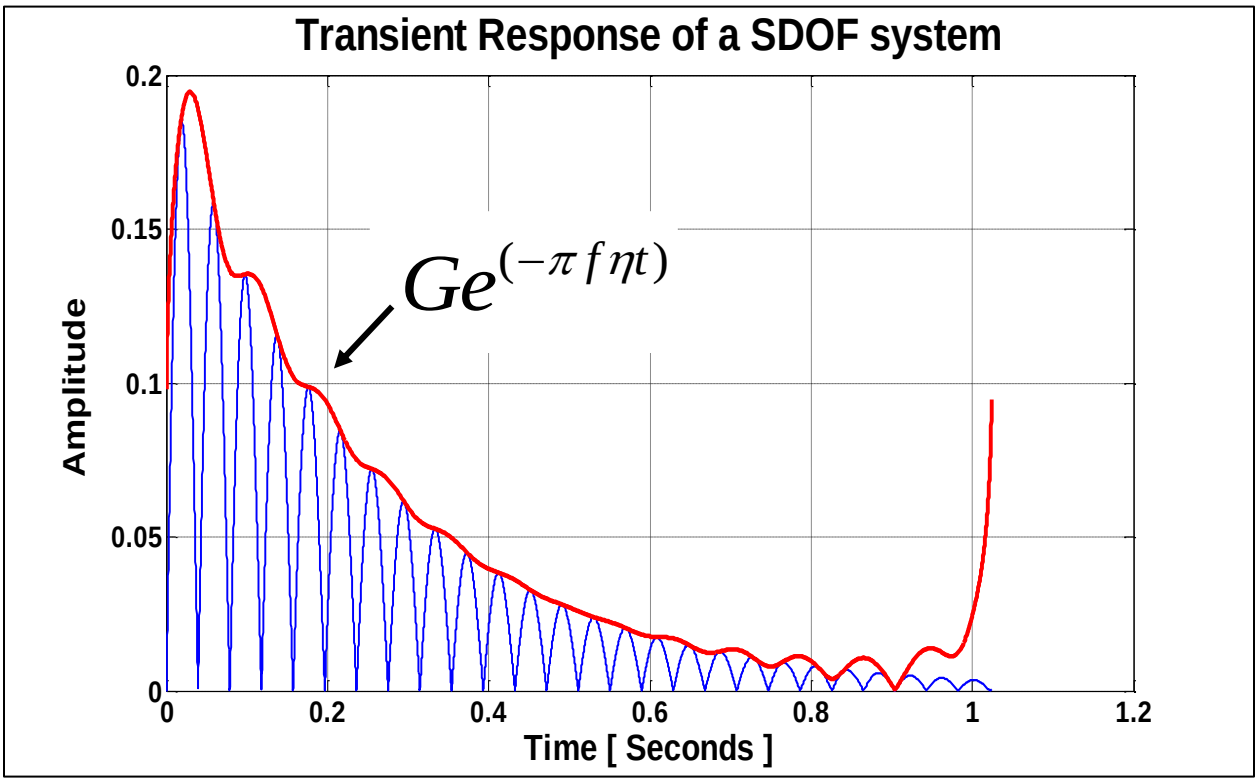

FIGURE 1-6 PEAK AMPLITUDE AND SLOPE OF THE TRANSIENT RESPONSE

The loss factor can be found for a single, well-defined modal resonance or as the average loss factor of many modal resonances over a given frequency range [6]. In both cases, the initial decay slope is found by plotting the system's response on a logarithmic amplitude scale, with a linear time scale. The loss factor is given by the slope of the logarithmic decrement shown in Figure 1-7. The loss factor is estimated with the following equation,

$$\eta = \frac{\Delta_t (dB/\sec)}{27.3 f_n}$$

where Δ_t is the decay rate in $dB/\sec$ and f_n is the natural frequency.

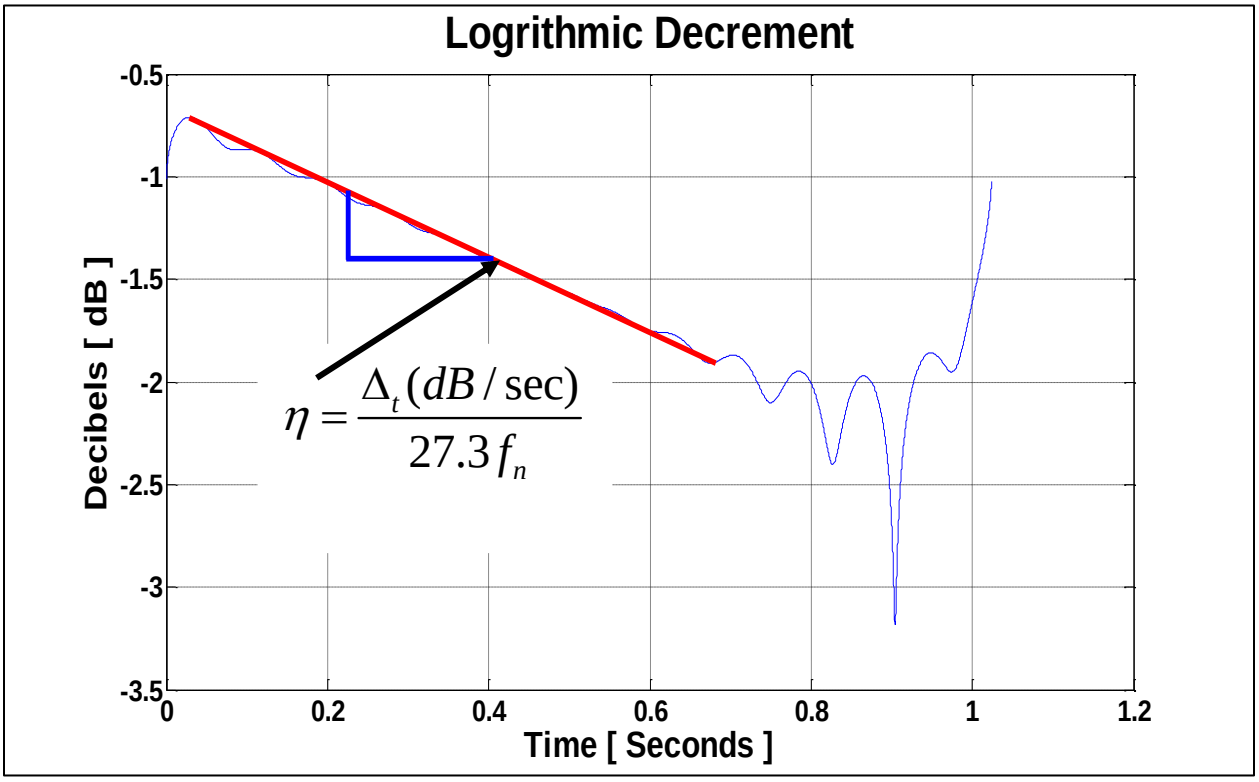

FIGURE 1-7 LOGARITHMIC DECREMENT OF THE TRANSIENT RESPONSE

1.2.2.3 LOGARITHMIC DECREMENT

The decay rate of the single degree of freedom spring-mass-damper system shown in Figure 1-7 can be used to estimate the damping, and the 'logarithmic decrement', δ, has sometimes been used to quantify the system damping[5]. The *logarithmic decrement* is defined as the natural log (base e) of the ratio of two successive peaks, for example the ratio (A_n / A_{n+1}) in Figure 1-8.

The single degree of freedom system under free decay is represented by Equation 1.9 and is stated here again

$$x(t) = e^{-\zeta\omega_n t}(A\cos\omega_d t + B\sin\omega_d t)$$

where ω_n is the undamped natural frequency and ω_d is the damped natural frequency, related to ω_n by:

$$\omega_d = \omega_n \sqrt{1-\zeta^2}$$

A and B are constants depending on the initial conditions.

In the decaying oscillation shown in Figure 1-8, the height of the first peak A_n, is given by

$$A_n = Ce^{-\zeta\omega_n t}$$

where C is a constant depending on A and B, and the height of the second peak, A_{n+1} which occurs $\frac{2\pi}{\omega_d}$ seconds later, is given by

$$A_{n+1} = Ce^{[-\zeta\omega_n(t_1+2\pi/\omega_d)]}$$

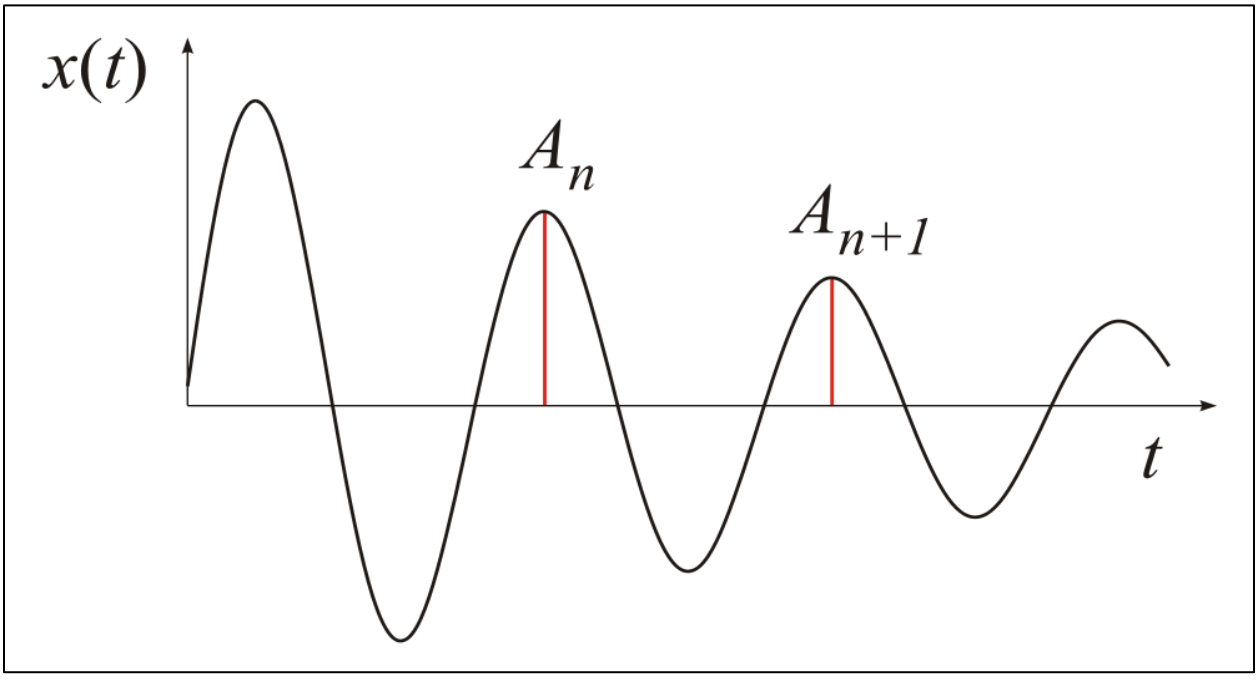

FIGURE 1-8 FREE DECAY OF AN UNDERDAMPED SYSTEM

then the ratio A_n / A_{n+1} is

$$\frac{A_n}{A_{n+1}} = e^{\left(\frac{2\pi\zeta}{\sqrt{1-\zeta^2}}\right)} \tag{1.27}$$

The logarithmic decrement δ is then defined as:

$$\delta = \log_e \frac{A_n}{A_{n+1}} = \frac{2\pi\zeta}{\sqrt{1-\zeta^2}} \tag{1.28}$$

From the above Equation (1.28) the viscous damping rate, ζ can be found by solving the following quadratic equations,

$$\delta^2 - \delta^2\zeta^2 = 2\pi\zeta$$

$$\delta^2\zeta^2 + 2\pi\zeta - \delta^2 = 0$$

1.2.2.4 FREQUENCY RESPONSE FUNCTION ESTIMATION

Assume the following form of the general input/output model shown in Figure 1-9.

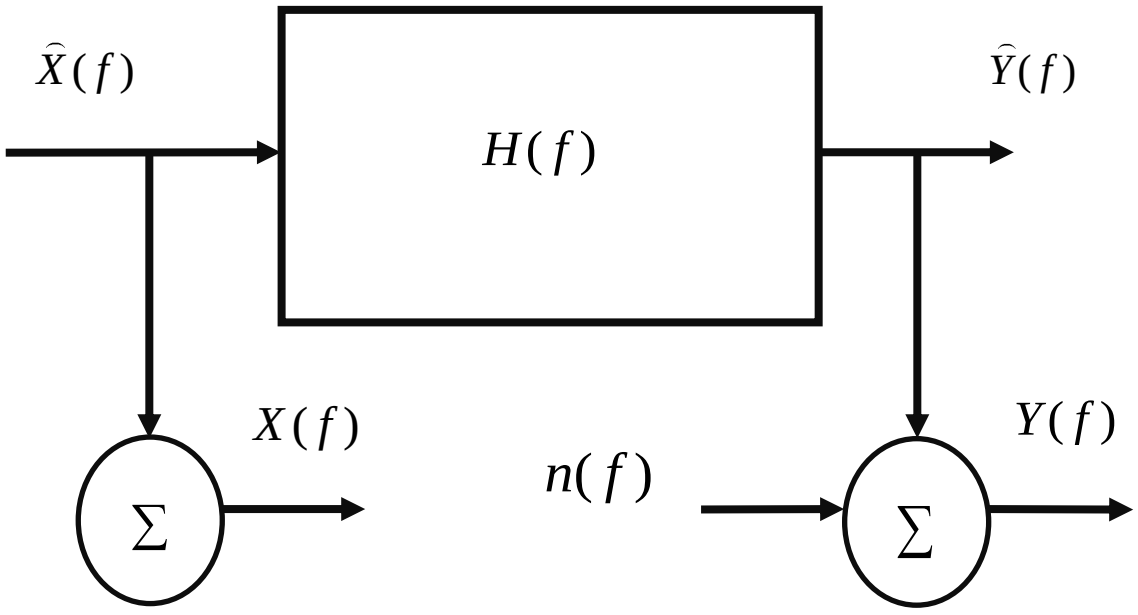

FIGURE 1-9 GENERAL INPUT/OUTPUT MODEL

Then,

$$\begin{aligned} X(f) &= \hat{X}(f) \\ Y(f) &= \hat{Y}(f) + n(f) \end{aligned} \tag{1.29}$$

where $X(f)$ is the measured input, which is equal to the correlated or ideal input $\hat{X}(f)$, and $Y(f)$ is the measured output, which is equal to the sum of the correlated or ideal output $\hat{Y}(f)$ and the uncorrelated output $n(f)$ which is noise [7].

The Frequency Response Function (F.R.F.) of the system is given as:

$$H = \frac{\sum_{k=1}^{K} X_k^* Y_k}{\sum_{k=1}^{K} X_k^* X_k} = \frac{\sum_{k=1}^{K} G_{xy}}{\sum_{k=1}^{K} G_{xx}} = \frac{cross-spectrum}{input-autospectrum} = H_1 \tag{1.30}$$

where X_k and Y_k are the individual Fourier Spectra of input x and output y.

The symbol * means complex conjugate. G_{xx} is the auto spectrum of the input point x, G_{xy} is the cross spectrum between the input point x and the output point y and H_1 is a complex valued function. The magnitude of the F.R.F. is referred to as gain, and the phase angle is the angle between the outputs relative to the input, which is obtained from the cross-spectrum in the numerator of the F.R.F. estimator.

The impulse response function of a system given by Equation (1.24) is the inverse Fourier Transform of the frequency response function.

The coherence function, $\gamma_{xy}^2(\omega)$ measures the degree of the correlation between the signals in the frequency domain. It is defined as

$$\gamma_{xy}^2(\omega) = \frac{\sum_{k=1}^{K} G_{xy} \sum_{k=1}^{K} G_{yx}}{\sum_{k=1}^{K} G_{xx} \sum_{k=1}^{K} G_{yy}} \tag{1.31}$$

where G_{yy} is the auto spectrum of the output point y and G_{yx} is the cross spectrum between the output point y and the input point x.The coherence function is such that $0 < \gamma_{xy}^2(\omega) < 1$, and it provides an estimate of the proportion of the output that is due to the input. For an ideal single input, single output system with no extraneous noise at the input or output stages the coherence function is equal to unity.

$$\gamma_{xy}^2(\omega) = \frac{\left|\mathrm{H}(\omega) G_{xx}(\omega)\right|^2}{G_{xx}(\omega)\left|\mathrm{H}(\omega)\right|^2 G_{xx}(\omega)} = 1 \tag{1.32}$$

The signal to noise ratio of a system is a function of the coherence function and is defined as

$$S/n = \frac{\gamma_{xy}^2(\omega)}{1-\gamma_{xy}^2(\omega)} \tag{1.33}$$

1.3 MEASUREMENT SETUP FOR LOSS FACTOR MEASUREMENTS

The experiments are carried out in the Structural Acoustics Laboratory (S.A.L.) at the University of Kansas. Aluminum and Steel plates are used to simulate aerospace structures, especially structural skin panels. Constrained layer damping (C.L.D.) treatment was applied to two plates; one has full covering C.L.D. and the other has partial covering C.L.D. The damping

material used here is visco-elastic damping polymer, 3MF9469PC. To ensure good bonding between the visco- elastic material and the structure, surfaces are cleaned before attachment and vacuum is drawn after the attachment to apply a pressure of about 1×10^5 Pascal. Plates were suspended from a stand by the use of elastic strands or aluminum wires to simulate free boundary conditions with respect to out-of-plane vibration [8]. The signal of excitation is in the form of white noise which was passed through the amplifier to a typical magneto-dynamic shaker. The output force is transmitted to the plate by using a thin steel rod known as a stinger as shown in Figure 1-10(b). [4].

(a) (b) (c)

FIGURE 1-10 SCANNING LASER VIBROMETER AND THE SHAKER CONFIGURATION

Laser Doppler vibrometers are used to precisely measure mechanical vibrations, and do so quickly, easily and without touching the test article. Vibrometers operate on the Doppler Principle, measuring the frequency shift of back-scattered laser light from a vibrating structure to determine its instantaneous velocity. The PSV-400 Scanning laser vibrometer is a single, automated, turnkey system. The vibrometer head used for acquiring experimental data is a

Polytec 056, which is shown in Figure 1-10(c). Software that controls the scanning laser vibrometer is Polytec version 7.1. All experiments used a frequency resolution of 1 Hz. This Vibrometer can only give up to 6400 frequency lines. To achieve a resolution of 1 Hz with data up to 6400 Hz, a sampling frequency of 16384 Hz is used. The Nyquist Frequency is more than twice of 6400 Hz, so we can have good loss factor estimation up to 6400 Hz. A typical experimental setup is shown in Figure 1-11.

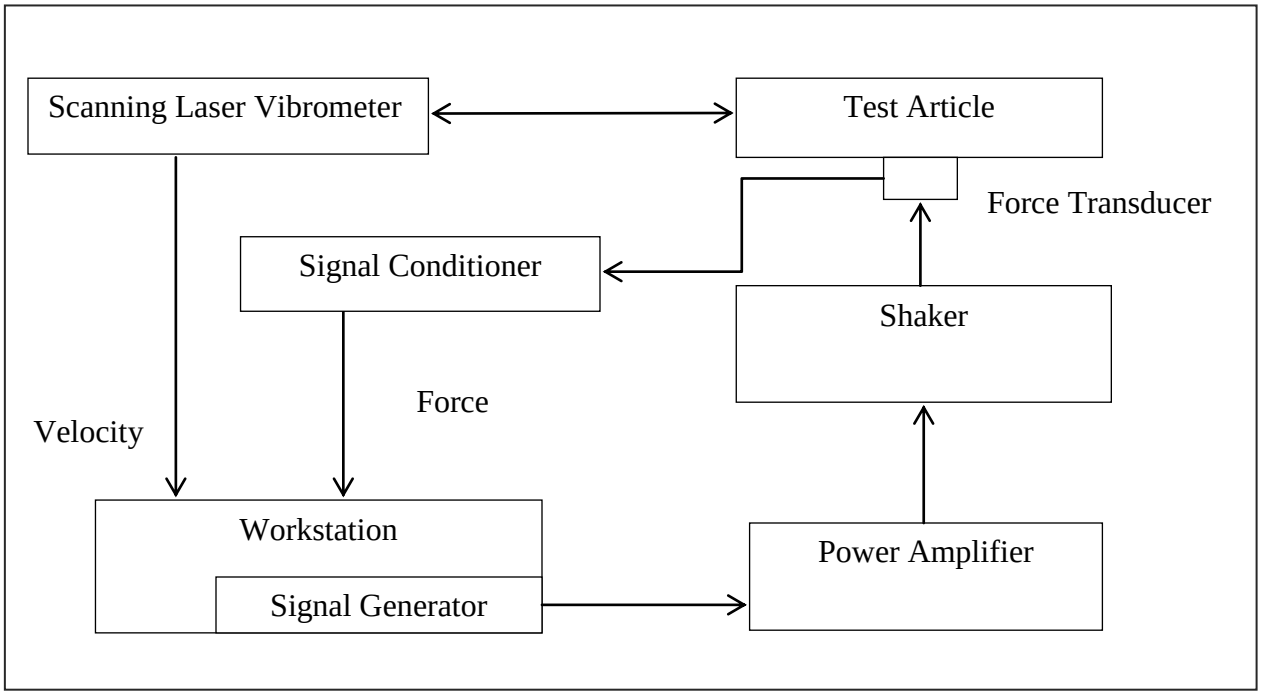

FIGURE 1-11 A TYPICAL EXPERIMENTAL SETUP USED

1.4 OVERVIEW OF STATISTICAL ENERGY ANALYSIS

Statistical energy analysis (S.E.A) is a modeling procedure for the estimation of the dynamic characteristics of, the vibrational response levels of, and the noise radiation from complex, resonant, built-up structures using energy flow relationships [9][10]. These energy flow relationships between the various coupled systems (e.g. plates) that comprise the built-up

structure have a simple thermal analogy. S.E.A. is also used to predict interactions between resonant structures and reverberant sound fields in acoustic volumes. Many random noise and vibration problems associated with large built-up structures, like aircraft, cannot be practically solved by classical methods, and S.E.A. therefore provides a basis for the prediction of average noise and vibration levels, particularly in high frequency regions where modal densities are high. The successful prediction of noise and vibration levels of coupled structural elements and acoustic volumes using the S.E.A. techniques depends to a large extent on an accurate estimate of three parameters:

1. The modal densities of the individual subsystems
2. The internal loss factors (damping) of the individual subsystems, and
3. The coupling loss factors (degree of coupling) between the subsystems.

S.E.A. is particularly attractive in high frequency regions where a deterministic analysis of all the resonant modes of vibration is not practical. This is because at these frequencies there are numerous resonant modes, and numerical computational techniques such as the finite element method have very little applicability.

1.4.1 BASIC ENERGY FLOW CONCEPTS

An individual oscillator driven in the steady-state condition at a single frequency has potential and kinetic energy stored within it. In the steady-state, the input power, Π_{in} has to balance with the power dissipated, Π_{diss}. The power dissipated is related to the energy stored in the oscillator via damping:

$$\Pi_{diss} = c\dot{x}^2 = 2\zeta\omega_n m\dot{x}^2 = 2\zeta\omega_n E = \omega_n E\eta \tag{1.34}$$

where c is the viscous-damping coefficient, ζ is the equivalent viscous damping ratio, ω_n is the natural frequency, m is the oscillator mass, E is the stored energy, and η is the damping loss factor.

The power dissipation concepts for a single oscillator can be extended to a collection of oscillators in specified frequency bands (e.g., full octave bands at one-third octave center frequencies). Here,

$$\Pi_{diss} = \omega E\eta, \tag{1.35}$$

where ω is the geometric mean center frequency of the band, and η is now the mean loss factor of all the modes within the band.

The time-averaged energy flow between the two oscillators is given by [5] [9] [10]

$$\langle \Pi_{12} \rangle = \beta \left\{ \langle E_1 \rangle - \langle E_2 \rangle \right\}, \tag{1.36}$$

where $\langle E_1 \rangle$ and $\langle E_2 \rangle$ are the time-averaged energies of the respective coupled oscillators, and β is a constant of proportionality. This equation is the fundamental basis of S.E.A.

1.4.2 THE TWO SUBSYSTEM MODEL

For two groups of lightly coupled oscillators with modal densities n_1 and n_2 respectively, the average energy flow, $\langle \Pi_{12} \rangle$ is expressed by extending Equation (1.36) as

$$\langle \Pi_{12} \rangle = \gamma \left\{ \langle E_1 \rangle / n_1 - \langle E_2 \rangle / n_2 \right\}, \tag{1.37}$$

where γ is another constant of proportionality, which is only a function of the oscillator parameters. It should be noted that $\langle E_1 \rangle$ and $\langle E_2 \rangle$ are total energies of the respective subsystems; $\langle E_1 \rangle / n_1$ and $\langle E_2 \rangle / n_2$ are the respective modal energies. The coupling loss factor, η_{ij}, relates to energy flow from subsystem i to subsystem j, and is a function of the modal density, n_i, of the subsystem i, the constant of proportionality, γ, and the center frequency, ω, of the band. Equation (1.37) can be expressed in power dissipation terms; the net energy flow from subsystem1 to subsystem 2 is the difference between the power dissipated during the flow of energy from subsystem 1 to subsystem 2 and the power dissipated during the flow of energy from subsystem 2 back to subsystem 1. Hence, using the power dissipation concepts from Equation (1.34),

$$\langle \Pi_{12} \rangle = \omega \langle E_1 \rangle \eta_{12} - \omega \langle E_2 \rangle \eta_{21} \tag{1.38}$$

where η_{12} and η_{21}, are the coupled loss factors between subsystems 1 and 2, and 2 and 1, respectively. From Equations (1.37) and (1.38) we have,

$$\frac{\gamma}{n_1} = \omega \eta_{12}, \text{ and } \frac{\gamma}{n_2} = \omega \eta_{21}.$$

Thus

$$n_1\eta_{12} = n_2\eta_{21} \tag{1.39}$$

Equation (1.39) is the reciprocity relationship between the two subsystems. By substituting this reciprocity relationship into Equation (1.38), we have

$$\langle \Pi_{12} \rangle = \omega\eta_{12}\left\{\langle E_1 \rangle - \frac{n_1}{n_2}\langle E_2 \rangle\right\}. \tag{1.40}$$

Figure 1-12 shows a two subsystem model (numerous modes in each subsystem) where subsystem 1 is driven directly by external force and the other subsystem, subsystem 2 is driven only through the coupling. Π_1 is the power input to subsystem 1; $\Pi_2 = 0$ is the power input to subsystem 2; n_1 and n_2 are the modal densities and η_1 and η_2 are the internal loss factors of subsystems 1 and 2 respectively; η_{12} and η_{21} are the coupling loss factors associated with energy flow from 1 to 2 and from 2 to 1; and E_1 and E_2 are the vibrational energies associated with subsystems 1 and 2.

Using the consistency relationship given by Equation (1.39) [11]

$$\frac{E_2}{E_1} = \frac{n_2\eta_{12}}{n_2\eta_2 + n_1\eta_{12}}, \tag{1.41}$$

and thus,

$$\frac{\eta_{12}}{\eta_2} = \frac{n_2 E_2}{n_2 E_1 - n_1 E_2}. \tag{1.42}$$

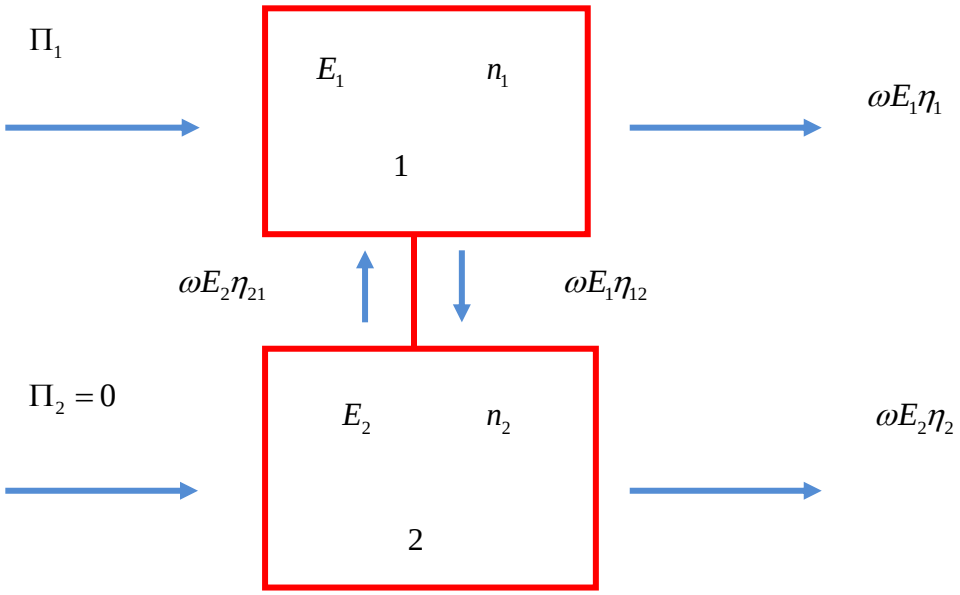

FIGURE 1-12 A TWO SUBSYSTEM S.E.A. MODEL

Equation 1.42 is only valid for direct excitation of subsystem 1, with subsystem 2 being excited indirectly via the coupling joint. If the experiment is reversed then we will have the following,

$$\frac{\eta_{12}}{\eta_1} = \frac{n_2 E_1}{n_1 E_2 - n_2 E_1}. \tag{1.43}$$

1.5 TEST ARTICLES CONSIDERED

1.5.1 ALUMINUM PLATE WITH FULL CONSTRAINED LAYER DAMPING

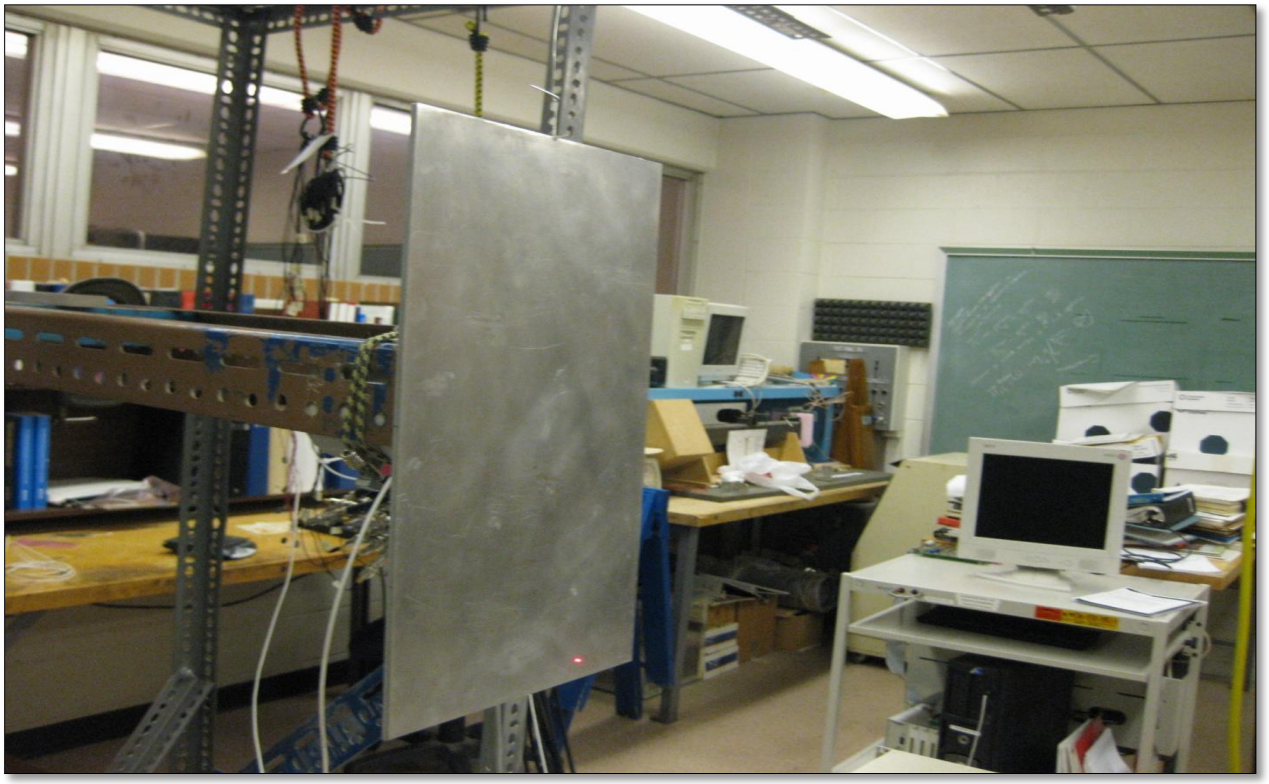

FIGURE 1-13 DAMPED ALUMINUM PLATE WITH FULL CONSTRAINED LAYER DAMPING

TABLE 1-1 DIMENSIONS OF DAMPED ALUMINUM PLATE WITH FULL CONSTRAINED LAYER DAMPING

	Material	Dimensions (m)	Mass(gms)
Base Layer	CLAD 2024-T3	0.349X0.2029X0.0016002	573.7
Damping Layer	3M F9469PC at20 ^{o}C	0.349×0.2029×0.000127	4.125
Constraining Sheet	CLAD 2024-T3	0.349X0.2029X0.0016002	48.06

1.5.2 UNDAMPED STEEL PLATE

FIGURE 1-14 UNDAMPED STEEL PLATE

TABLE 1-2 MATERIAL PROPERTIES OF THE UNDAMPED STEEL PLATE

Material	Dimensions(m)	Mass (gms)
Steel	0.39 x 0.28 x 0.003	2750

1.5.3 TWO STEEL PLATES JOINED ALONG A LINE

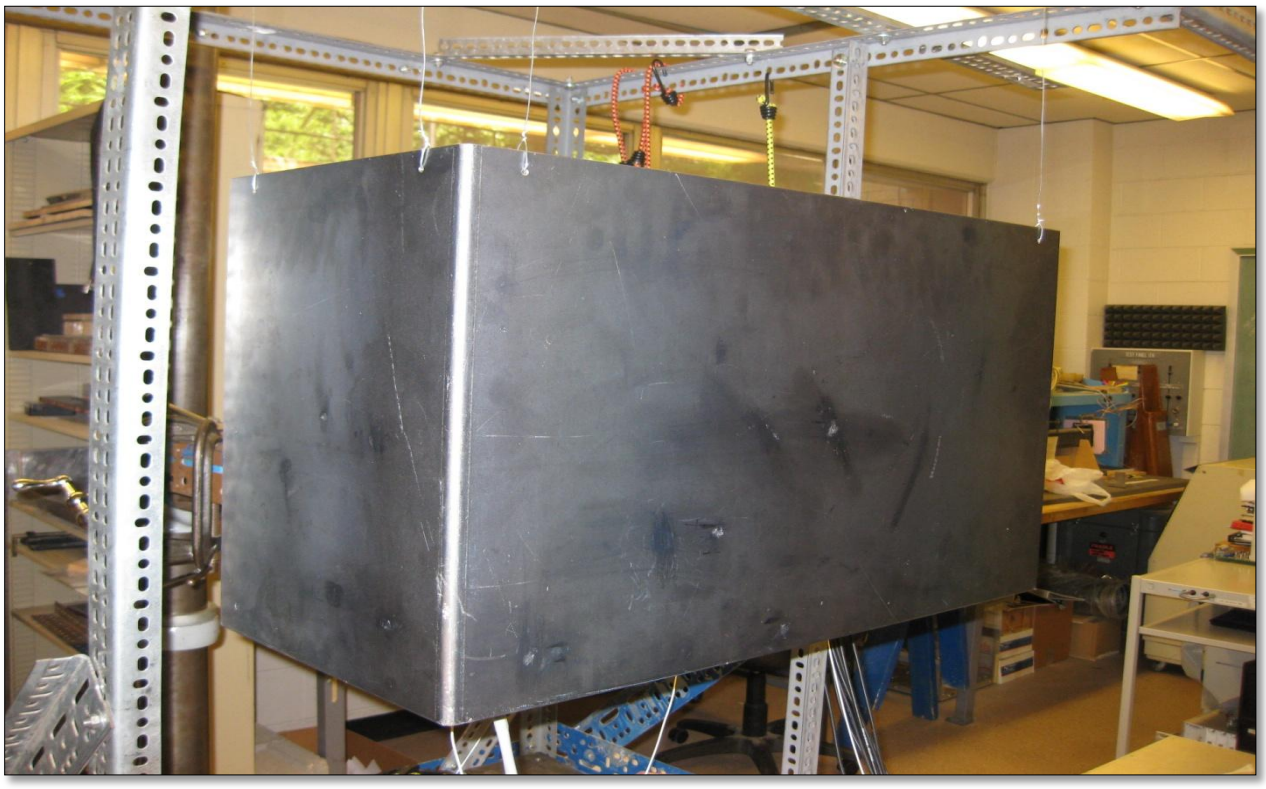

FIGURE 1-15 TWO UNDAMPED STEEL PLATES JOINED ALONG A LINE

TABLE 1-3 MATERIAL PROPERTIES OF THE STEEL PLATES JOINED ALONG A LINE

	Material	Dimensions (m)	Mass (gms)
Plate 1 (Small Plate)	Steel	0.39 x 0.28 x 0.003	2750
Plate 2 (Large Plate)	Steel	0.625 x 0.28 x 0.003	6000

1.5.4 UNDAMPED ALUMINUM PLATES JOINED AT A POINT

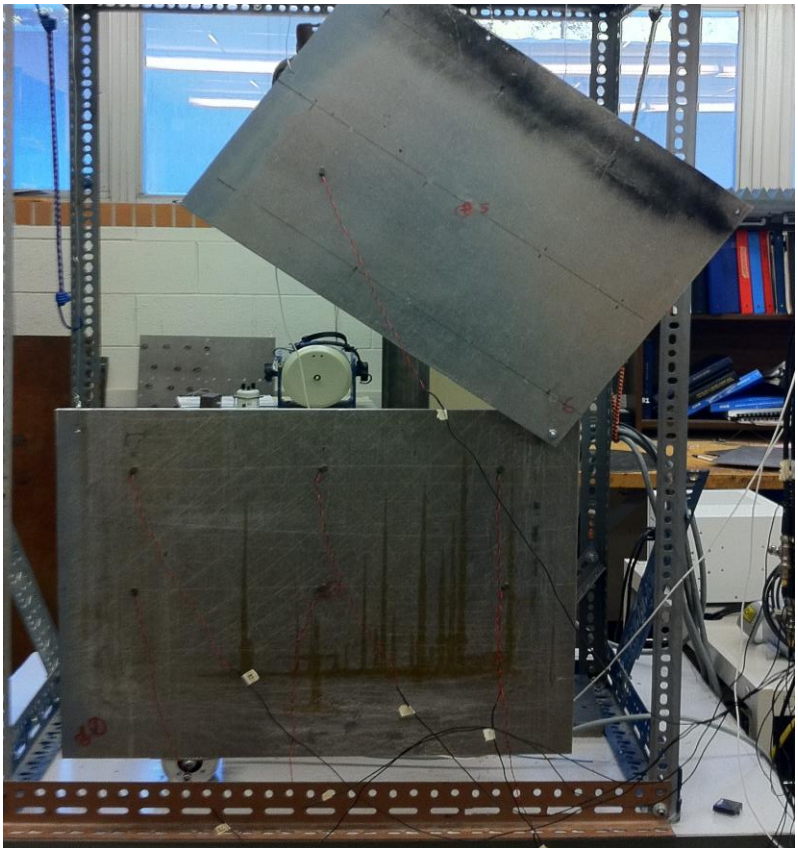

FIGURE 1-16 TWO UNDAMPED ALUMINUM PLATES CONNECTED AT A POINT

TABLE 1-4 MATERIAL PROPERTIES OF ALUMINUM PLATES JOINED AT A POINT

	Material	Dimensions (m)	Mass(gms)
Top Plate	CLAD 2024-T3	0.53 x 0.40 x 0.00635	3628
Bottom Plate	CLAD 2024-T3	0.61 x 0.46 x 0.00635	4820

The plates are connected through a force transducer.

2 LOSS FACTOR ESTIMATION USING THE POWER INPUT METHOD

2.1 THEORY OF THE POWER INPUT METHOD

The Power Input Method (P.I.M.) is based on a comparison of the dissipated energy of a system to its maximum total energy under steady state vibration. Some errors may be introduced through the measurement technique, but the P.I.M. is fundamentally unbiased at the natural frequencies of well-defined modes or when the loss factors are frequency-band averaged over many modes. These "frequency-averaged" damping loss estimates are widely used in the automotive and aerospace industry for vehicle computer models based on Finite Element Method (F.E.M.) and Statistical Energy Analysis (S.E.A.) [6].

The damping loss factor per cycle in the frequency band centered at ω, for a structural system is defined as [4]

$$\eta(\omega) = \frac{E_{diss}}{E_{Total}} = \frac{E_{IN}}{E_{Total}} \tag{2.1}$$

where E_{IN} is the input energy, E_{diss} is the energy dissipated from damping and E_{Total} is the time averaged total energy of the system. Assuming a stationary input energy at the fixed location, the energy dissipated, E_{diss} can be replaced with input energy E_{IN} because the input energy is equal

to the dissipated energy under steady state conditions. Unfortunately, E_{IN} cannot be measured directly. But the input energy can be calculated from the simultaneous measurements of the force and velocity at the point of energy input. E_{diss} can then be computed as

$$E_{IN} = E_{diss} = \frac{1}{2\omega} \mathrm{Re}[\mathrm{H}_{ff}(\omega)] G_{ff}(\omega), \tag{2.2}$$

where H_{ff} is the driving point mobility function (the force-to-velocity transfer function), and G_{ff} is the power spectral density of the input force. Obtaining an estimate for E_{Total} requires making a few assumptions. First, since the total energy cannot be calculated directly from force and velocity measurements, it can be replaced with twice the maximum kinetic energy –which holds true at the natural frequencies of an undamped system. But, the error in making this assumption is, for instance only 0.5% for a damping level of 10%. Secondly, the system being measured should be approximated by a summation as opposed to a volume integral when taking measurements. Thus the kinetic energy is evaluated by the following equation:

$$E_{KE} = \frac{1}{2} \sum_{i=1}^{N} m_i G_{ii}(\omega), \tag{2.3}$$

where, E_{KE} is the system kinetic energy, N is the number of measurement locations, m_i is the mass of the discrete portion of the system, and G_{ii} is the power spectral density of the velocity response at each measurement location. Finally, assuming that the system is linear, allows use of:

$$\left|H_{ff}(\omega)\right|^2 = \frac{G_{ii}(\omega)}{G_{ff}(\omega)}, \tag{2.4}$$

where, H_{ff} is the driving point mobility function. With the above mentioned assumptions, and all measurement points uniformly spaced throughout the system in equal mass portions, we have the damping in the structure defined as,

$$\eta(\omega) = \frac{\mathrm{Re}\left[H_{ff}(\omega)\right]}{\omega m \sum_{i=1}^{N}\left|H_{if}(\omega)\right|^2} \tag{2.5}$$

where H_{if} is the mobility between the driving point f and the point i. To obtain accurate loss factors estimations, it is essential to have highly accurate measurements of the driving point FRF (H_{ff}) [4]; otherwise, large errors could be introduced. In particular, if the phase information in H_{if} is not carefully resolved, the loss factor estimation may be negative which is physically unrealizable. One way to address deficiencies in phase information is to increase frequency resolution in the measurement.

2.2 SINGLE DEGREE OF FREEDOM ANALYSIS

2.2.1 INTRODUCTION TO SINGLE DEGREE OF FREEDOM SYSTEMS

A system with a single degree of freedom (S.D.O.F. system) is the simplest among the vibratory systems. It consists of three elements: inertia element (mass), elastic element (spring),

and damping element. The dynamic state of the system is fully described by one variable that characterizes deflection of the inertia element from the equilibrium position. One key assumption for the spring-mass-damper system is that the spring has no damping or mass, the mass has no stiffness or damping; and the damper has no stiffness or mass. Furthermore, the mass is allowed to move in only one direction. The role of single degree of freedom systems in vibration theory is very important because any linear vibratory system behaves like an S.D.O.F. system near an isolated natural frequency and as a connection of S.D.O.F. systems in a wider frequency range.

The general form of the differential equation describing a single degree of freedom oscillator is,

$$m\ddot{x}(t) + c\dot{x}(t) + kx(t) = f(t),\ x(0) = x_0,\ \dot{x}(0) = v_0 \tag{2.6}$$

where $x(t)$ is the position of the mass, m is the mass, c is the viscous damping rate, k is the stiffness, and $f(t)$ is the external dynamic load. The initial displacement is x_0, and the initial velocity is v_0

Free vibrational response of lightly damped systems decay over time. Damping may be introduced into a structure through diverse mechanisms, including linear viscous damping, friction damping, and plastic deformation. All but linear viscous damping are somewhat complicated to analyze with closed form expressions, so we will restrict our attention to linear viscous damping, in which the damping force f_D is proportional to the velocity,

$$f_D = c\dot{x}$$

The two types of energies in a system are kinetic energy, T, and the potential energy, U. Their sum $T+U$ is the total energy of vibration. Generally, it is the time-averaged energy values $\langle T \rangle$ and $\langle U \rangle$, that are required. Since it is known that $\langle T \rangle = \langle U \rangle$ and $E = m\langle v \rangle^2$.

For a damped system, the energy decays exponentially with time. The mean square velocity is obtained by differentiating the underdamped solution given by

$$x(t) = X_T e^{-\zeta \omega_n t} \sin\left\{(1-\zeta^2)^{1/2}\omega_n t + \phi\right\} \tag{2.7}$$

In the above equation the viscous damping ratio ζ, is now replaced with the structural loss factor η and the relation between the two is given by $\eta = 2\zeta$.

$$x(t) = X_T e^{-\eta \omega_n t/2} \sin\left\{(1-(\eta/2)^2)^{1/2}\omega_n t + \phi\right\} \tag{2.8}$$

The mean-squared velocity is obtained by differentiating Equation (2.8) and subsequently integrating the square value over a time interval. It is

$$\left\langle \upsilon^2 \right\rangle \approx \frac{V^2 e^{-\eta \omega_n t}}{2}, \tag{2.9}$$

where V is the maximum velocity level. The corresponding mean-square displacement is

$$\left\langle x^2 \right\rangle \approx \frac{\left\langle \upsilon^2 \right\rangle}{\omega_n^2} \tag{2.10}$$

The above equations are approximations and assume small damping, i.e. $\omega_d \approx \omega_n$. For the case of the underdamped oscillator, $\langle T \rangle = \langle U \rangle$, so the total time averaged energy is, $\langle E \rangle \approx 2\langle T \rangle = m\langle \upsilon^2 \rangle,$. Therefore, the time-averaged power dissipation is given by

$$\langle -dE/dt \rangle = \langle \Pi \rangle = c\langle \upsilon^2 \rangle = \eta\omega_n m\langle \upsilon^2 \rangle = \eta\omega_n \langle E \rangle. \tag{2.11}$$

Hence, the structural loss factor is [6] [12]

$$\eta = \frac{\langle \Pi \rangle}{\omega_n \langle E \rangle} \tag{2.12}$$

The structural loss factor is thus related to the time-averaged power dissipation and the time averaged energy of vibration.

2.2.2 ANALYTICAL LOSS FACTOR ESTIMATION OF SDOF SYSTEMS

2.2.2.1 USING A TRUE RANDOM FORCE

The most popular excitation signal used for shaker testing to estimate loss factors is the random signal. A true random signal (the time history of the signal is neither periodic nor transient but is continuous and does not repeat itself) is synthesized with a random number generator, and is an unending (non-repeating) random sequence. Typical example of a random vibration is the turbulent flow over an aircraft body. A time domain window (a Hanning window or one like it), must always be used with true random signals during testing to minimize leakage. The force and the response of the system should satisfy the Dirchlet condition which states that

these signals and the first time derivative of the signals are zero at the beginning and end of the time record.

The single degree of freedom system is excited with a random force. The random force is created using a random phase angle approach. A typical true random signal before and after applying a Hanning window is shown in Figure 2-1. The MatLAB code to generate the random signal is given in Appendix A. The SDOF system has a mass of $0.5\,Kg$, damping rate of 0.5 Ns/m and a stiffness of $1000\,N/m$.

The natural frequency of the system ω_n which is given by $\omega_n = \sqrt{k/m}$ is calculated as 44.7214. The damping coefficient ζ which is given by $\zeta = \frac{c}{2m\omega_n}$ is calculated to be 0.0112. Since the structural damping loss factor η of the system is given as $\eta = 2\zeta$, the input loss factor for the SDOF system is 0.224. The damped natural frequency ω_d of the system given by $\omega_d = \omega_n\sqrt{1-\zeta^2}$, is calculated to be 44.7186. Note that $\omega_d \approx \omega_n$.

The response of the system for this true random excitation signal is given by the impulse function, shown in Equation (1.25) and stated here

$$h(t) = \frac{1}{m\omega_d} e^{-\zeta\omega_n t} \sin \omega_d t$$

The velocity is then obtained by differentiating the velocity in the time domain.

Figure 2-2 shows the velocity response of the single degree of freedom system subjected to random excitation. Again a Hanning window is used for the velocity response to minimize leakage.

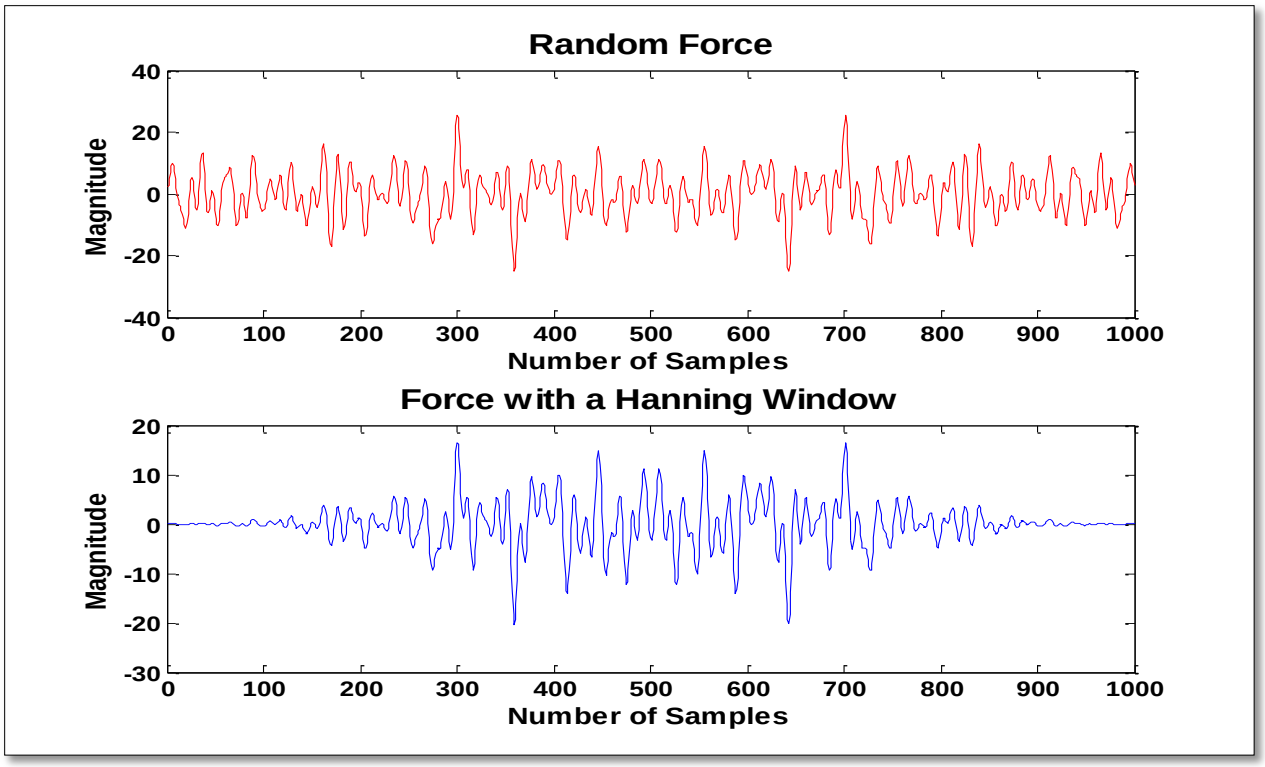

FIGURE 2-1 RANDOM FORCE AND THE FORCE WITH THE HANNING WINDOW

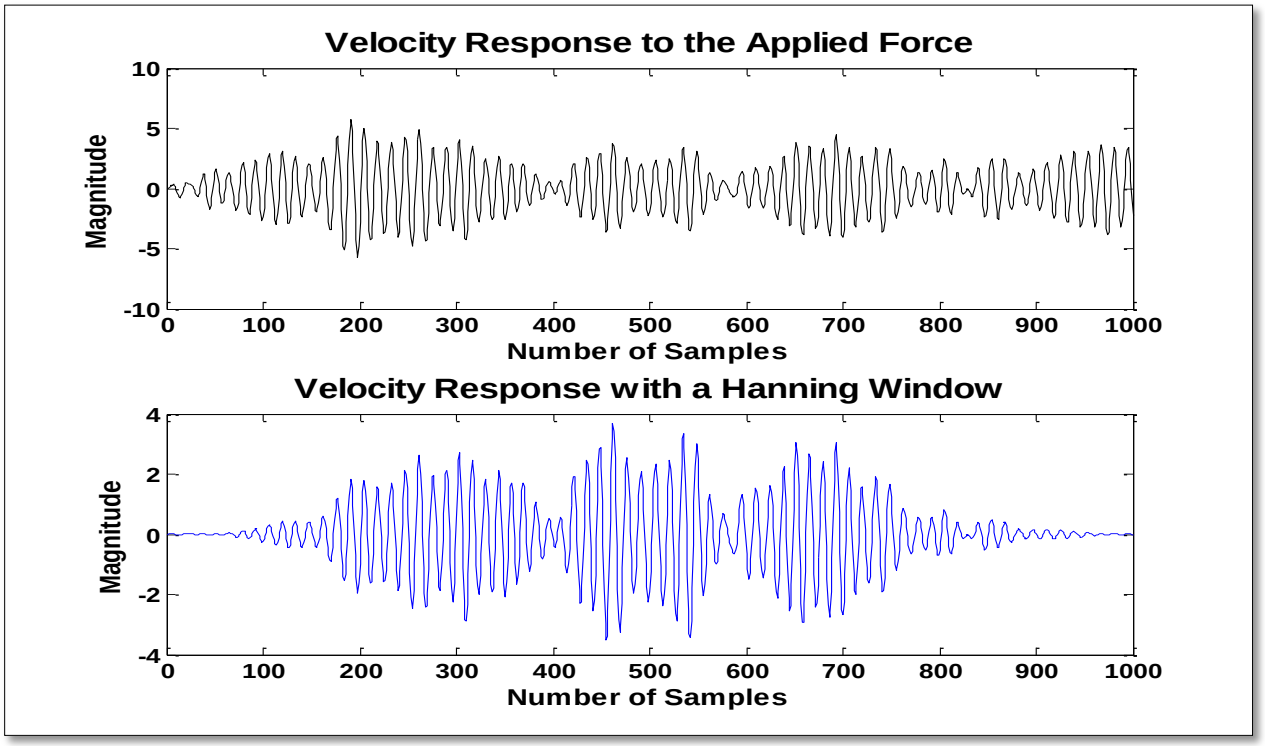

FIGURE 2-2 VELOCITY RESPONSE AND VELOCITY AFTER APPLYING THE HANNING WINDOW

The structural loss factor by the power input method is the total energy input (and dissipated) divided by the total time averaged energy of the system. The energy input by the single degree of freedom system is given by $f*v$ and the total energy of the system is the kinetic energy of the system given by $\frac{1}{2}mv^2$. Thus, the loss factor of the system is given by

$$\eta = \frac{f*v}{\frac{1}{2}mv^2} \tag{2.13}$$

The input structural loss factor η of the system is 0.224 as mentioned earlier, the expected loss factor is 0.224. Figure 2-3 shows the input loss factors and the corresponding loss factors calculated by the P.I.M. for 10 samples. The estimated loss factors are accurate with a mean variation of less than 1%.

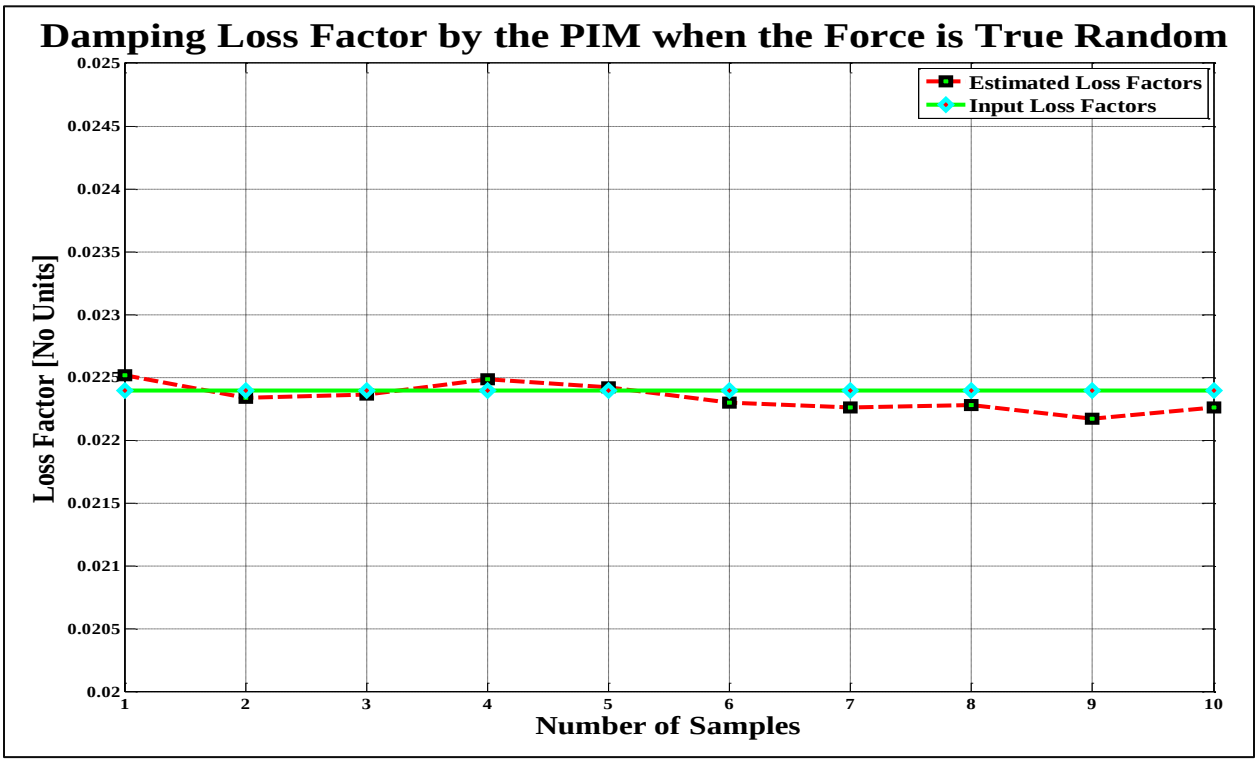

FIGURE 2-3 COMPARISON BETWEEN THE INPUT LOSS FACTORS AND THE ANALYTICALLY ESTIMATED LOSS FACTORS OF A SINGLE DEGREE OF FREEDOM SYSTEM FOR A TRUE RANDOM EXCITATION.

2.2.2.2 USING A SINUSOIDAL FORCE

The single degree of freedom system is dynamically forced to vibrate with a sinusoidal forcing function, $f(t) = F_o \cos(\omega t)$ where ω is the frequency of the forcing function in radians per second. If $f(t)$ is persistent, then after several cycles the system will respond only at the frequency of vibration of the external forcing ω.

The sine wave excitation signal has been used since the early days of structural dynamic measurements. It was the only signal that could be effectively used with traditional analog instrumentation. Even after broad band testing methods (like impact testing), have been developed for use with Fast Fourier Transforms (F.F.T.) analyzers, sine wave excitation is still useful in some applications. The primary purpose for using a sine wave excitation signal is to put energy into a structure at a specified frequency. Slowly sweeping sine wave excitation is also useful for characterizing non-linearities in structures.

The single degree of freedom system with a mass of 0.5 Kg, damping rate of 0.5 Ns/m and a stiffness of 1000 N/m is excited with a sinusoidal input force of frequency, which is equal to the damped natural frequency of the system. The natural frequency of the system ω_n which is given by $\omega_n = \sqrt{k/m}$ is calculated as 44.7214. The damping coefficient ζ which is given by $\zeta = \frac{c}{2m\omega_n}$ is calculated to be 0.0112. Since the structural damping loss factor η of the system is given as $\eta = 2\zeta$, the input loss factor for the S.D.O.F. system is 0.224. The damped natural frequency ω_d of the system given by $\omega_d = \omega_n\sqrt{1-\zeta^2}$ is calculated to be 44.7186. Note that $\omega_d \approx \omega_n$.

The response of the system for this periodic excitation signal is given by the impulse function, shown in Equation (1.25) and stated here again

$$h(t) = \frac{1}{m\omega_d} e^{-\zeta\omega_n t} \sin \omega_d t$$

The sinusoidal excitation force and the velocity response of the single degree of freedom system are plotted in Figure 2-4. The force and the response must satisfy the Dirchlet condition and so a Hanning window is used.

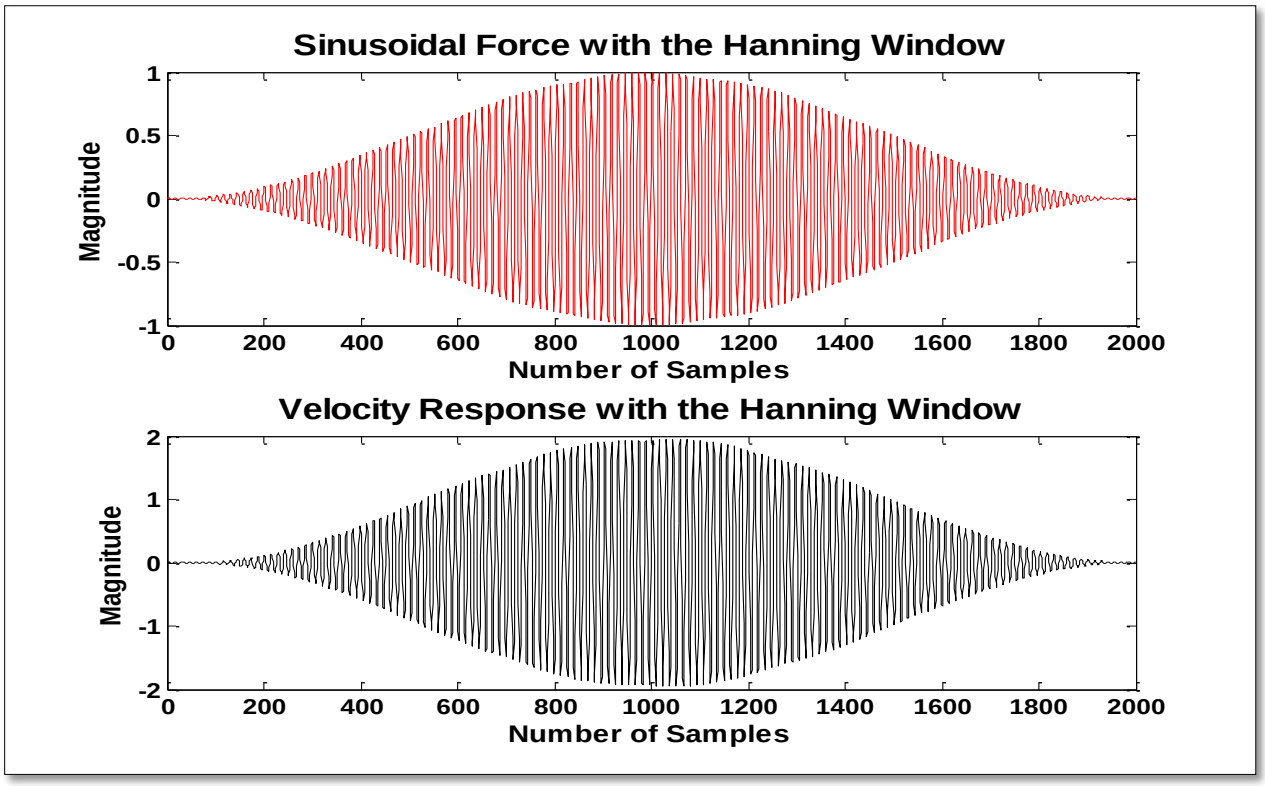

FIGURE 2-4 FORCE AND VELOCITY WITH A HANNING WINDOW APPLIED

Once we have the response of the system to the periodic excitation signal the velocity of the system is calculated by simple differentiation and the total energy is measured as the kinetic

energy given by $\frac{1}{2}mv^2$ and the dissipated energy is the product of impulse and velocity and the loss factor is calculated by

$$\eta = \frac{f * v}{\frac{1}{2}mv^2}.$$

The input loss factor of the system is varied by varying the spring constant k and thus by changing the frequency of the periodic signal with which the system is excited. The input and the estimated loss factors for various levels of structural loss factor are plotted in Figure 2-5. From Figure 2-3 and Figure 2-5 it is shown that the Power Input Method is fairly accurate in estimating the damping of the single degree of freedom systems with a mean variance of less than 1% for a wide range of loss factors. By averaging a large number of measurements, the random variations can be removed.

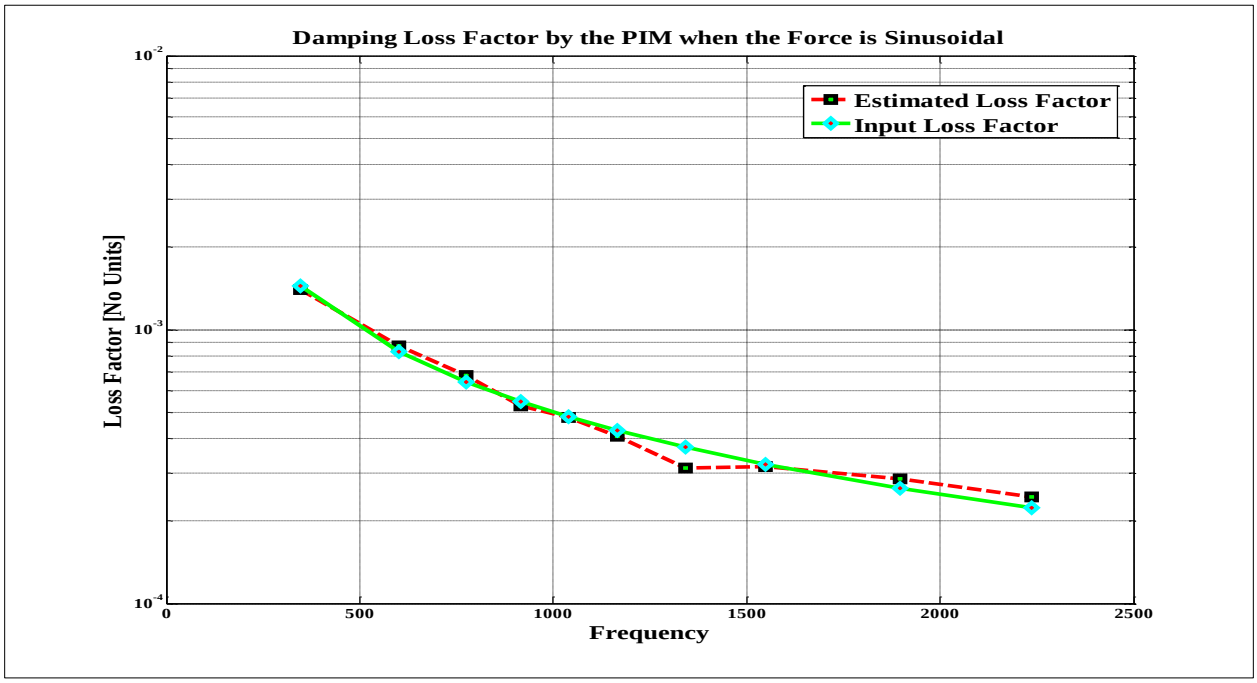

FIGURE 2-5 COMPARISON BETWEEN THE INPUT LOSS FACTORS AND THE ANALYTICALLY ESTIMATED LOSS FACTORS OF A SINGLE DEGREE OF FREEDOM SYSTEM FOR A SINUSOIDAL EXCITATION

2.3 PLATE – EXPERIMENTS

For the experimental validation of the Power Input Method a couple of relatively simple systems are chosen. A 2024-T3 aluminum plate with a full covering constrained layer damping treatment and a steel plate with no damping are used as the test articles. Plates are chosen over other simple structures (i.e., bars, etc.) because plates have a higher modal density. Most of the concepts of the single degree of freedom systems can be directly extended to the case of the multiple degree of freedom systems [1]. There are n natural frequencies each associated with its own mode shape, for a system having n degrees of freedom. Plates are typically modeled analytically as a finite-numbered collection of modal responses or a finite element approximation [5].

As discussed in the introduction section of Chapter 2, the Power Input Method [13], [11], [14] approximates the loss factor of the system by the ratio of energy dissipated within the system per radian of motion to its total strain energy. Hence the loss factor is given by

$$\eta(\omega) = \frac{E_{diss}}{E_{Total}} = \frac{E_{IN}}{E_{Total}}$$

the numerator in the equation can be replaced with

$$E_{IN} = \frac{1}{2\omega} \mathrm{Re}[H_{if}(\omega)] G_{ff}(\omega)$$

where H_{if} is the mobility (velocity/force) between the driving point f and the point i,

The total energy of the system i.e., the total time averaged kinetic energy of the system is given by

$$E_{KE} = \frac{1}{2}\sum_{i=1}^{N} m_i G_{ii}(\omega), .$$

The mobility transfer function, which is the ratio of the Power Spectral Density (P.S.D.) of velocity response at the measurement location i to the P.S.D. of input force at the chosen input location, is given by [14]

$$\left|H_{ff}(\omega)\right|^2 = \frac{G_{ii}(\omega)}{G_{ff}(\omega)}$$

where H_{ff} is the mobility of the driving point.

Hence the loss factor of the multi degree of freedom system is determined by the equation,

$$\eta(\omega) = \frac{\mathrm{Re}\left[H_{ff}(\omega)\right]}{\omega m \sum_{i=1}^{N}\left|H_{if}(\omega)\right|^2} \tag{2.14}$$

2.3.1 ALUMINUM PLATE WITH FULL CONSTRAINED LAYER DAMPING

The 2024-T3 aluminum plate is suspended with a thin aluminum wire to create free-free boundary condition as shown in Figure 1-10(a, b). The other end of the wire is attached to a massive and stiff frame, so vibrational energy is reflected back to the test article with minimum energy loss at the boundary. Wolf Jr. [8] provided a rule-of-thumb for designing suspension systems: to simulate free boundary conditions; the first rigid body mode under the constraint of the suspension should be no more than 1/10 of the first elastic mode. For example, the most dominant rigid body mode (the vertical translational mode) for this damped aluminum plate is measured to be at 1.43 Hz, which is much less than 1/10 of the plate's first bending mode which

is 90.6Hz. As mentioned in the discussion about the measurement techniques, to eliminate the effects of mass loading due to an accelerometer, a Polytec laser, model OFV 056 is used. Vibrational response of the plate due to a steady excitation is measured at 225 points by placing a grid of scanning points over the entire surface of the plate. This is similar to using a Finite Element approach where we divide the test specimen in to finite elements of smaller size and the response of each finite element is calculated to give a close representation of the entire plate. In a finite element analysis the solution should asymptotically approach a constant value as the total number of finite elements is increased. Similarly as the number of scanning points are increased, the loss factor measurements should asymptotically approach a constant value. The plate is excited from 0 Hz to 6.4 KHz with a resolution of 1 Hz via a LDS Model V203 electrodynamic shaker and a LDS PA25E power amplifier. A PCB force gage was connected to the shaker with a stinger and attached to the back of the plate to measure the input force while the scanning laser vibrometer measures the vibrational responses of the system.

It must be noted here that the laser vibrometer cannot measure the driving point mobility directly; instead it measures the velocity of the point on the front of the plate immediately opposite the forcing point. The accurate measurement of the driving point mobility is critical to get a good estimation of loss factors. Figure 2-6, presents the loss factors as a function of frequency for one excitation point. The loss factors estimated in 1/3 octave frequencies by averaging the loss factors in the respective full octave band are also shown in the graph. The oscillatory behavior of the estimated loss factors is attributed to the limitations of the experimental technique and a curve fit through the local minima is a closer estimate of the loss factors for the plate [17].

Figure 2-7 shows the estimation in full octave frequency bands with one third octave frequency spacing for the 6 different excitation points as well as the average. Explanation of the periodicity or the sinusoidal variation of the loss factor curves is explained elsewhere [16]. An accurate measurement of loss factor can be accomplished by doing a curve fit through the local minima [17]. It should be noted that the variation in the loss factor estimation is about 30% depending on the location of the excitation point, so averaging a number of different response measurements, typically four or more, is required for a good estimation of loss factor.

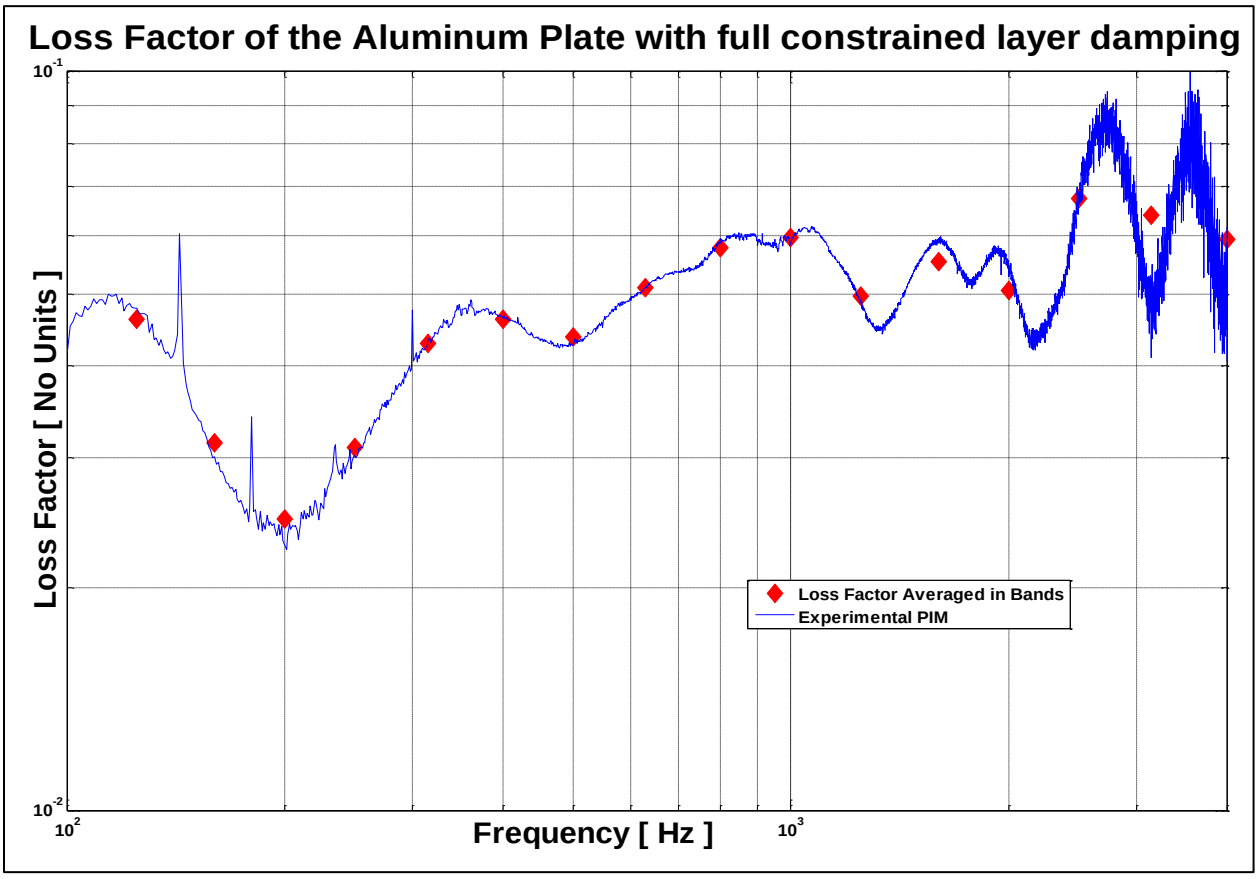

FIGURE 2-6 ESTIMATION OF LOSS FACTOR FOR THE HIGHLY DAMPED ALUMINUM PLATE WITH CONSTRAINED LAYER DAMPING BY THE POWER INPUT METHOD IN FULL FREQUENCY SPECTRUM

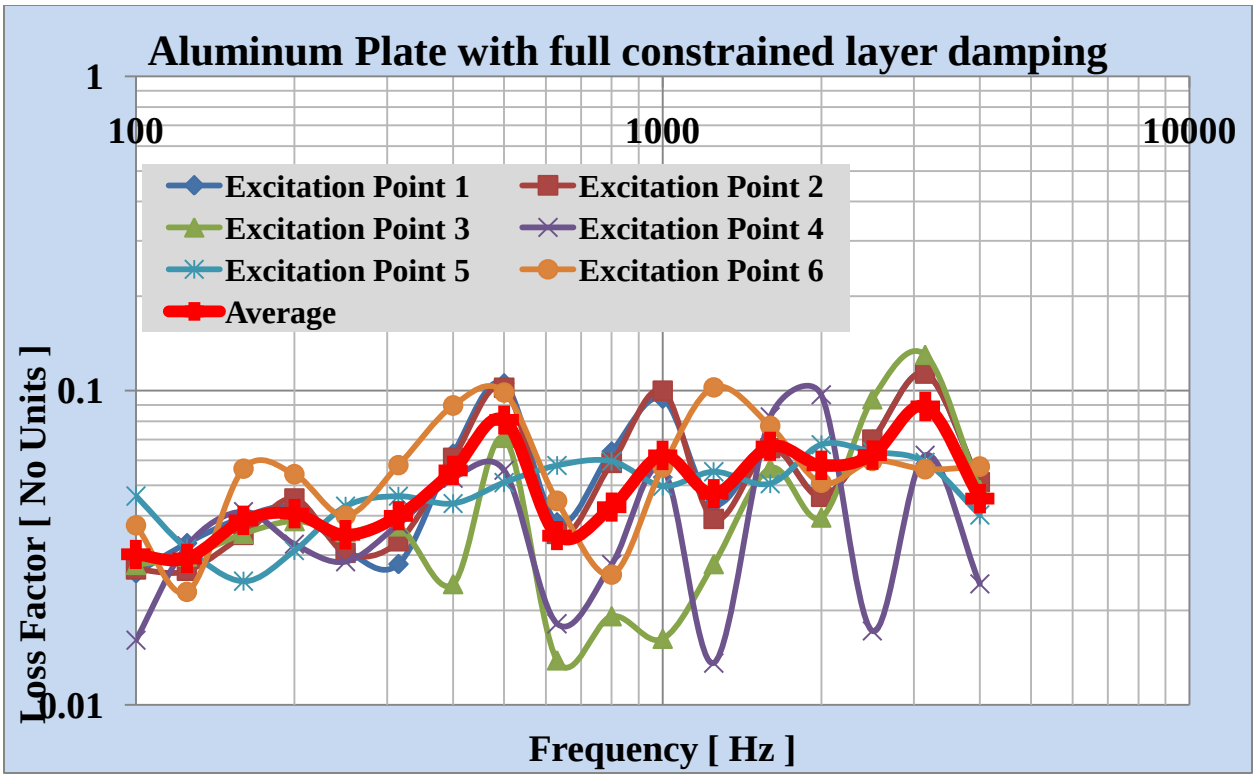

FIGURE 2-7 LOSS FACTOR FOR THE ALUMINUM PLATE WITH FULL CONSTRAINED LAYER DAMPING ESTIMATED IN FULL OCTAVE BANDS WITH 1/3RD OCTAVE CENTER FREQUENCIES

2.3.2 UNDAMPED STEEL PLATE

The undamped steel plate is shown in Figure 1-14. Although the plate has no external damping treatment applied it has an inherent material damping. Steel has very low internal damping but the purpose of this experiment is to determine the limitations of the power input method. The steel plate is suspended with metal cords but could still be considered as free-free boundary conditions. To simulate free boundary condition the first rigid body mode under the constraint of suspension should be no more than 1/10th of the first elastic mode [8], [4] which it is in this case. It can be seen from Figure 2-8 that the damping loss estimation of the plate fails as it predicts negative loss factors. It is hence concluded that although the power input method

provides reasonable accuracy for estimating the loss factors for a moderate and highly damped plates, it is not recommended to use the power input method for lightly damped plates.

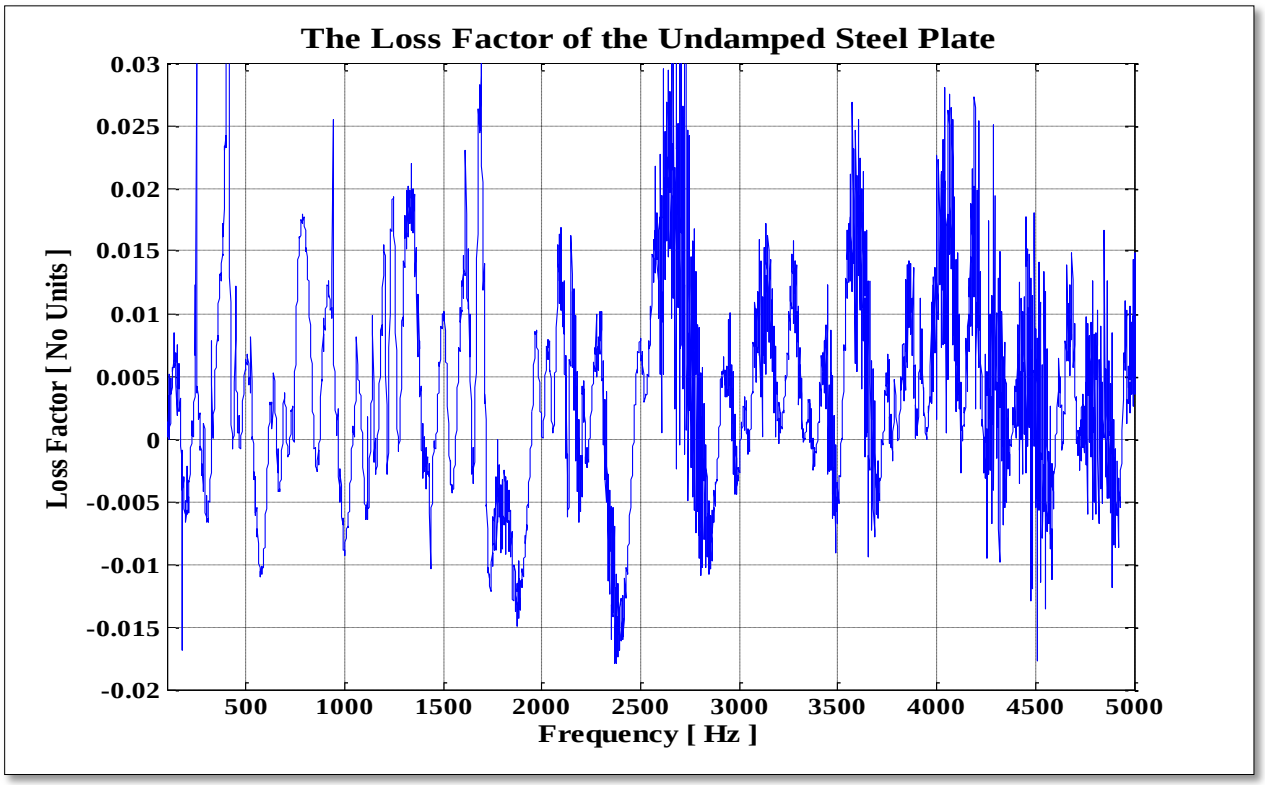

FIGURE 2-8 LOSS FACTOR ESTIMATION BY THE POWER INPUT METHOD FOR THE UNDAMPED STEEL PLATE

2.3.3 EFFECT OF FREQUENCY RESOLUTION ON DAMPING ESTIMATION

The highly damped aluminum plate is used to investigate the effect of frequency resolution. The study is based on the experimental analysis of the model at a 1 Hz resolution. Lower levels of frequency resolution are created through simple decimation. Figure 2-9 shows the loss factors estimated at different individual one-third octave bands for a frequency resolution of 1, 2, 4 and 8 Hz. As it can be seen from the graph for low frequency resolution, the loss factor estimation in the low modal density region (< 300 Hz) fails as the variation is more

than 100% over the loss factors with adequate frequency resolution. For low resolution there will not be adequate information to capture all the modes in a particular band that is centered at these 1/3rd octaves and so the damping cannot be estimated accurately.

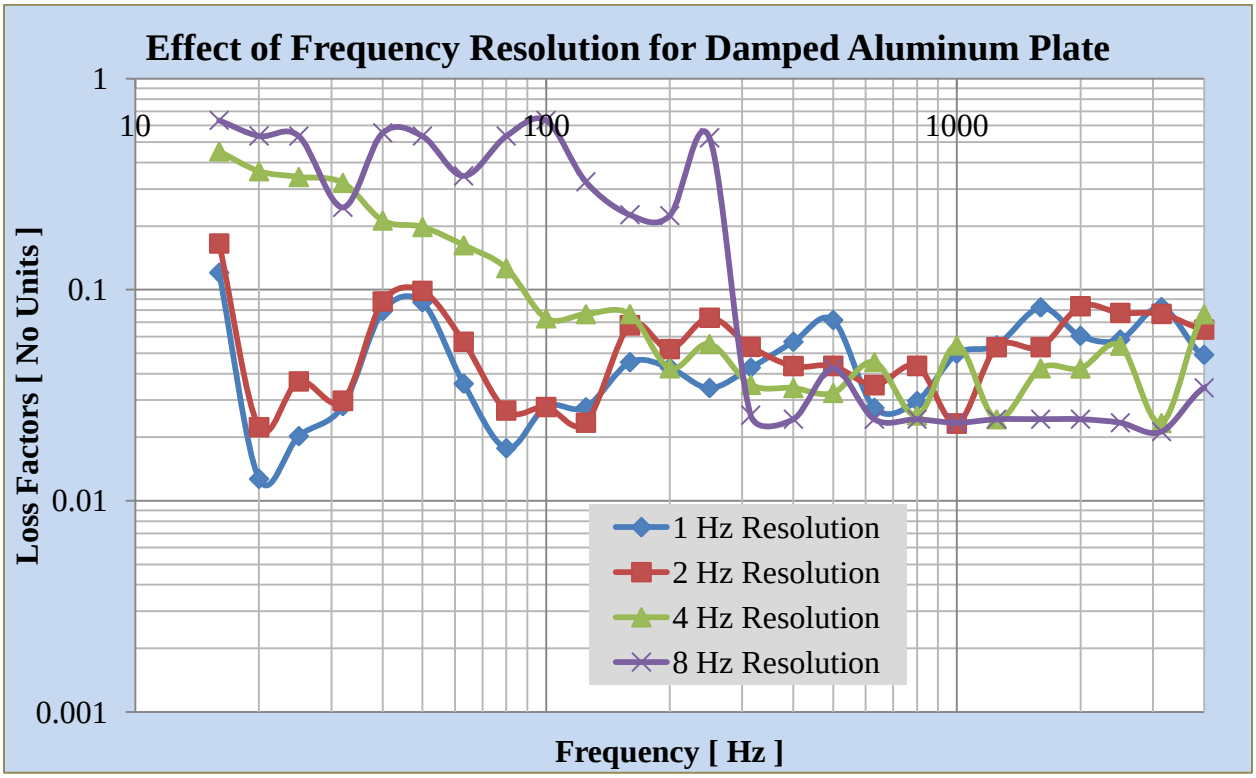

FIGURE 2-9 EFFECT OF FREQUENCY RESOLUTION ON THE ESTIMATED LOSS FACTORS FOR THE ALUMINUM PLATE WITH FULL CONSTRAINED LAYER DAMPING TREATMENT

3 IMPULSE RESPONSE DECAY METHOD

3.1 THEORY OF THE IMPULSE METHOD FOR LOSS FACTORS

The Impulse Response Decay Method (I.R.D.M.) and other decay rate methods are motivated by the realization that damping is proportional to the decay rate in transient response [6]. The system's response amplitude when plotted versus time will have a slope proportional to $e^{(-\pi f \eta t)}$, where f is the frequency, η is the damping loss factor, and t is time. A typical transient response of a SDOF system is shown in Figure 3-1.

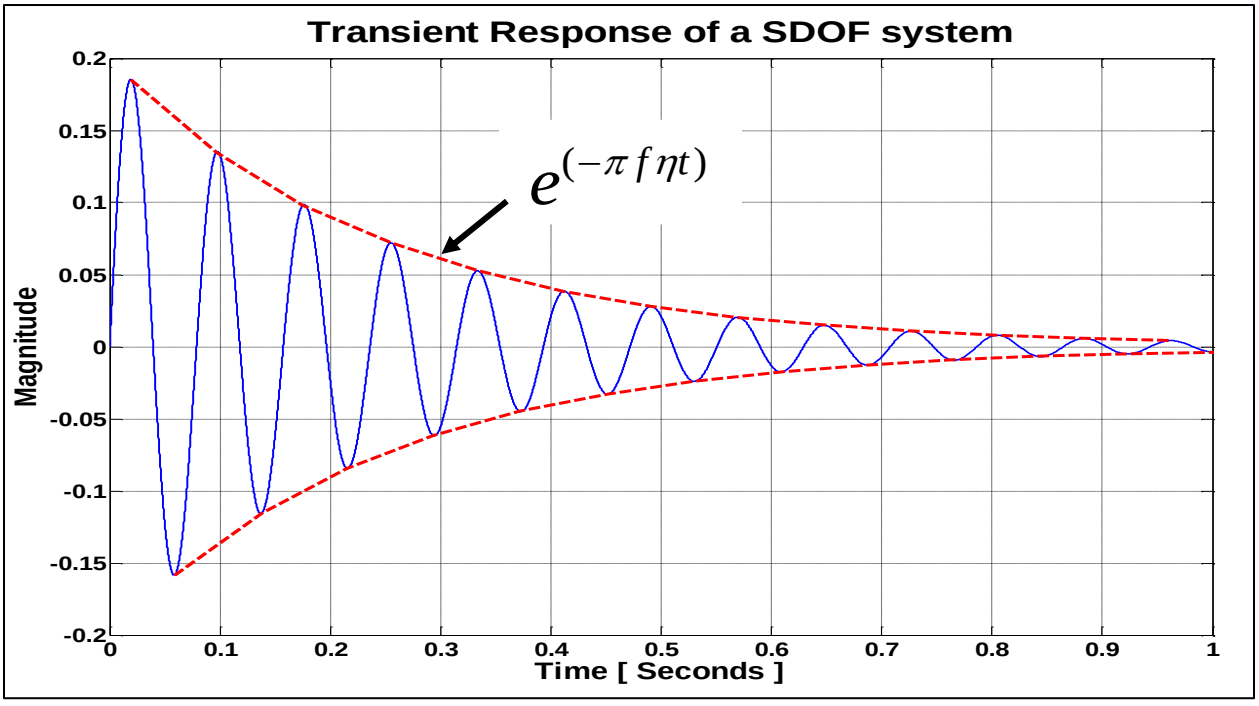

FIGURE 3-1 TRANSIENT RESPONSE OF A SINGLE DEGREE OF FREEDOM SYSTEM

The energy of the system is proportional to the peak amplitude squared; therefore, the system response will decay at a rate equal to $Ge^{(-\pi f \eta t)}$ where G is related to the peak response amplitude of the system. The peak amplitude of the response is shown in Figure 3-2.

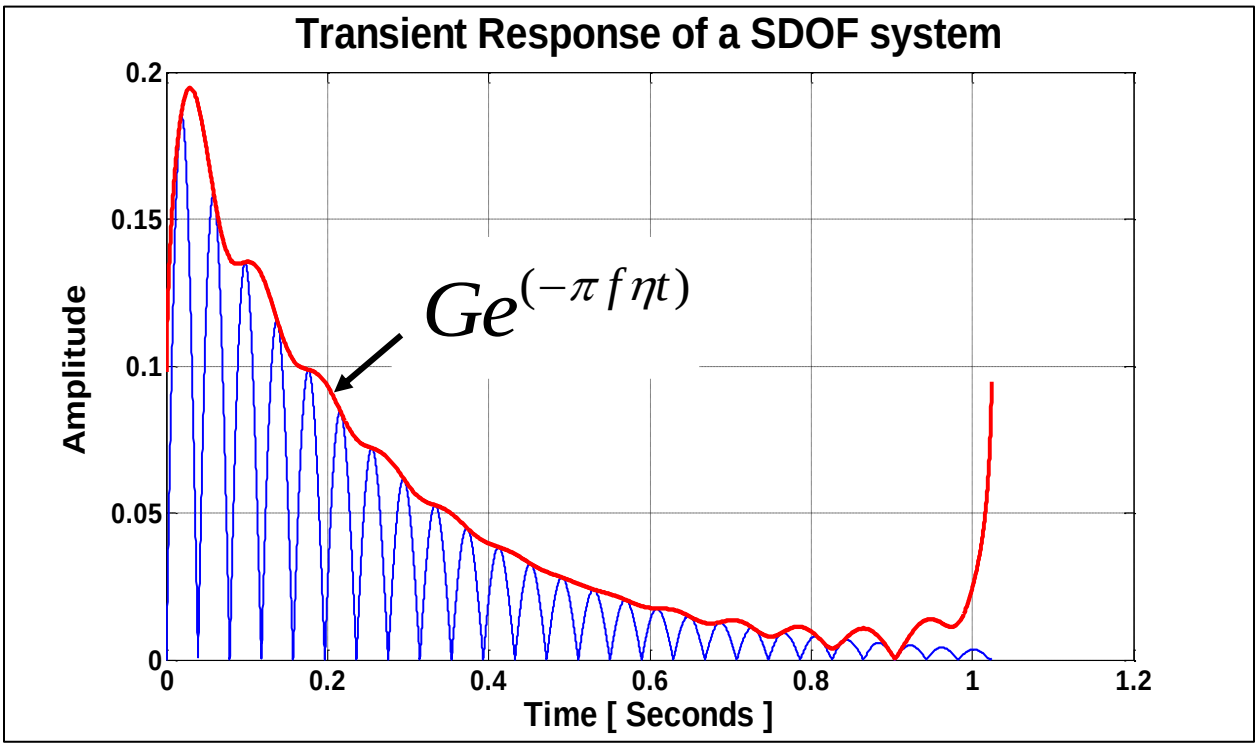

FIGURE 3-2 PEAK AMPLITUDE OF THE TRANSIENT RESPONSE

The loss factor can be found for a single, well-defined modal resonance or as the average loss factor of many modal resonances over the particular frequency range. The initial decay slope is found by plotting the system's response on a logarithmic amplitude scale, with a linear time scale. The plot of the decay rate is shown in Figure 3-3. The loss factor is estimated by the following equation,

$$\eta = \frac{\Delta_t (dB/\sec)}{27.3 f_n}$$

where Δ_t is the decay rate in $dB/\sec$ and f_n is the natural frequency.

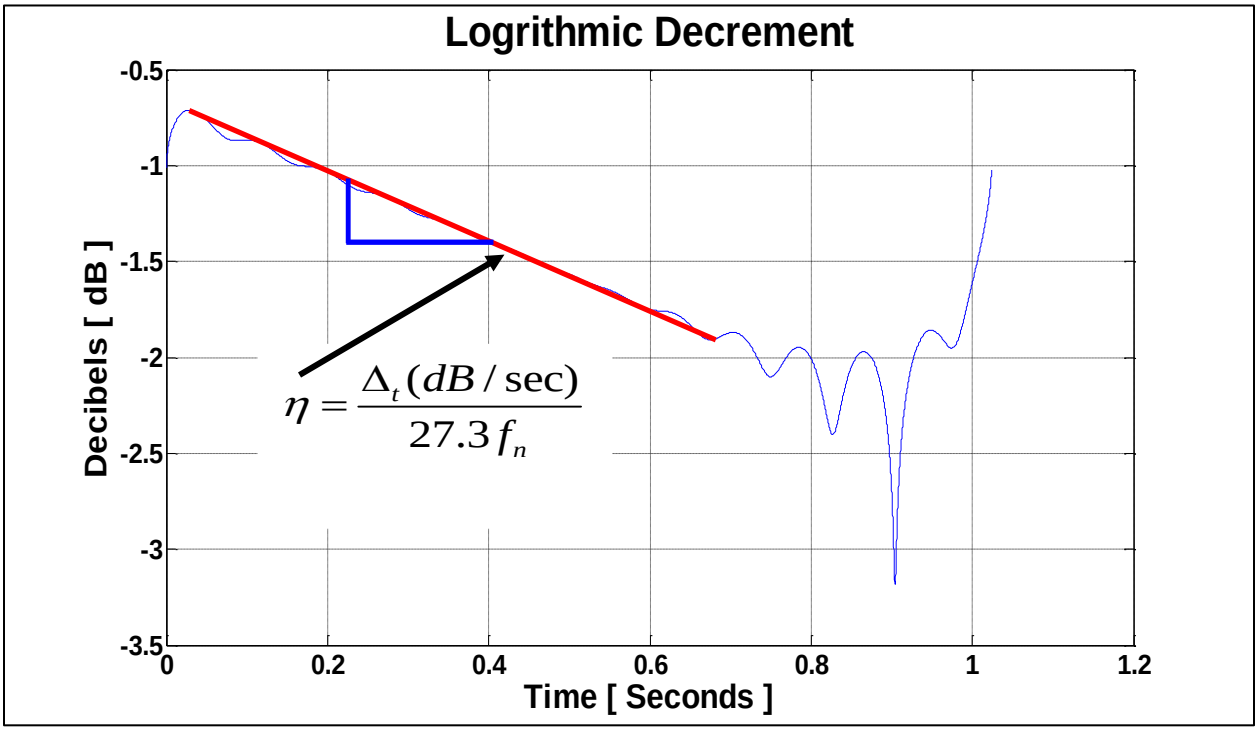

FIGURE 3-3 LOGARITHMIC DECAY OF THE SINGLE DEGREE OF FREEDOM SYSTEM

The I.R.D.M. is similar to the initial decay rate method described above, but utilizes the impulse response of the system instead of the output response. The impulse response can be obtained from an inverse Fourier transform of a system's frequency response function (F.R.F.) or using the maximum length sequence (M.L.S.) method [18]. In the M.L.S. method, the impulse response is obtained by calculating the cross correlation between the M.L.S. input and the system output with a great amount of accuracy and repeatability [19]. The initial decay rates can often be difficult to identify especially since more than one slope will appear in the time domain.

3.2 SINGLE DEGREE OF FREEDOM SYSTEMS

3.2.1 LOSS FACTOR USING THE IMPULSE FUNCTION

The impulse function is a mathematical function which is zero for all time except at a single instant of time. The impulse response function of a underdamped system is given by the Equation (1.25) and re-stated here,

$$h(t) = \frac{1}{\omega_d m} e^{(-\zeta\omega_n t)} \sin(\omega_d t)$$

where ω_n is the natural frequency, ω_d is the damped natural frequency, m is the mass and ζ is the viscous damping co-efficient. The response of a single degree of freedom system with a mass of 0.5 Kg, damping rate of 0.5 Ns/m and a stiffness of 1000 N/m is calculated by the impulse response function. The natural frequency of the system ω_n which is given by $\omega_n = \sqrt{k/m}$ is calculated as 44.7214. The damping coefficient ζ which is given by $\zeta = \frac{c}{2m\omega_n}$ is calculated to be 0.0112. Since the structural damping loss factor η of the system is given as $\eta = 2\zeta$, the input loss factor for the SDOF system is 0.224. The damped natural frequency ω_d of the system given by, $\omega_d = \omega_n\sqrt{1-\zeta^2}$ is calculated to be 44.7186. Note that $\omega_d \approx \omega_n$. A plot of the impulse response function as a function of time is shown in Figure 3-4.

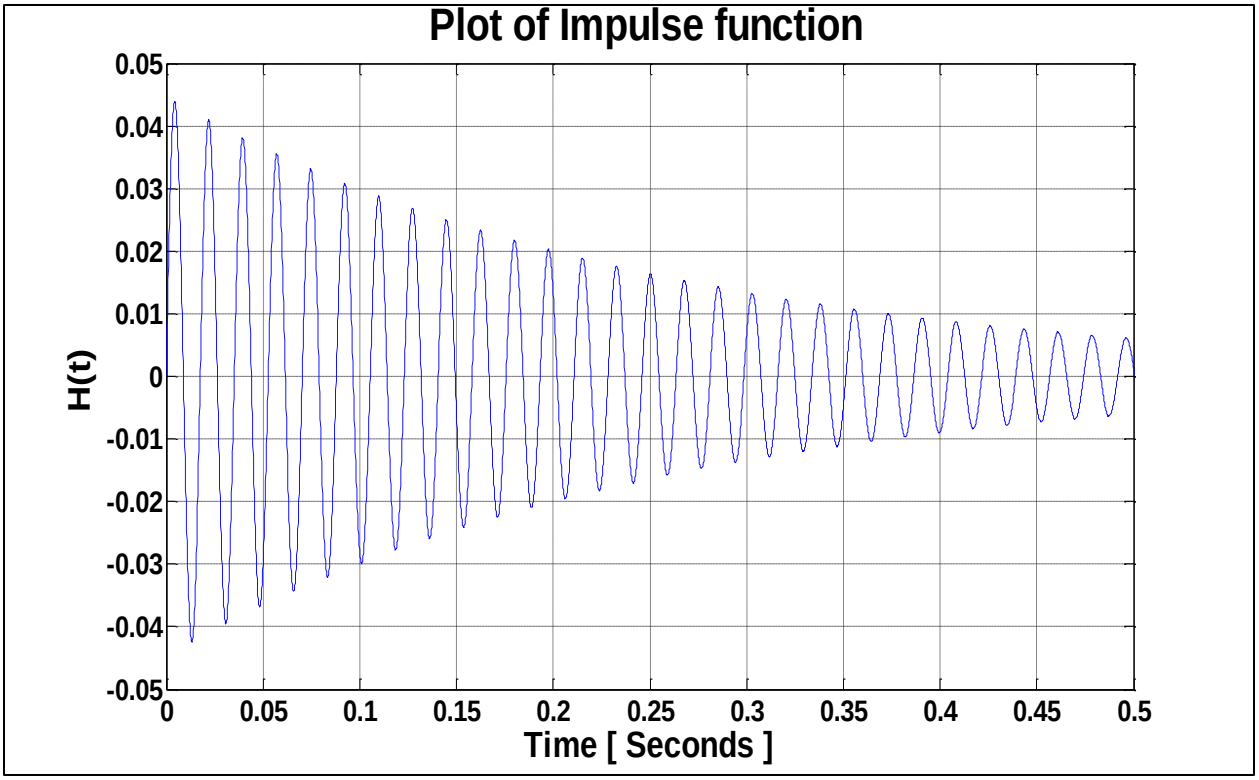

FIGURE 3-4 PLOT OF THE IMPULSE FUNCTION

The response of the single degree of freedom system is defined as the convolution of the Impulse Response Function with the applied force. The response of the system to a unit impulse, the impulse response function is then used in convolution with the applied force to get the response. The convolution integral is given by Equation (1.26) and is re-stated here,

$$x(t) = \int_0^t F(\tau)h(t-\tau)d\tau = \frac{1}{m\omega_d} e^{-\zeta\omega_n t} \int_0^t F(\tau)e^{\zeta\omega_n t} \sin\omega_d(t-\tau)d\tau \qquad (2.15)$$

The Hilbert transform of this response has the real and imaginary components which can be seen in Figure 3-5. Also plotted in Figure 3-5 is the absolute value of the Hilbert transform as a function of time.

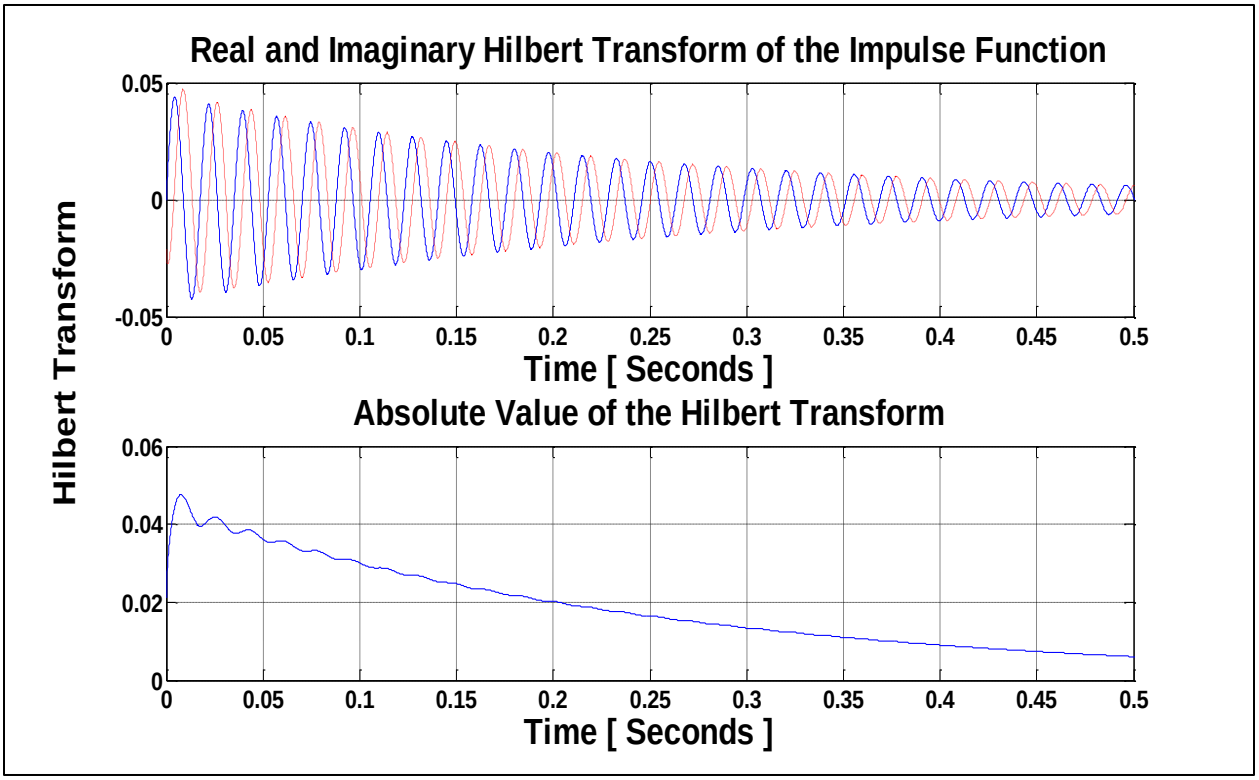

FIGURE 3-5 REAL AND IMAGINARY OF HILBERT TRANSFORM OF THE IMPULSE FUNCTION (TOP) AND THE ABSOLUTE VALUE OF THE HILBERT TRANSFORM (BOTTOM)

The logarithmic decrement of the Hilbert transform of the response denoted by δ represents the response decay of the system. It is used to find the damping loss factor for the damped or undamped systems in time domain. It is the natural logarithm of the amplitudes of any two successive peaks. The logarithmic decrement in the mathematical terms is given by $\delta = \frac{1}{n} \ln \frac{x_0}{x_n}$ where x_0 is the greater of the two amplitudes and x_n is the amplitude of a peak n periods away. The logarithmic decrement of the S.D.O.F. subjected to the unit impulse function is shown in Figure 3-6.

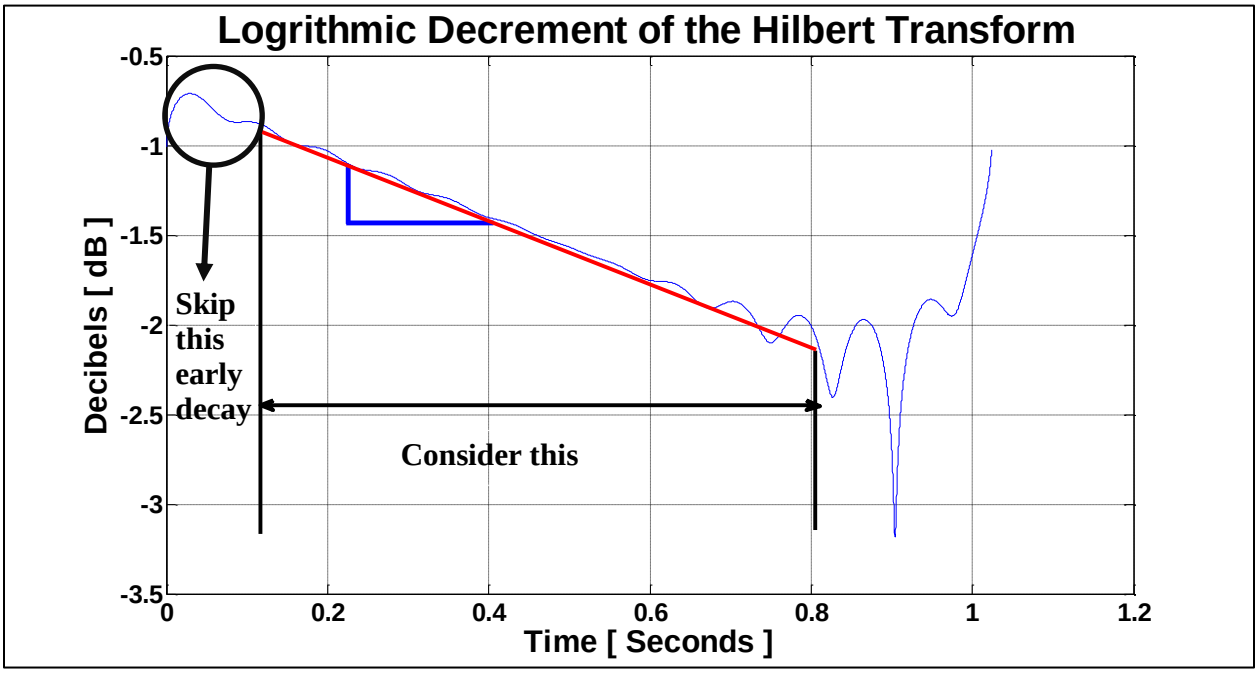

FIGURE 3-6 LOGARITHMIC DECREMENT OF THE HILBERT TRANSFORM

The slope of the logarithmic decrement curve is the loss factor of the system. It was necessary for the user to determine the initial slope of decay signals manually. It becomes apparent that this user input could be a possible source of error for the loss factor calculation. So a study of the effect of skipping different lengths of time from the impulse before starting the slope fit and considering the decay for different lengths of time is done. In this study the '*skip*' and '*consider*' time periods were varied systematically [20]. The loss factors of the system are then plotted as a function of various skip and consider periods and are shown in Figure 3-7. The estimated loss factor is 0.224, except when the initial decay of the response is used for slope determination, in which case there is apparent under prediction of loss factor.

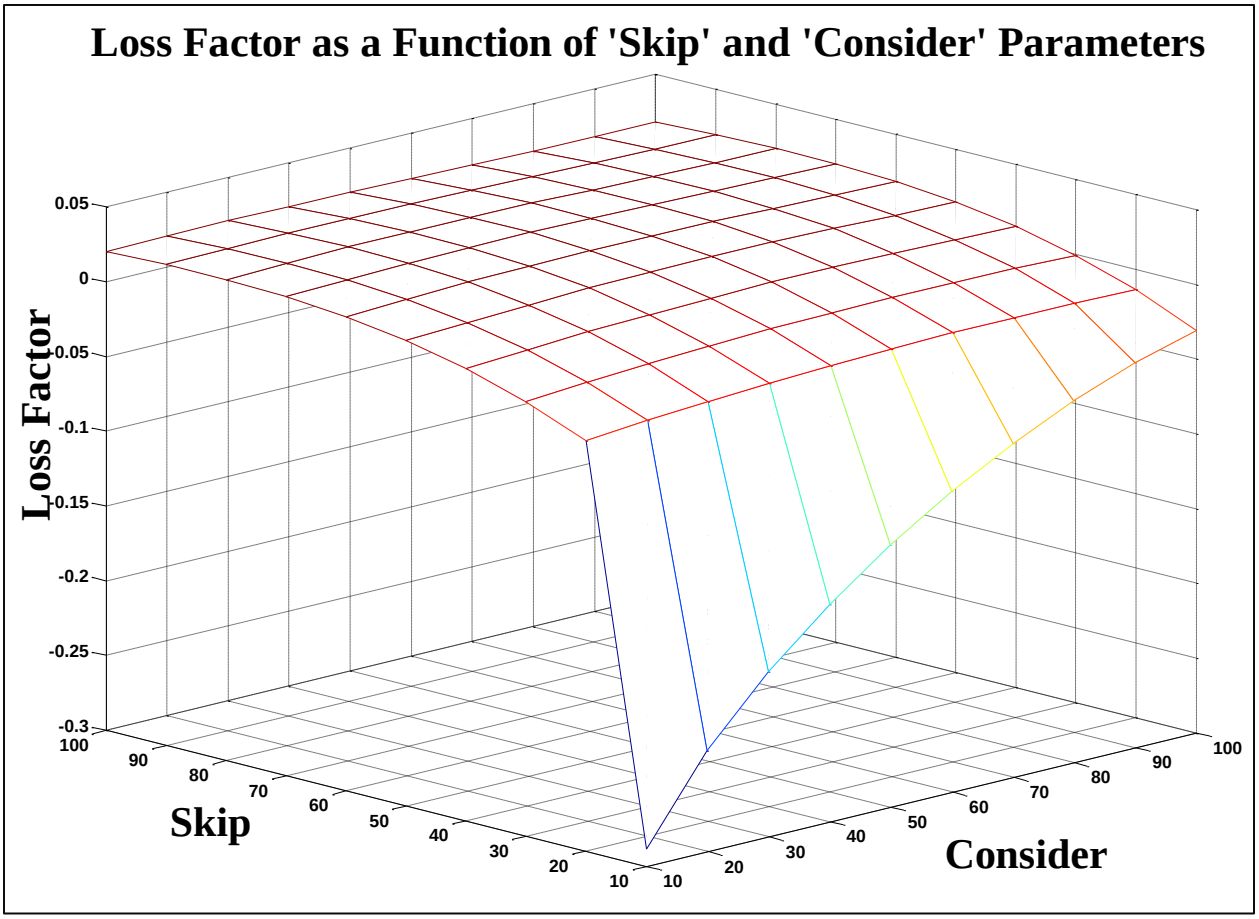

FIGURE 3-7 LOSS FACTOR WITH VARIOUS 'SKIP' AND 'CONSIDER' PARAMETER VALUES FOR A SDOF SYSTEM WITH A TRUE IMPULSE EXCITATION

3.2.2 LOSS FACTOR USING A SINUSOIDAL IMPULSE FORCE

The impulse function which causes a S.D.O.F. system to have the impulse response discussed in the previous section, if viewed from a purely mathematical standpoint, is not strictly a function, because no real function is equal to zero everywhere but a single point. So a real unit impulse function cannot be observed in a real world situation. The I.R.D.M. is then validated for a S.D.O.F. system by simulating the impulse with a half sine pulse of short duration. The single degree of freedom system has a mass of $0.5\,Kg$, damping rate of 0.5 Ns/m and a stiffness of

1000 N/m. The natural frequency of the system ω_n which is given by $\omega_n = \sqrt{k/m}$ is calculated as 44.7214. The damping coefficient ζ which is given by $\zeta = \dfrac{c}{2m\omega_n}$ is calculated to be 0.0112. Since the structural damping loss factor η of the system is given as $\eta = 2\zeta$, the input loss factor for the SDOF system is 0.224.

The response of the single degree of freedom system is given by the convolution integral which is given by Equation (1.26) and restated here

$$x(t) = \int_0^t F(\tau)h(t-\tau)d\tau = \frac{1}{m\omega_d} e^{-\zeta\omega_n t} \int_0^t F(\tau) e^{\zeta\omega_n t} \sin\omega_d (t-\tau) d\tau$$

The half sine impulse and the calculated response are shown in Figure 3-8.

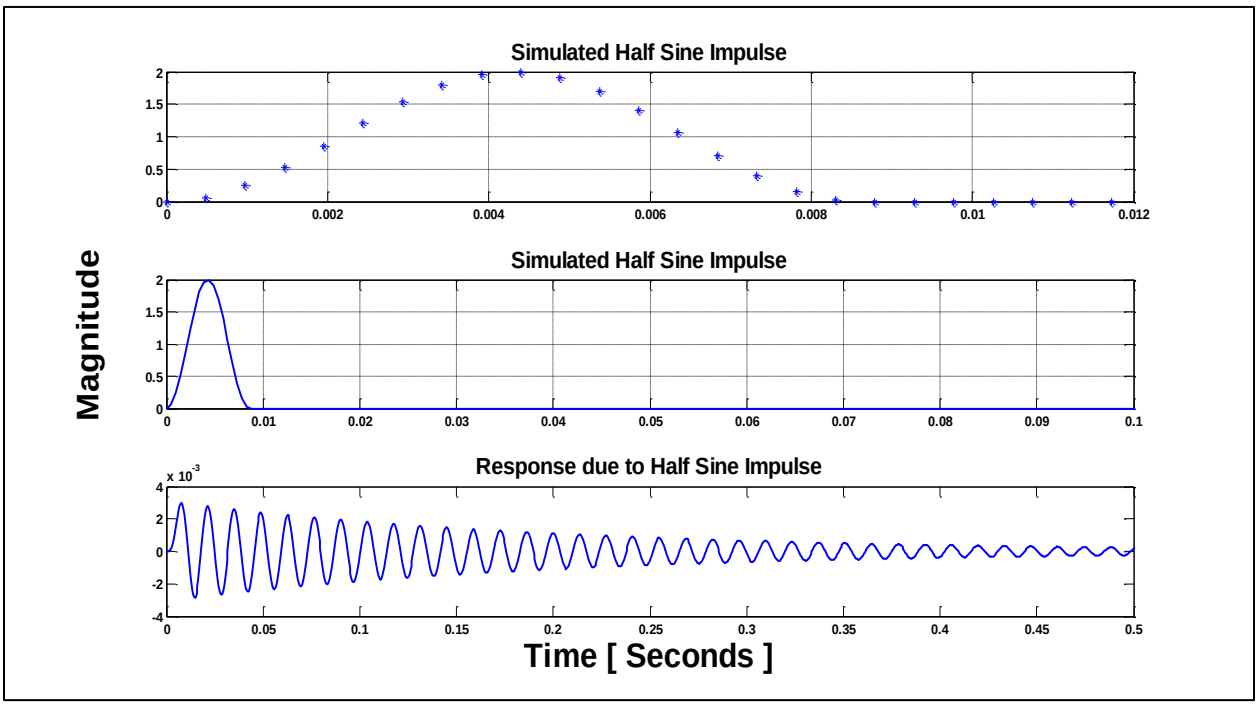

FIGURE 3-8 SIMULATED IMPULSE AND THE RESPONSE BY THE CONVOLUTION INTEGRAL

The force and the response of the system are converted from time domain to frequency domain to determine the frequency response function by the Fourier transform. The frequency response function is the complex ratio of output displacement to the input force, $\frac{X}{F}$ and is called receptance as discussed in Chapter 1. This frequency domain function is then converted into the time domain by employing the inverse Fourier transform. The impulse response function is used in convolution with the half sine force. The natural logarithm of the Hilbert transform of the response gives the logarithmic decrement and the slopes of the logarithmic decrement is calculated by the same skip and consider method as described in the earlier section. The Fourier transform of the force and response and of the impulse function is shown in Figure 3-9.

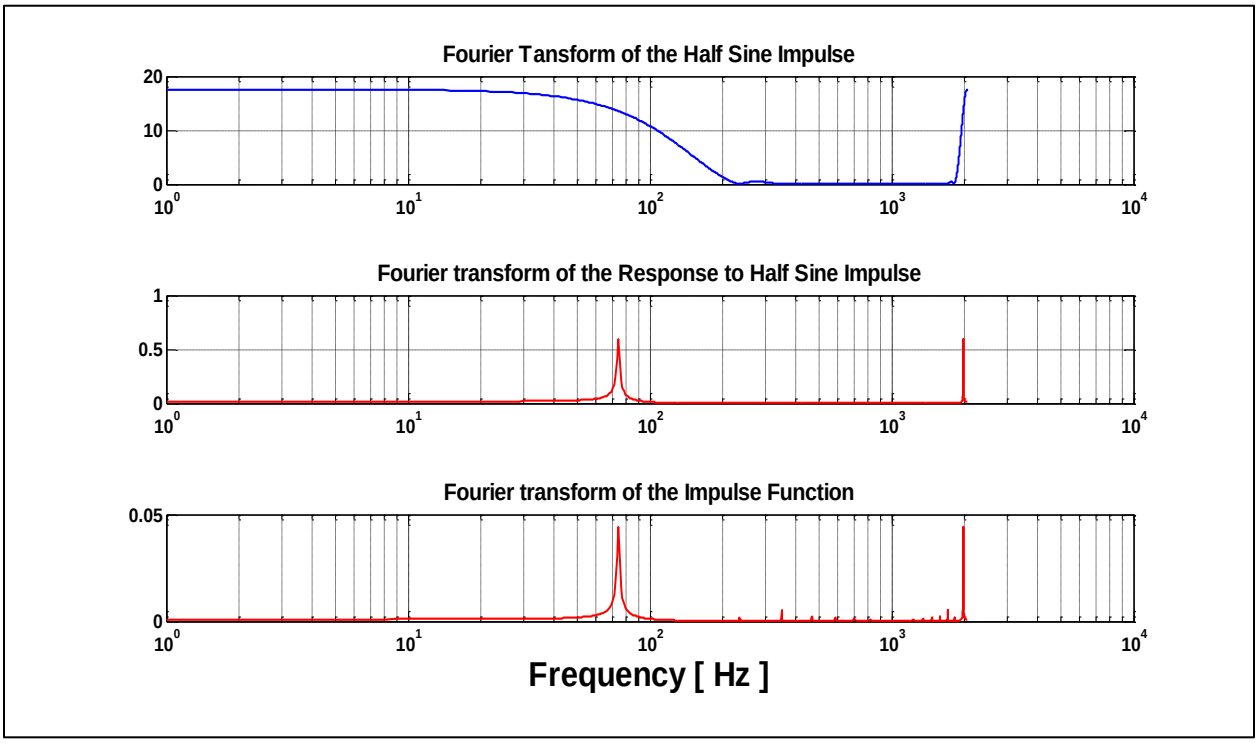

FIGURE 3-9 FOURIER TRANSFORM OF THE FORCE, RESPONSE AND THE IMPULSE FUNCTION

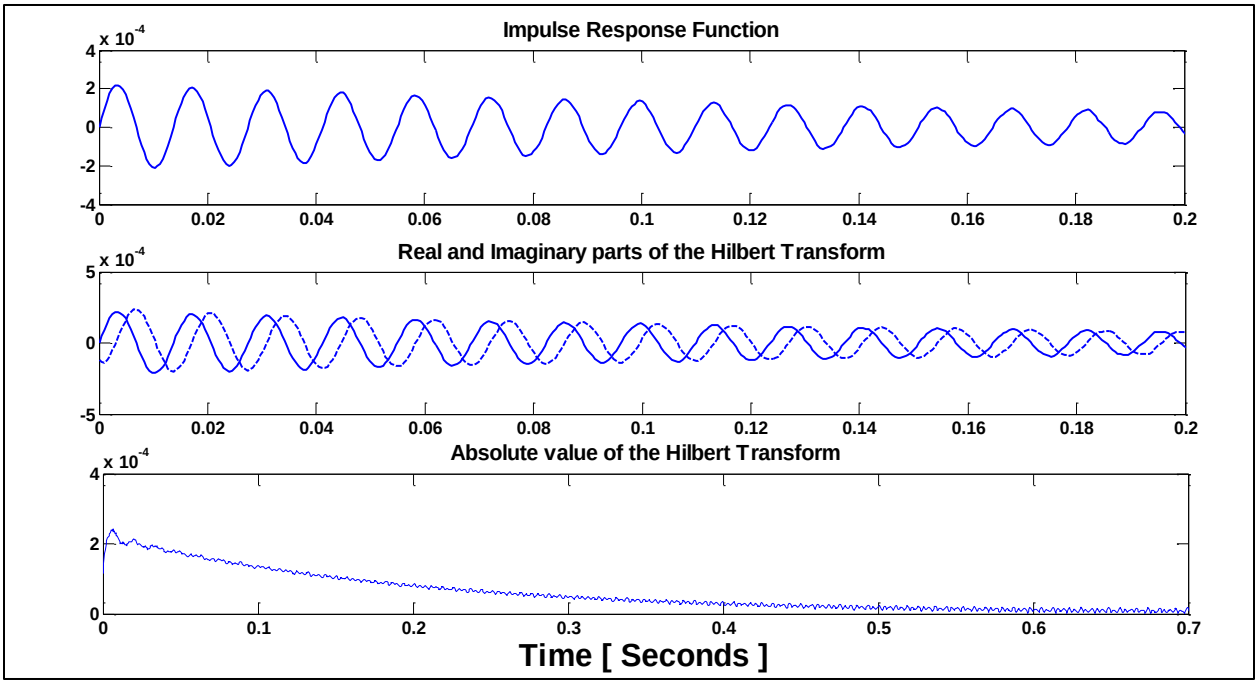

FIGURE 3-10 IMPULSE RESPONSE FUNCTION AND THE HILBERT TRANSFORM

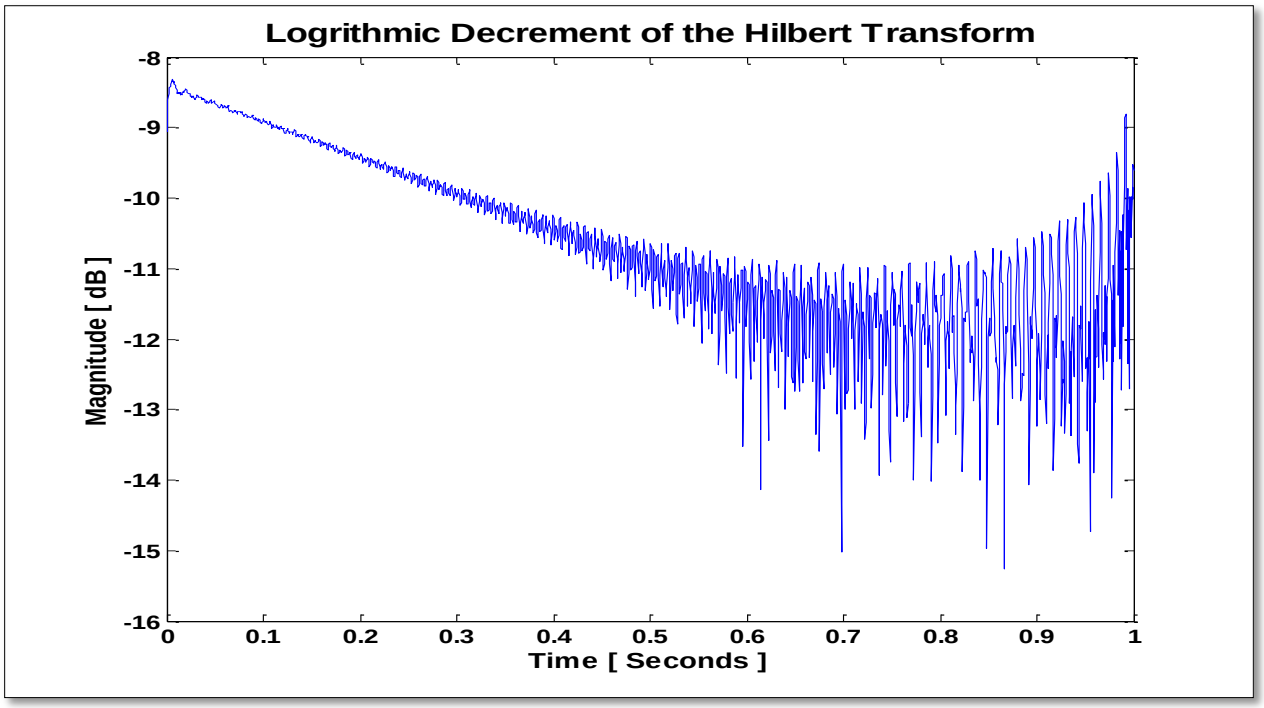

FIGURE 3-11 LOGARITHMIC DECREMENT OF THE HILBERT TRANSFORM OF THE RESPONSE OF A SDOF SYSTEM WITH A SINUSOIDAL EXCITATION

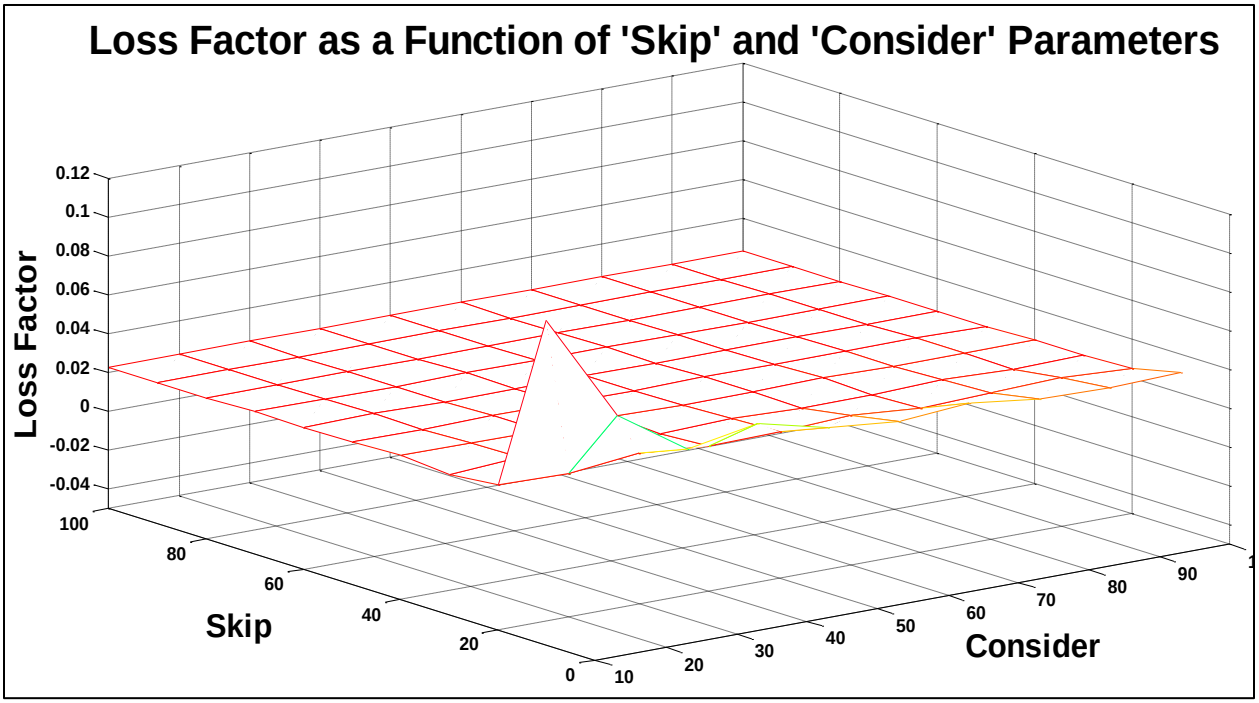

FIGURE 3-12 LOSS FACTORS WITH VARIOUS 'SKIP' AND 'CONSIDER' PARAMETERS FOR A SDOF SYSTEM WITH A SINUSOIDAL EXCITATION

The impulse response function and the real, imaginary, and absolute value of the Hilbert transform are then plotted and are shown in Figure 3-10. Figure 3-11 shows the logarithmic decrement, in decibels, of the response decay of the S.D.O.F. system which is excited with a half sine impulse and the subsequent loss factors estimated are shown in Figure 3-12. The estimated loss factor is 0.224 which is equal to the input loss factor, except when the initial decay is taken into consideration.

From the analytical studies of estimation of loss factors by the I.R.D.M. applied to the single degree of freedom systems excited with a half sine impulse it can be concluded that the estimation of loss factors is quite accurate with a variation of less than 1% for the single degree of freedom systems. In subsequent sections, the analytical and experimental validation of the impulse response decay method for multiple degree of freedom systems is discussed.

3.3 PLATES – ANALYTICAL AND EXPERIMENTAL IRDM

3.3.1 ANALYTICAL ESTIMATION- NASTRAN MODEL

The thin plate (of in-plane dimensions, $a \cdot b$) has an aspect ratio of 1.5 (a/b), a thickness ratio of 385 (b/t) and a specific stiffness (E/ρ) of $2.59*10^7\ N.m/Kg$. The damping loss factor, η, is assigned values from 0.001[0.1%] to 0.01[1%] and 0.1[10%]. The plate is considered to be free of external supports and is loaded by a concentrated mechanical force.

Although an analytical model is undoubtedly available, a computational model has been developed using MSC/NASTRAN Version 2008. There are a total of 14065 Nodes and 13824 elements are used to represent the whole model. QUAD4 elements (of dimensions, $A \cdot B$) with a quadrilateral element fineness of approximately 80 (b/B or a/A) have been used to create a regular, rectangular mesh. As such, the spatial Nyquist frequency—at which modal half-wavelengths approaches the element width (A or B)—is estimated at approximately 10 kHz. The mechanical loads are applied in the center of one quadrant of the plate to a single node, modeling physical loading via the bottom surface of a small force gage. Responses to excitation at the single forcing point were computed at approximately the 17 points indicated in Figure 3-13, below, wherein each square region represents 100 elements. 4 different excitation points are used for the study and for each excitation point the responses are computed at the above mentioned 17 points. The four excitation points are shown as red dots in Figure 3-13. The input points are named as Point 1, Point 2, Point 3 and Point 4 named clockwise from the top left and are shown in Figure 3-13.

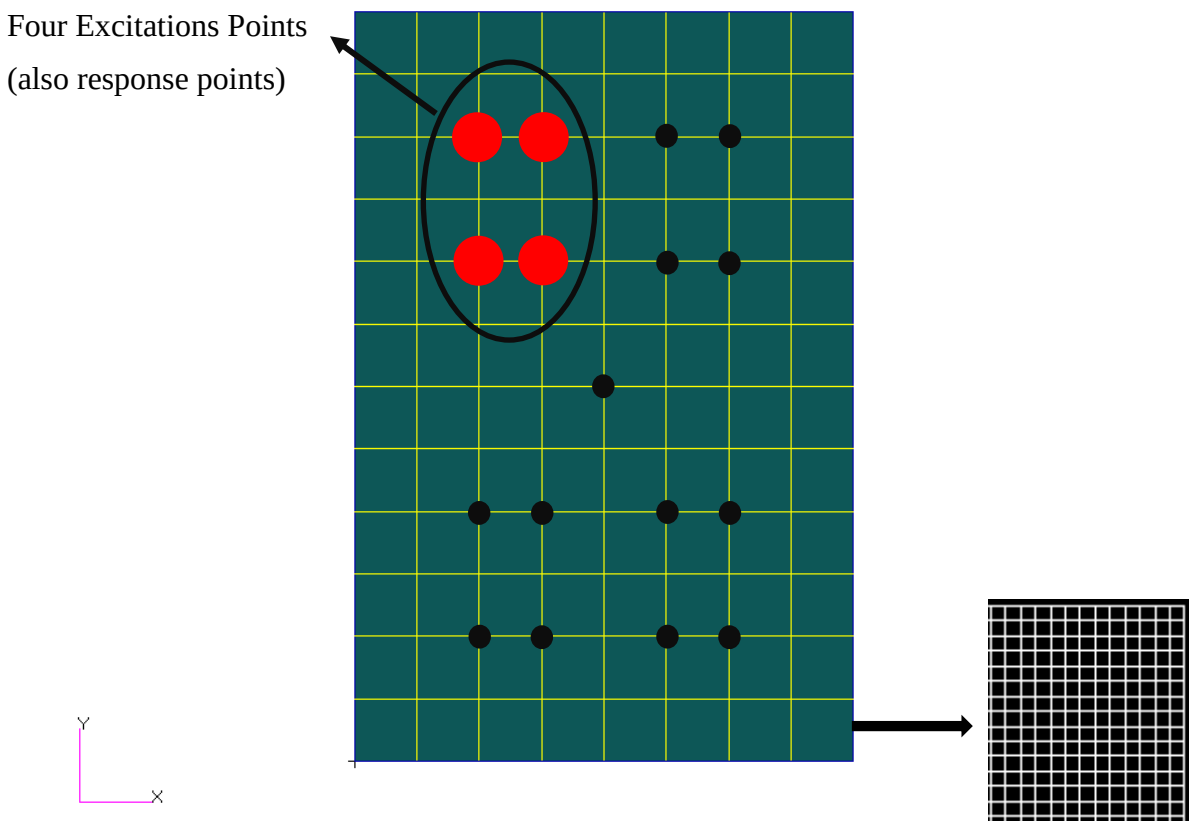

FIGURE 3-13 COMPUTATIONAL MODEL WITH REGULAR PATTERN OF EXCITATION AND RESPONSE POINTS

For the computational studies, the best frequency resolution for a frequency response function (F.R.F.) attempted is 1 Hz over a 10 kHz frequency range. This F.R.F.s are inverted using the inverse Fourier transform, resulting in the analogous impulse response functions (I.R.F.s). Based on the frequency resolution, Δf = 1 Hz, and the number of "lines" in the F.R.F., N = 10,000, the length of the IRF is 1/ Δf = 1 second. Since there were "N" lines in the F.R.F., the number of response points in the IRF is 2N = 20,000, which corresponds to a temporal

resolution of 1/20,000 = 50 microseconds. As such, the temporal resolution in the computational studies allows resolution of responses up to 10 kHz, but only good responses up to about 4 kHz.

For experimental studies, the sampling frequency is 64.4 kHz, which provides a temporal resolution of 15.52 microseconds. The expectation, then, is that vibration frequencies may be resolved poorly to 32.2 kHz, but rather well to 13 kHz.

The damping loss factor, whether for a structural element or an entire structure, is known to have frequency dependence. This frequency-dependence is partly due to frequency-dependent material properties of the constituent materials and partly due to the distribution of material strain as a function of frequency [16]. Assigning a single damping loss factor for a structure requires specifying some sort of process to account for the spatially-variable response, mobility or accelerance upon which the damping loss factor is based. Analytically, an integrated response can be used, allowing the prediction of a frequency- and spatially-dependent loss factor to be expressed. Experimentally, of course, only a finite number of points is available, which suggests averaging the response from multiple points. Some researchers have shown that responses from a small number of randomly-selected points seem to show convergence to a common value [23]. In this study convergence is studied with regard to the number of and location of response measurements.

The impulse response decay method is based on the estimation of the decay rate in a spring-mass-damper system. But, for a real structure, there are many modes of vibration excited by an impulse (or any other type of excitation). A popular means of estimating damping loss factor uses band-limited segments of the F.R.F., which, when inverted in the Fourier sense, yield a decaying response with arbitrarily narrow frequency content. The assumption is that the decay observed in these frequency bands tends to represent the frequency-dependent damping loss

factor. In this study the center frequencies f_c for the analysis bands are standard one-third octave frequencies (i.e., 630, 800, 1000, 1250, 1600, 2000 etc.). However, the bandwidth of each band, or "bin", is a full octave. The frequency-dependent damping loss factor is then estimated to be [6]:

$$\eta(f_c) = \frac{\Delta_t}{27.3 f_c}$$

where f_c the band center frequency and Δ_t is the (assumed constant) decay rate in dB/sec. Figure 3-14 is the accelerance FRF for a selected point (Point 1) of the computational model based on a frequency resolution of 10 Hz (Δf) over a frequency range of 10 kHz. Note that this corresponds to a temporal resolution of 50 microseconds. Also shown is the narrow band response, found by frequency domain filtering of the full octave bandwidths at 1250 Hz.

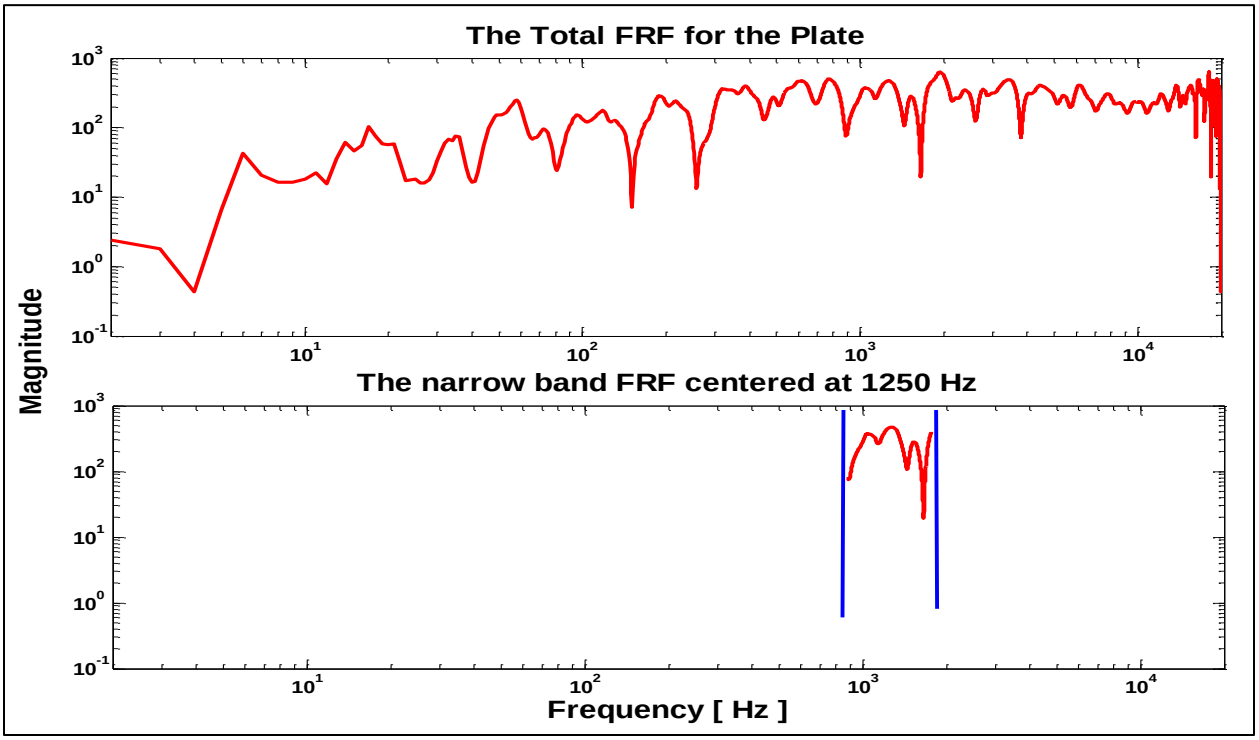

FIGURE 3-14 ACCELERANCE FRF FOR THE THIN PLATE, FOR THE FULL SPECTRUM (TOP) AND IN THE OCTAVE BAND CENTERED AT 1250 HZ (BELOW)

The inverse fourier transform of the full octave, band-limited F.R.F. at each of the one-third octave frequencies is first computed. The value of the loss factor η is then estimated from the slope of the envelope of the decay signatures. Figure 3-15 is a composite of average acceleration free decay signatures for a set of 16 regularly-spaced response points. From these average decay signatures, the frequency-dependent loss factors were estimated. The estimated loss factors for the responses of the computational model with an input loss factor of 0.01 are shown in Figure 3-16. The loss factors estimated for the four different excitation points are plotted. It is evident that the I.R.D.M. is fairly accurate with an acceptable variation of 10% for estimating this relatively moderate loss factors. The location of the excitation point has some induced errors as one location point may excite greater number of modes than the other.

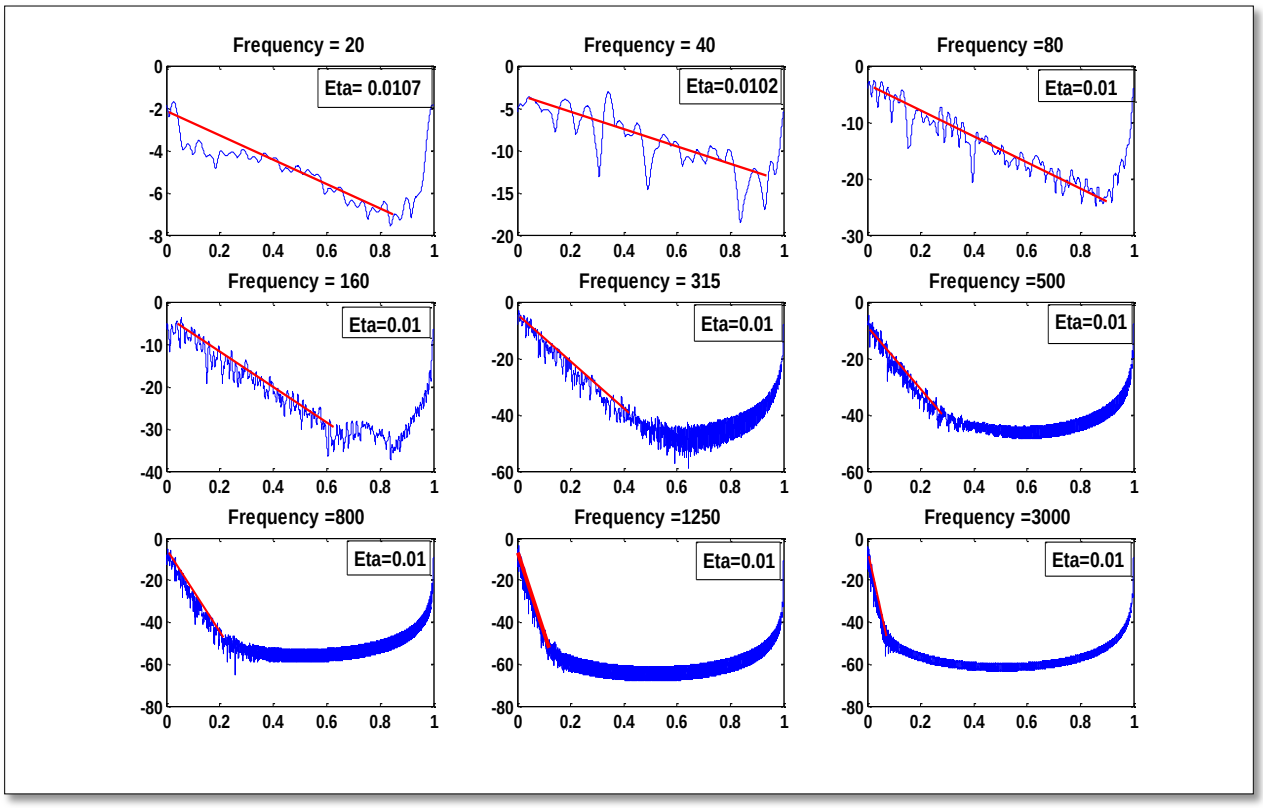

FIGURE 3-15 AVERAGED DECAY SIGNATURES FOR A RANGE OF FULL OCTAVE BANDS, WITH THE LINEAR ESTIMATE OF SLOPE AND THE RESULTING LOSS FACTOR SHOWN FOR INPUT LF OF 0.01

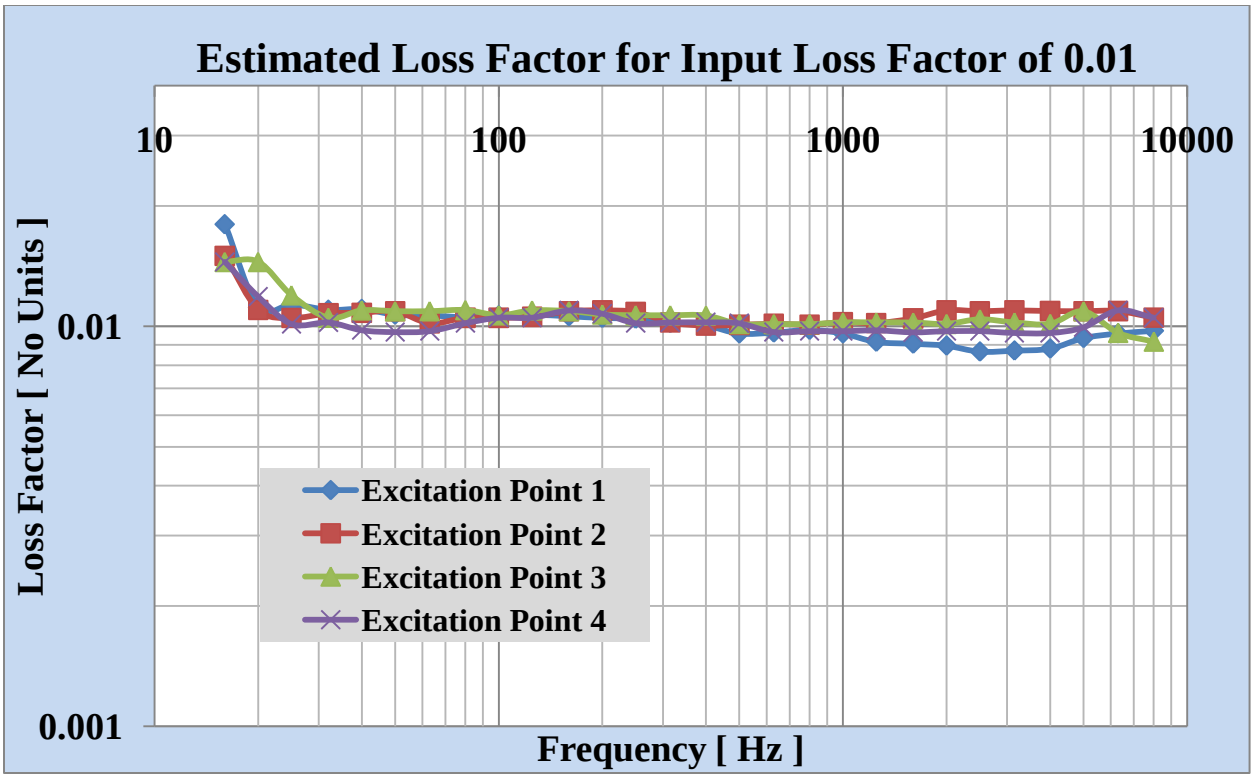

FIGURE 3-16 ESTIMATED LOSS FACTOR FOR A INPUT LOSS FACTOR OF 0.01 [1 %]

For a very low input loss factor of 0.001[0.1%] the estimated loss factors by the I.R.D.M. is shown in Figure 3-17. The loss factors for the four different excitation points are estimated. It can be seen that in the low frequency range (< 200 Hz) the estimated loss factors are not accurate However in the 200 Hz – 8000 Hz frequency range the estimated loss factors are accurate within 2% of the input loss factor. As mentioned earlier some error is introduced as a result of the location of the excitation point. Within few limitations in the low frequency zone for systems that are lightly damped the impulse response decay method yields consistent results (98% accurate) and it is shown to be better than the power input method (P.I.M.). Also it is suggested that averaging more input-output pairs is an added advantage for increasing the accuracy of measured loss factors when using the I.R.D.M. for lightly damped structures.

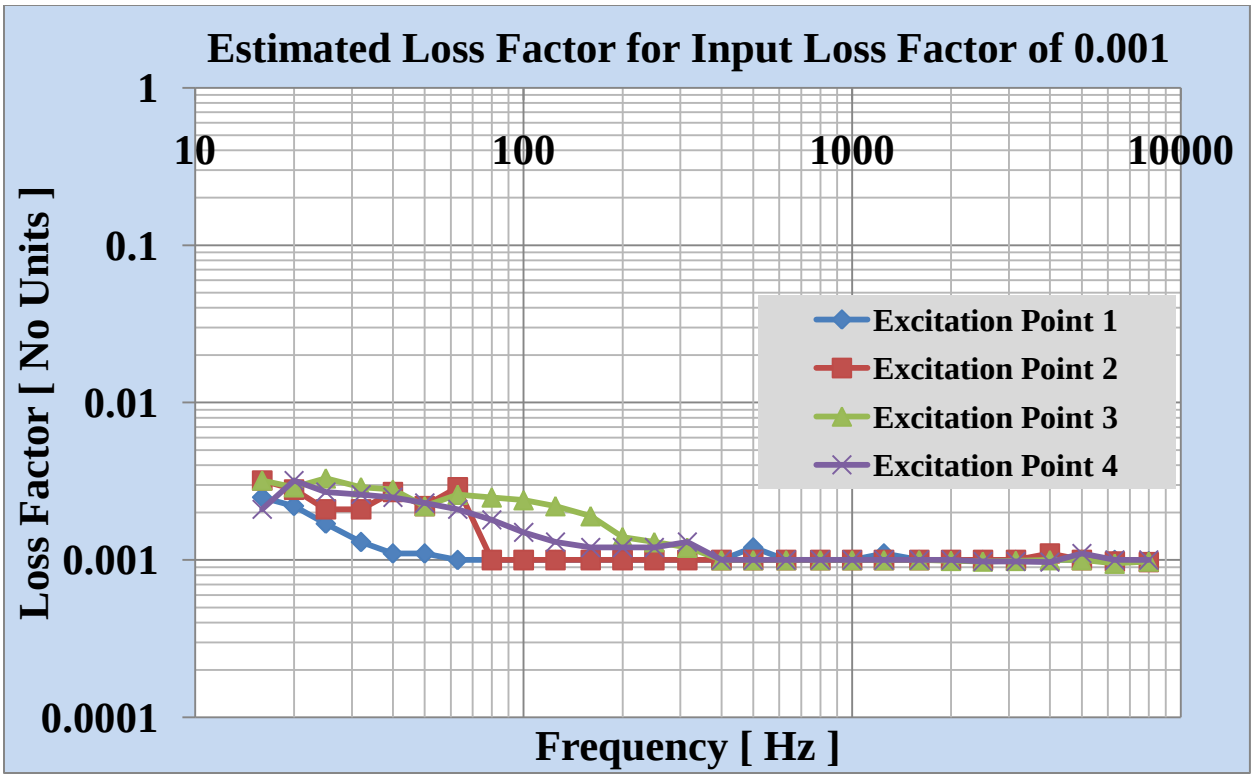

FIGURE 3-17 ESTIMATED LOSS FACTOR FOR A INPUT LOSS FACTOR OF 0.001 [0.1 %]

Figure 3-18 shows the estimated loss factors of the panel for a very high input damping level of 10 %. The loss factors from the four different excitation points are plotted showing some variation (approximately 10% mean variation) based on the location of the excitation point. The loss factors are under estimated at frequencies above 1000 Hz. Some of the response points are in the direct field of vibration, where the response is significantly higher than the other response points which results in under prediction of loss factors.

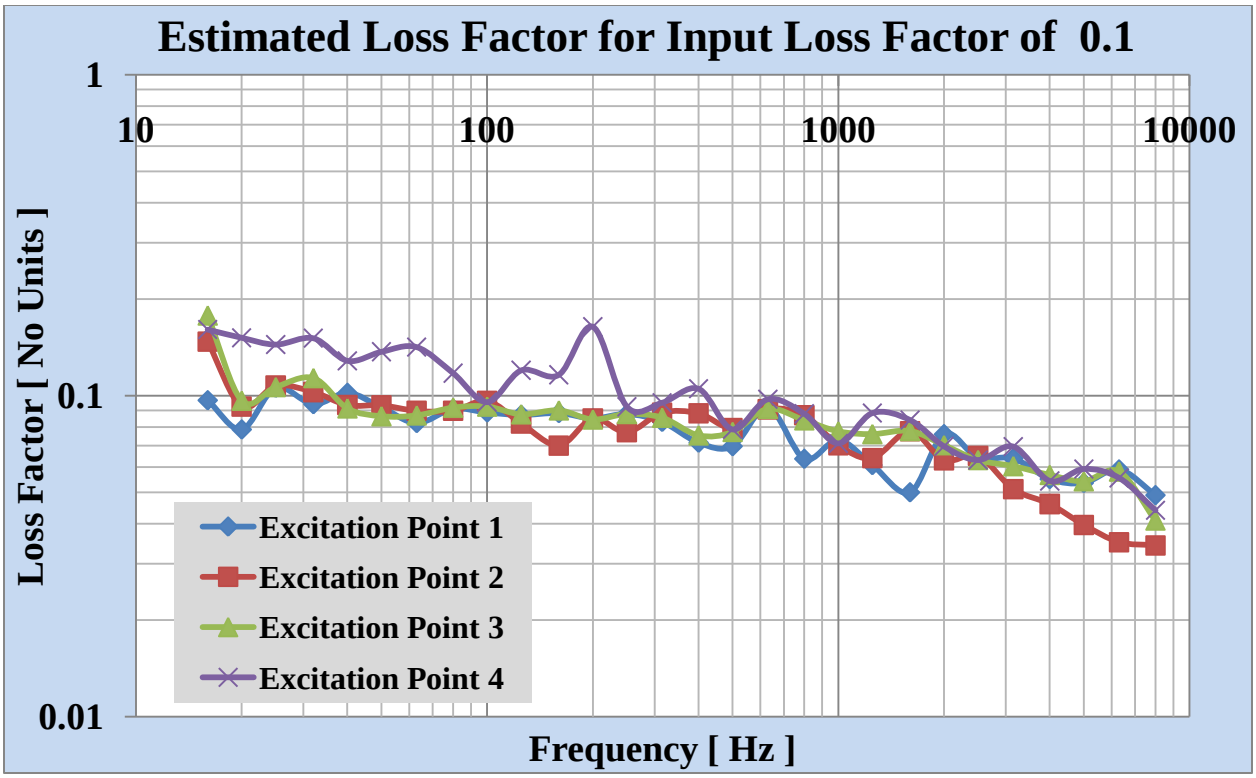

FIGURE 3-18 ESTIMATED LOSS FACTOR FOR A INPUT LOSS FACTOR OF 0.1 [10 %]

3.3.2 EXPERIMENTAL RESULTS

3.3.2.1 ALUMINUM PLATE WITH CONSTRAINED LAYER DAMPING

The analytical estimation of the loss factors uses the accelerance frequency response functions; however the mobility functions can also be used to estimate the loss factors. Using a scanning laser vibrometer the mobility functions for the aluminum plate with constrained layer damping treatment were measured. The mobility response functions are measured at 225 response points and the plate is excited at 4 different locations across the plate. In the computations 8 response points, (two response points randomly chosen from each quarter) are used, so well averaged loss factor measurements are achieved. Figure 3-19 shows the estimated

loss factors for the plate. As discussed in previous sections, since the plate is rather highly damped (approx. 0.1), the estimated loss factors should be fairly accurate, well within 10% mean variation, except at lower frequencies where the variation is greater than 10%. Clearly there is an apparent under-prediction above 2000 Hz. The variation introduced by the location of the excitation point is also seen.

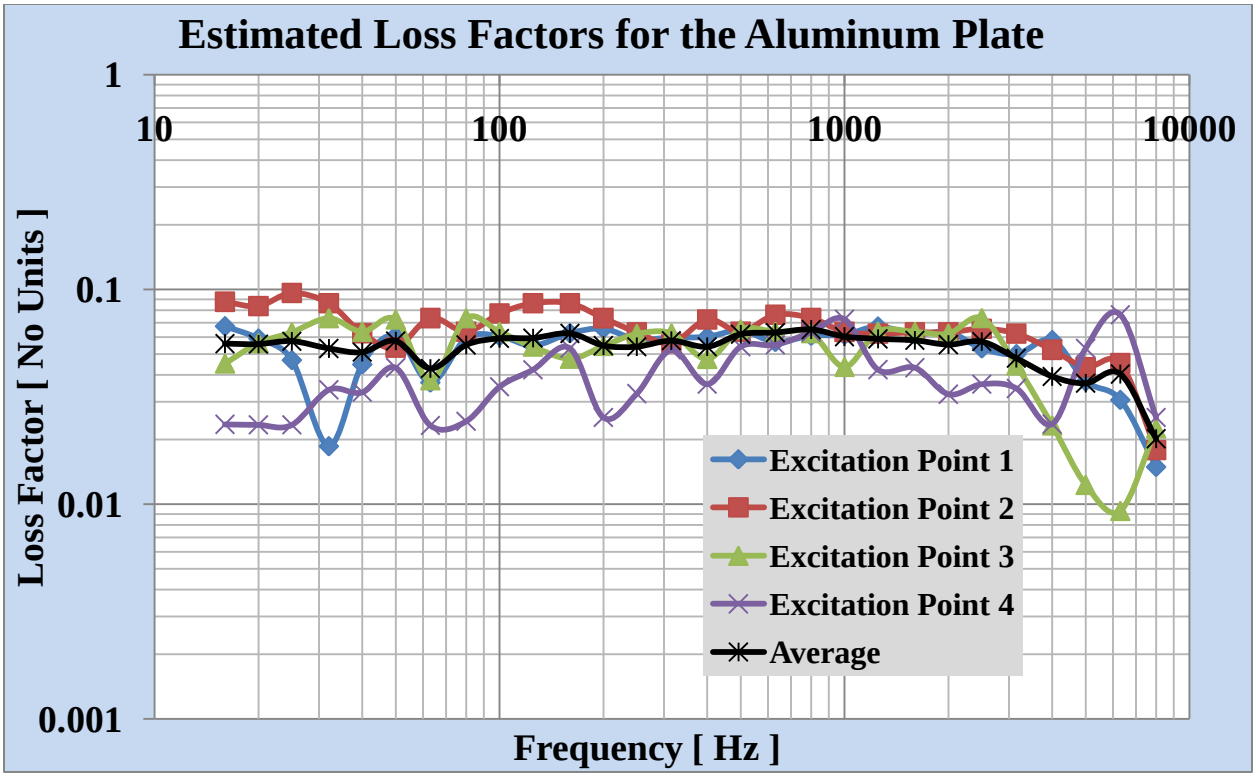

FIGURE 3-19 LOSS FACTORS OF DAMPED ALUMINUM PLATE BY THE IMPULSE RESPONSE DECAY METHOD

3.3.2.2 UNDAMPED STEEL PLATE

The mobility data for the undamped steel plate is collected at 187 response points for each of the 4 excitation points. Figure 3-20 shows the loss factors estimated for four different excitation points and the averaged loss factors. The loss factors estimated by the power input method show that the plate has an inherent damping of about 1%. The experimental impulse response decay method provides fairly consistent estimates for different excitation points, well

within 10%variation for this plate with some variance introduced in the estimations based on the location of different excitation points.

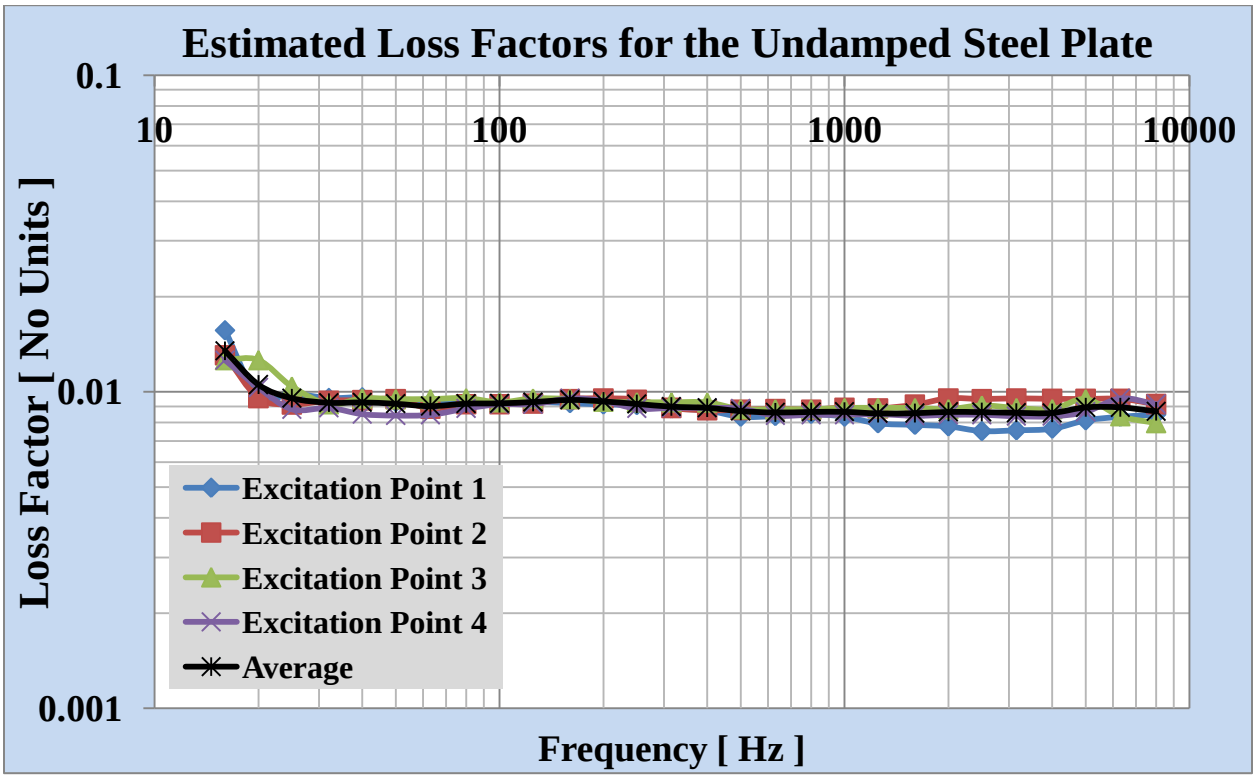

FIGURE 3-20 ESTIMATED LOSS FACTORS OF THE UNDAMPED STEEL PLATE

3.3.2.3 OBSERVATIONS

The comparison between the estimated loss factors for the aluminum plate with full constrained layer damping is shown in Figure 3-21. The loss factors estimated by the I.R.D.M. technique are expected to be accurate based on the computational studies and as expected the variation is well within 10%. The loss factors estimated with the P.I.M. technique show a large variation, greater than 50%, and the cyclic behavior of the results are observed. This plate being highly damped the P.I.M. estimate is reasonably accurate well within 10% at higher frequencies and it can be seen that in the 500 Hz – 4000 Hz frequency range the estimated loss factors with both the techniques are fairly close (less than 10% error).

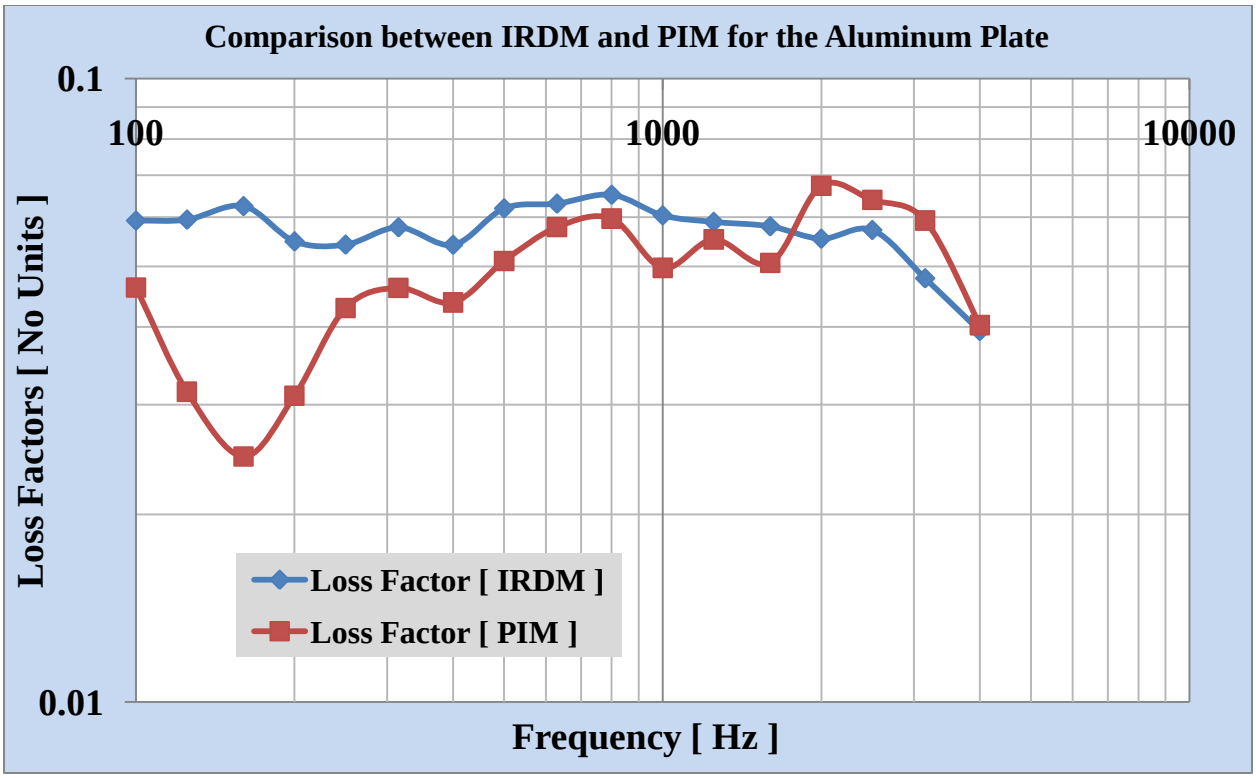

FIGURE 3-21 COMPARISON OF THE EXPERIMENTAL IRDM AND EXPERIMENTAL PIM FOR THE ALUMINUM PLATE WITH FULL COVERAGE CONSTRAINED LAYER DAMPING

3.3.3 SELECTION OF APPROPRIATE PROCESSING PARAMETERS FOR IRDM

The computational model was used to investigate the effects of the following four "processing variables" used in the impulse response decay method.

1. Frequency Bandwidth
2. Frequency Resolution
3. Number of Measurement Points
4. Signal to Noise Ratio

3.3.3.1 Effect of Frequency Bandwidths

The loss factors for standard one-third octave center frequencies have been found using full octave bins. To investigate this choice, a study has been conducted using full, one-third, one-sixth, and one-twelfth octave bins for the computational model with an input loss factor of 1%. Figure 3-22 shows the predicted loss factors by changing the band width which shows there is no increase in accuracy of the estimations for larger octave bins. Apparently, there is no reason to choose any one bandwidth over another. So, a full octave bin will be used in all the subsequent work as narrower octave bins are proportionally, computationally intensive.

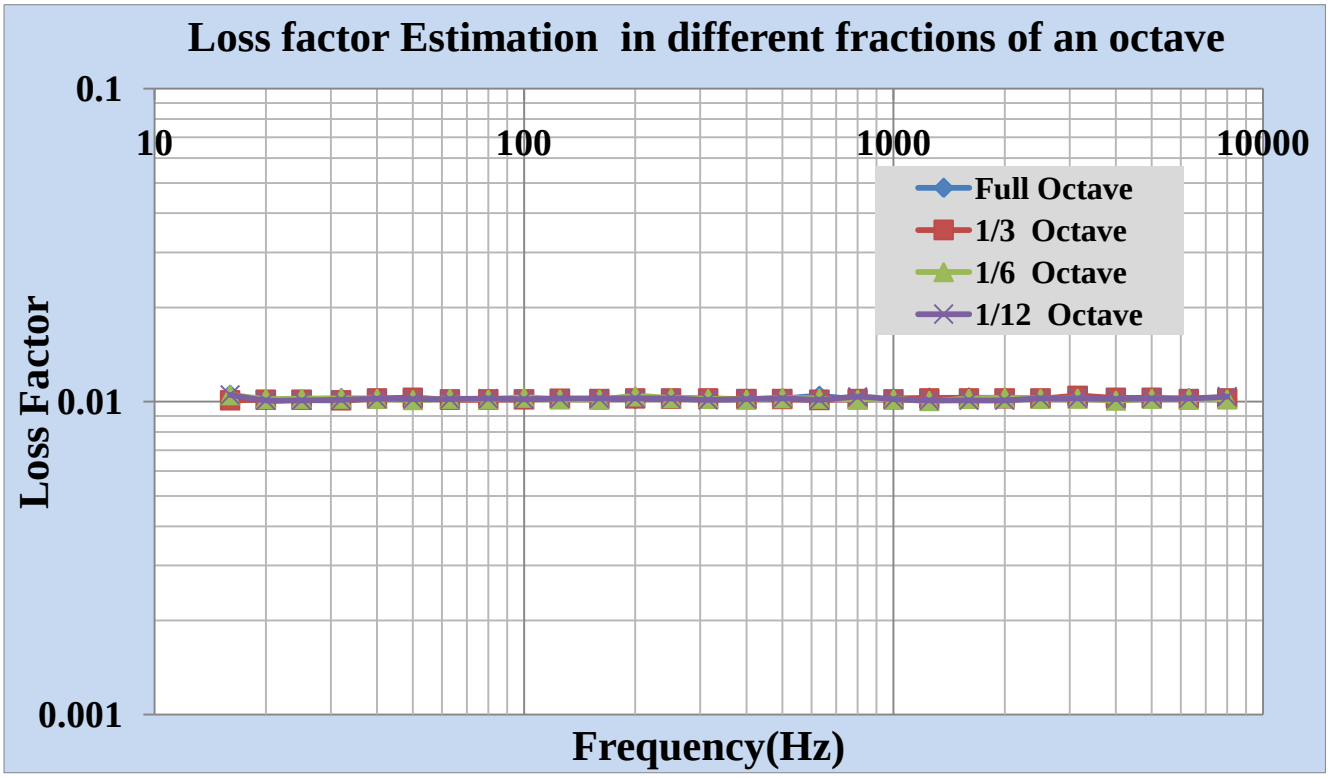

Figure 3-22 Variation of Loss Factor for a Range of Octave Bandwidth's Centered at 1/3 Octave Center Frequencies.

3.3.3.2 Effect of Frequency Resolution

The effect of frequency resolution has been studied for the loss factor levels of 0.001, 0.01 and 0.1. This study was based on the frequency response functions from the computational model, for which the frequency resolution is 1 Hz. Lower levels of frequency resolution are created through simple decimation of the accelerance frequency response function before applying the impulse response decay method.

The estimated loss factors for the three levels of loss factors in the computational model for five different frequency resolutions is shown in Figure 3-23, Figure 3-24 and Figure 3-25. Figure 3-23, for the case of a 0.1% damping, shows that only the 1 Hz resolution allows successful estimation; say within 1% above 300 Hz.

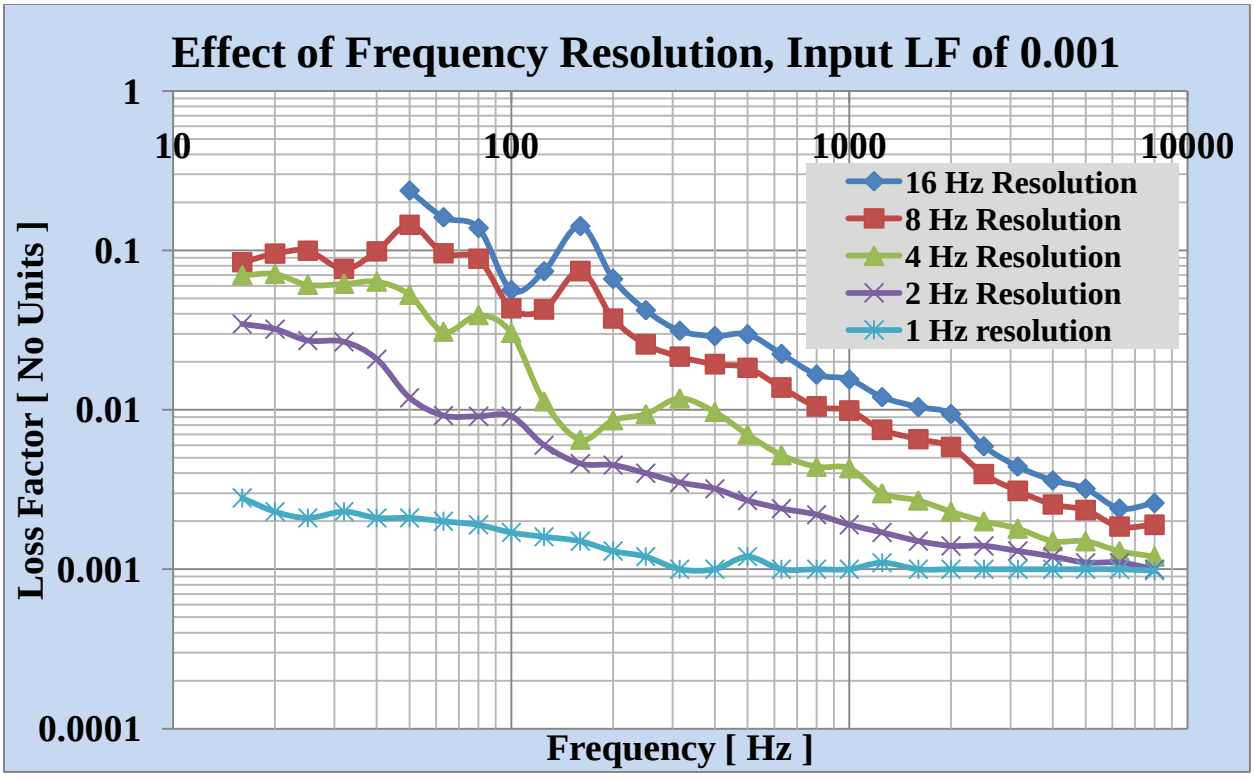

Figure 3-23 Effect of Frequency Resolution for a Input Loss Factor of 0.001 [0.1%]

Figure 3-24, for the case of 1% damping, shows that very successful estimation is achieved for frequency resolutions of 4 Hz or less above 200Hz but, just like the low damping case, the loss factor is over estimated for coarser resolution.

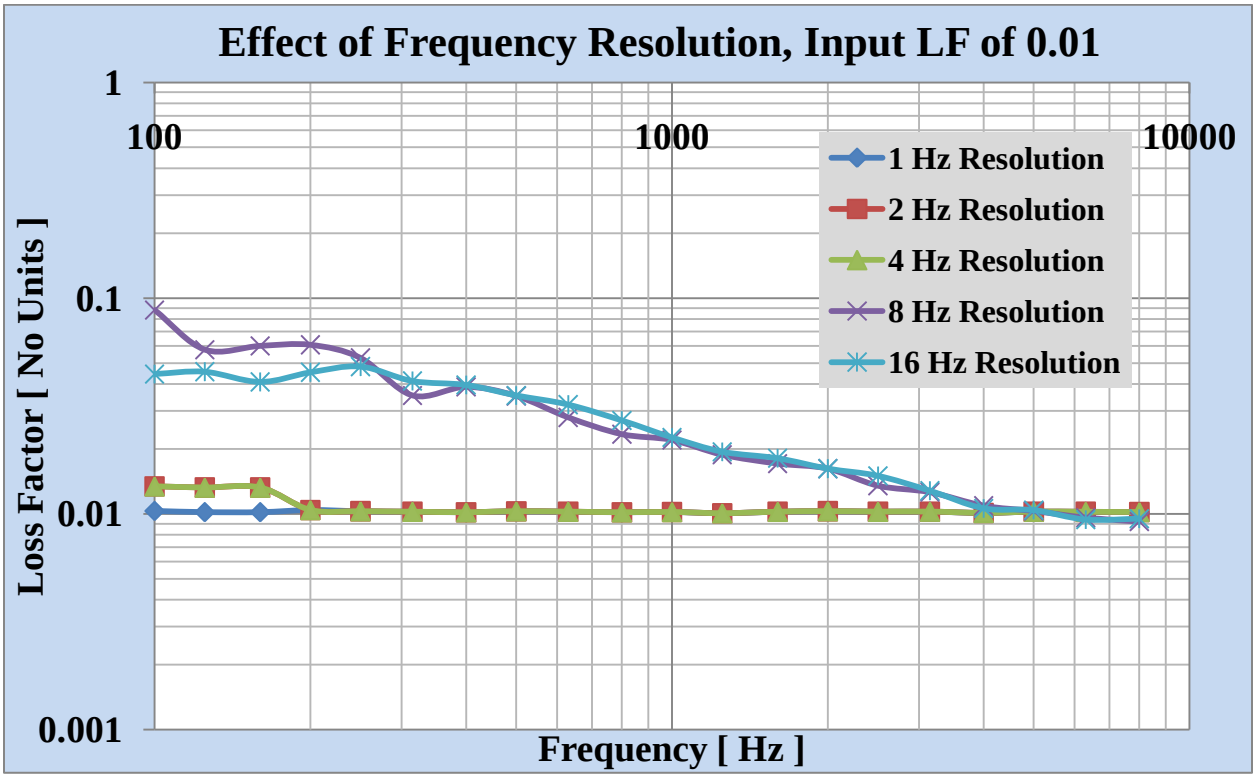

FIGURE 3-24 EFFECT OF FREQUENCY RESOLUTION FOR A INPUT LOSS FACTOR OF 0.01 [1%]

Finally, and most importantly, Figure 3-25 shows the estimation for the case of 10% damping. The loss factor is over estimated for 8 Hz and 16 Hz resolution below 1000 Hz. Above 1000 Hz there is a poor estimation for all frequency resolution cases. This failure is believed to be due to the fact that responses used in the estimation which happened to be in the "near field" response region—where the magnitude of response is systematically larger than the "reverberant field" region—skewed the estimation to a low loss factor, especially at the higher frequencies.

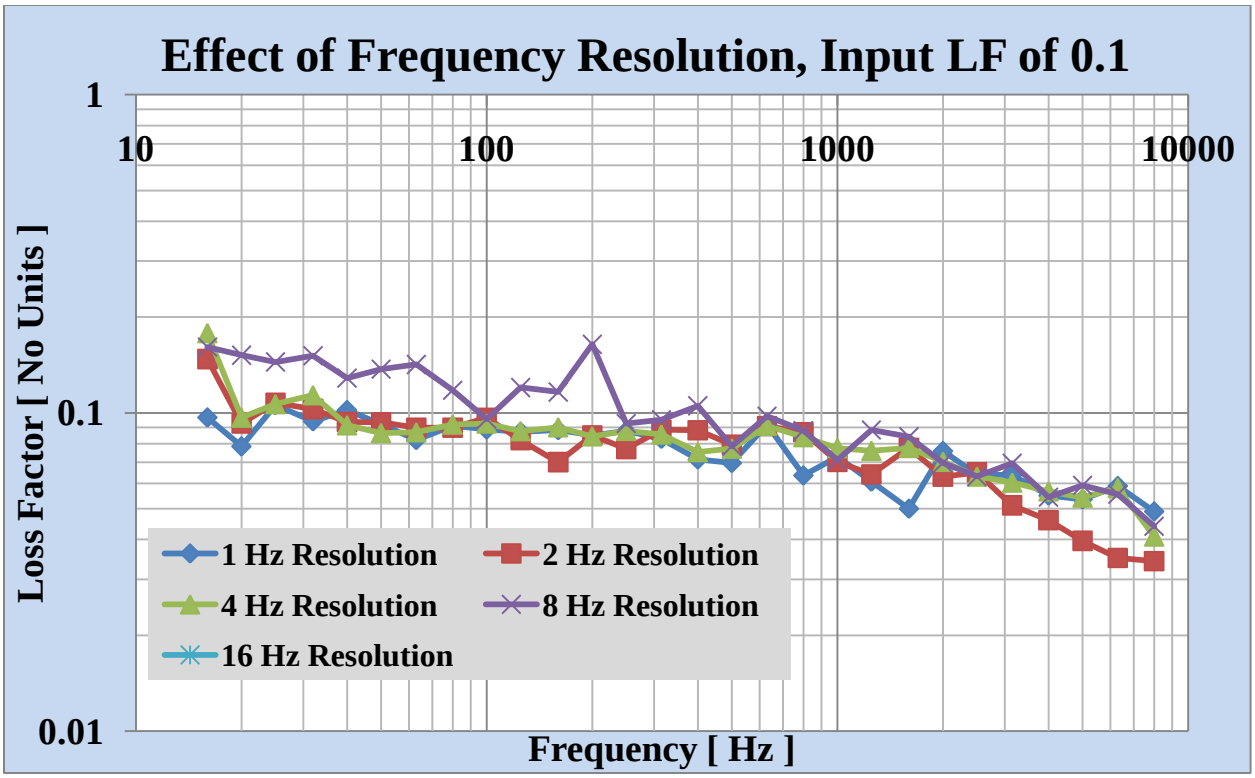

FIGURE 3-25 EFFECT OF FREQUENCY RESOLUTION FOR A INPUT LOSS FACTOR OF 0.1 [10%]

3.3.3.3 EFFECT OF VARIABLE NUMBER OF MEASUREMENT POINTS

One of the goals of the study reported here is to determine the variance of estimated loss factors as a function of the number of response points averaged. Although more information is typically better, knowledge of the number of response points ***needed*** to get an ***acceptable*** estimation of the loss factor results would be useful. Figure 3-26 shows the damping loss factor estimates resulting from averages of 20, 15, 10 and 5 sets of 4, 8, 12 and 16 responses, respectively, due to excitation at a single excitation point for the lightly damped computational model. For this study, the sets of 4, 8, 12 and 16response points were selected at random from the set of 4 excitations and 16 responses for each excitation that are considered. Note that in this case, data from 8 response points are needed to get acceptable estimates of damping loss factor (within 1% of the known value of 0.01) in the 40-8000 Hz range.

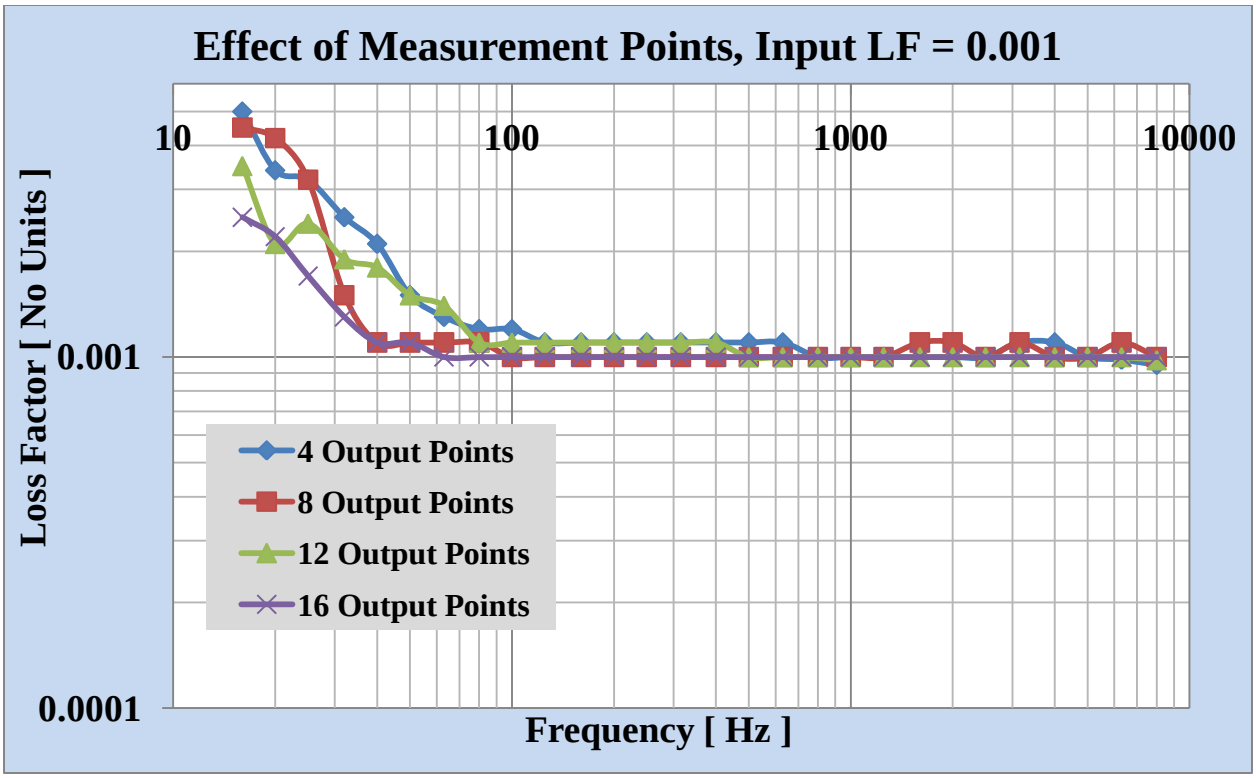

FIGURE 3-26 ESTIMATION OF LOSS FACTORS BY VARYING THE NUMBER OF MEASUREMENT POINTS FOR A INPUT LOSS FACTOR OF 0.001 [0.1%]

Figure 3-27 shows the estimated loss factors for the moderately damped case and there is very little improvement above 100 Hz is apparent when more points are considered (less than 10%). From Figure 3-28, shown below, which is a highly damped case it can be seen that there is very little improvement (less than 1% variation) in estimation of loss factor when using more than 4 response points.

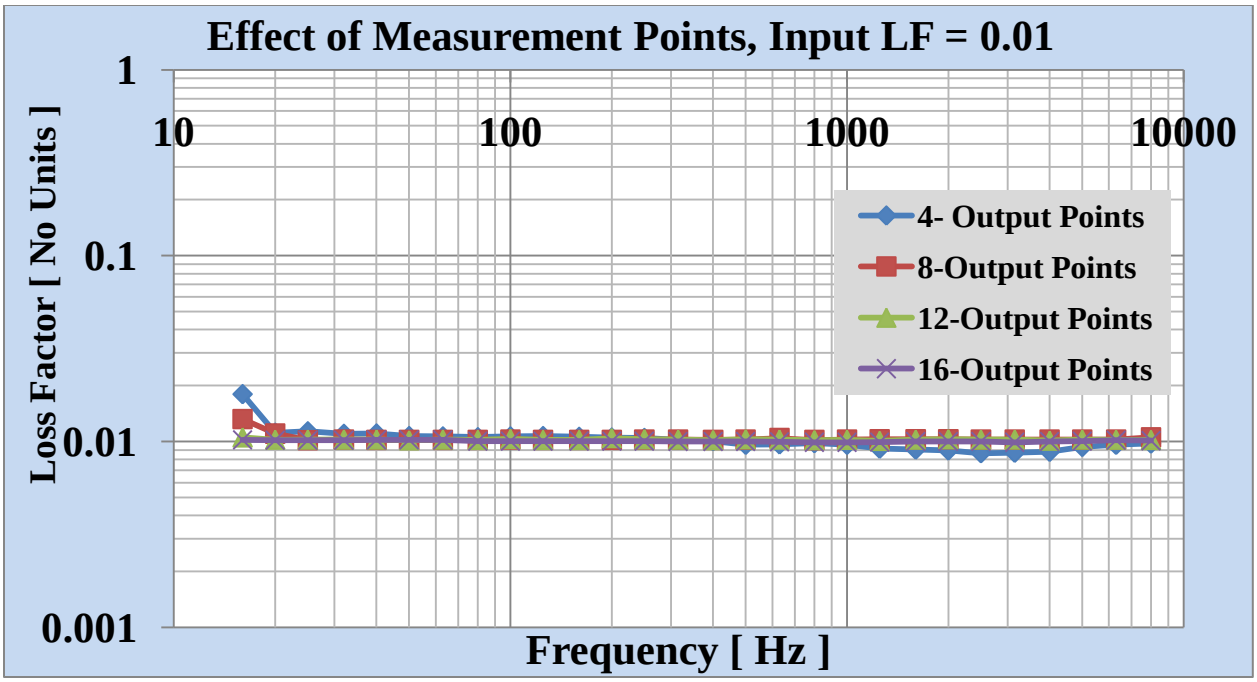

FIGURE 3-27 ESTIMATION OF LOSS FACTORS BY VARYING THE NUMBER OF MEASUREMENT POINTS FOR A INPUT LOSS FACTOR OF 0.01 [1%]

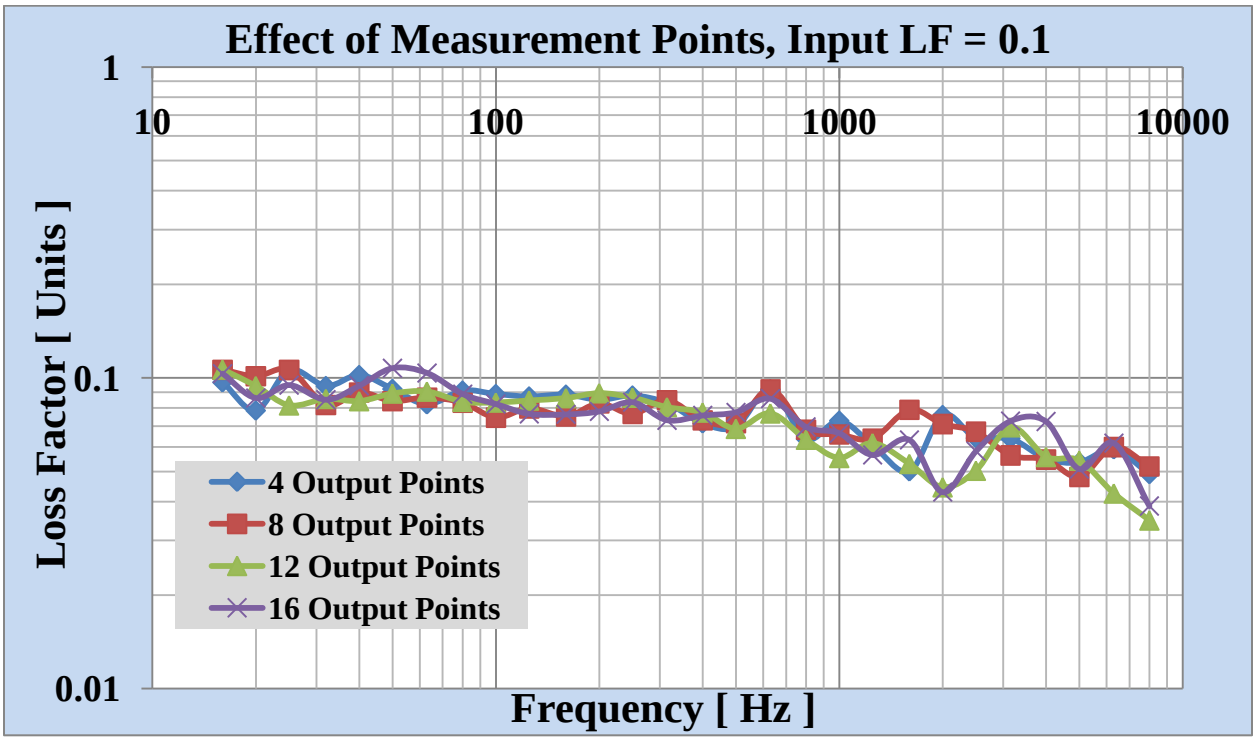

FIGURE 3-28 ESTIMATION OF LOSS FACTORS BY VARYING THE NUMBER OF MEASUREMENT POINTS FOR A INPUT LOSS FACTOR OF 0.1 [10 %]

3.3.3.4 EFFECT OF NOISE

Experimental measurements will always be affected by surrounding noise and the atmosphere, so the effect of noise on the estimated loss factors for the three damping levels is investigated. The signal to noise ratio is given a function of the coherence and is given by Equation (1.33) and is restated here,

$$S/n = \frac{\gamma_{xy}^2(\omega)}{1-\gamma_{xy}^2(\omega)}$$

Noise was added to the accelerance frequency response measurements before employing the I.R.D.M. and the loss factors are estimated. Three different signal to noise levels (100, 50, and 10) are investigated to account for various experimental conditions. Eight measurement points, randomly selected from the four quarters (two from each quarter) are used to compute the loss factors. The estimated loss factors for an input loss factor of 0.1 are shown in Figure 3-29. The effect of noise is felt in the low frequency level (below 100 Hz) where there is significant over estimation of loss factors (50% variation) but above 100 Hz there is no apparent affect except at few discrete frequency bands around 1000 Hz (less than 10% variation). Reasons for this behavior have to be investigated and are suggested for further study. Figure 3-30 and Figure 3-31 show the estimated loss factors for input loss factor of 0.01 and 0.001. For the plate with moderate damping there was no effect of noise for frequencies above 500 Hz and there is less than 10% error for the frequencies below 500 Hz which is admissible. For lightly damped model there is very little effect of noise above 500 Hz (well within 1% variation), and at low frequencies the estimation is inaccurate (greater than 50% variation).

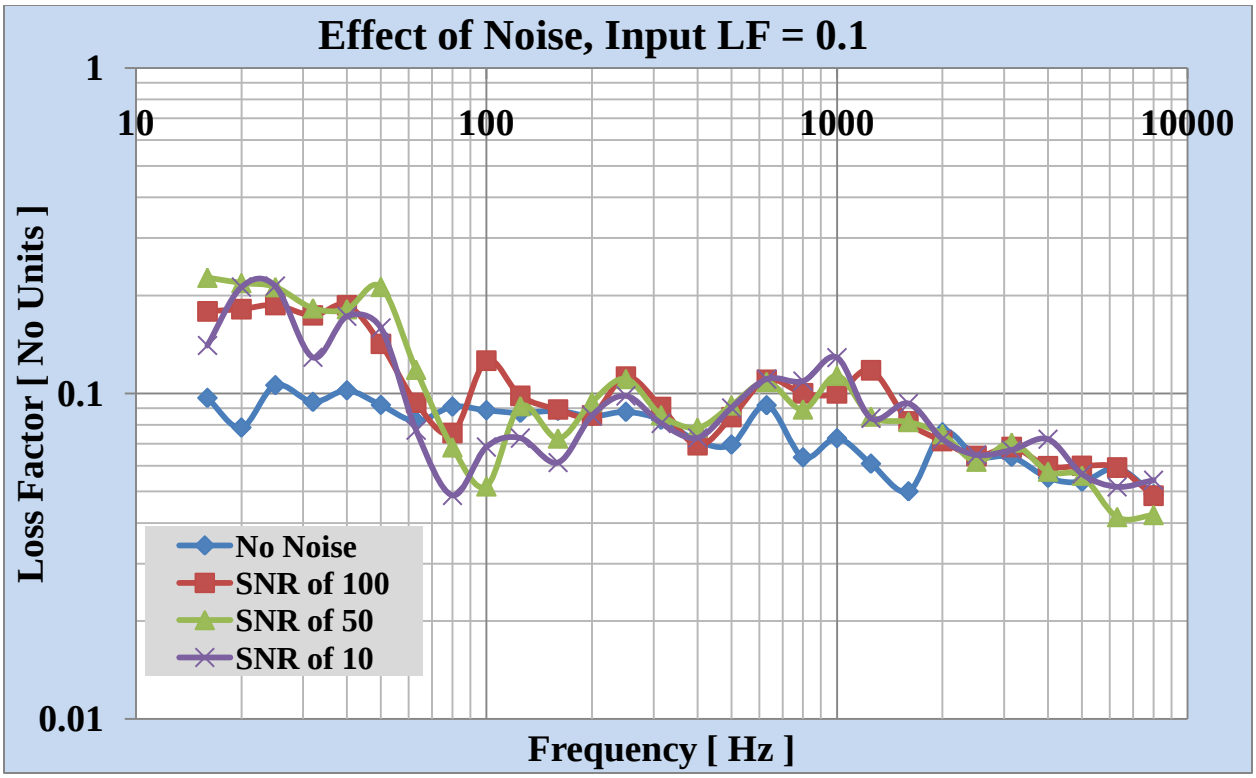

FIGURE 3-29 LOSS FACTOR ESTIMATION FOR VARIOUS NOISE LEVELS, INPUT LOSS FACTOR OF 10 %

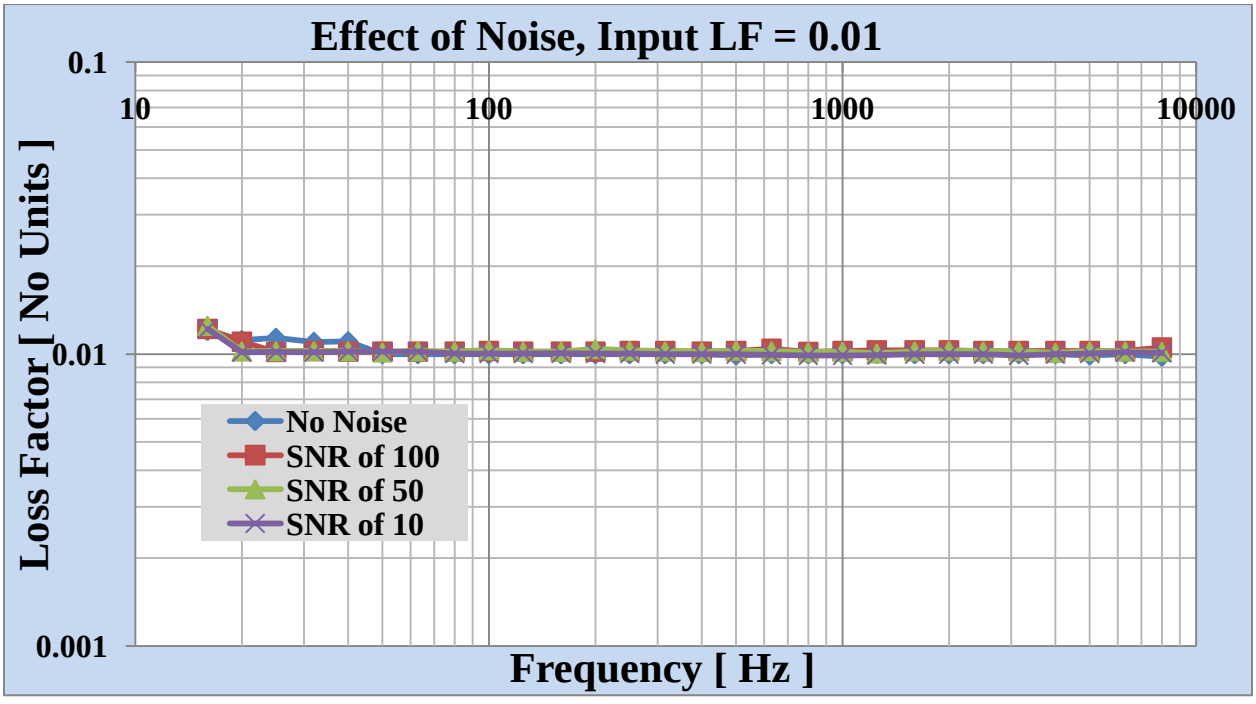

FIGURE 3-30 LOSS FACTOR ESTIMATION FOR VARIOUS NOISE LEVELS, INPUT LOSS FACTOR OF 1 %

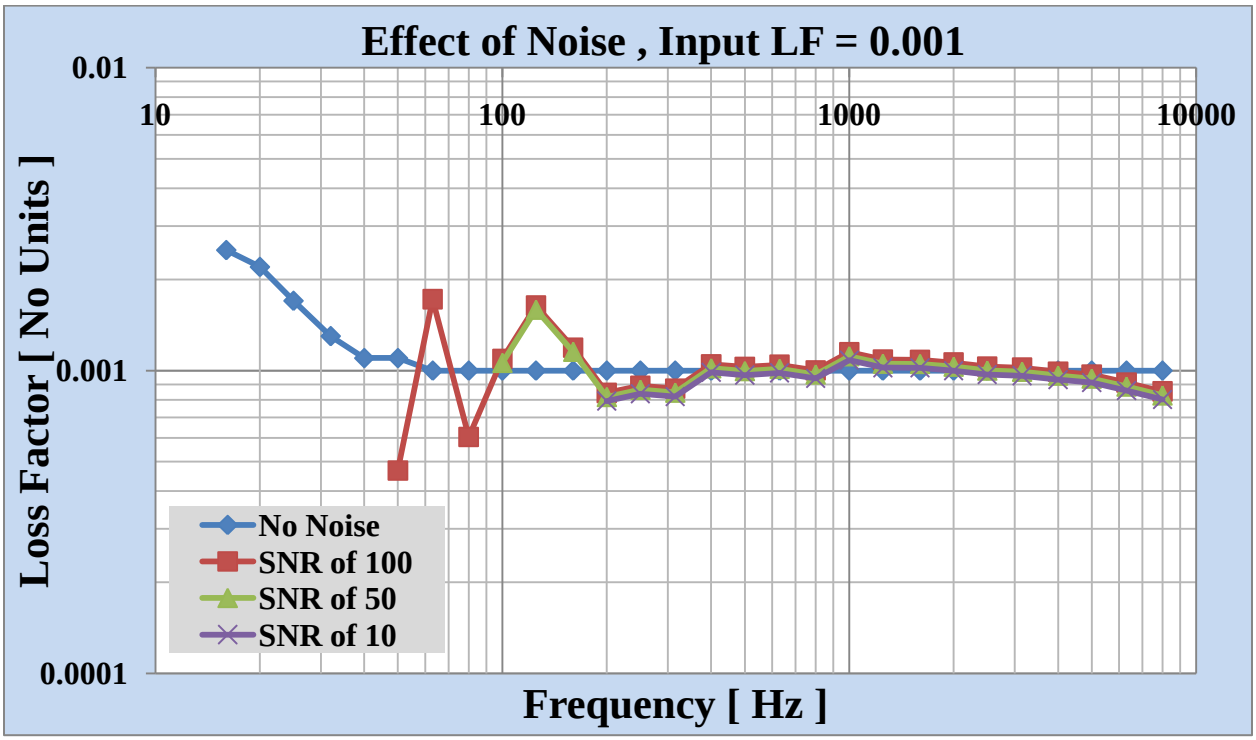

FIGURE 3-31 LOSS FACTOR ESTIMATION FOR VARIOUS NOISE LEVELS, INPUT LOSS FACTOR OF 0.1 %

4 STATISTICAL ENERGY ANALYSIS

4.1 MODAL DENSITY [AND MODES IN BAND]

Following the theory from Lyon and DeJong [9] , the modal density is based on measurements or computation of the average conductance in a plate based on power input at a point, y_s in a frequency band centered on ω_c :

$$< G >_{w_c, y_s} = \frac{\pi}{2} \frac{n(\omega_c)}{M} = (4M\bar{\delta}\,\bar{f}_c)^{-1}$$

Here, M is the mass of the structure, $n(\omega_c)$ is the Modal Density of the structure in the frequency band ω_c , and $\Delta\omega_c$ is the bandwidth of the frequency band centered on ω_c

In the interval $\Delta\omega_c$ the number of modes that can contribute to the average, the "modes in band" is given by $N(\omega_c) = n(\omega_c)\Delta\omega_c$

4.1.1 UNDAMPED STEEL PLATE

Based on the techniques given in above section, the modal densities of the plates and modes per band were calculated. For the experimental study, the plate is hung by bungee cords, thereby enforcing essentially free-free boundary conditions [8]. For these experiments, excitation was applied with an electrodynamic shaker at one of four essentially randomly-selected

locations. The responses at several hundred points were recorded using a Polytec laser vibrometer, leading to experimental estimates of modal density and modes in band. Analytically and computationally, the modal densities were calculated using S.E.A. and the finite element method, within VA One. The modal density of the undamped steel plate measured analytically, calculated by the finite element method and the experimentally calculated modal density are plotted in Figure 4-1.

The sinusoidal behavior of the experimental results is expected as the modal density depends on the experimentally calculated loss factors from the power input method. In the frequency range of interest of this current study, i.e., 500 Hz to 2500 Hz the experimentally calculated modal density, the modal densities calculated by the finite element method and the modal densities calculated analytically with Auto-SEA are in some agreement (30% mean variation). The cyclic behavior is also present in the F.E.A. results which show that the modal densities calculated from the experimentally estimated energies will not be necessarily a straight line as are obtained from the modal densities obtained by solving the wave equation.

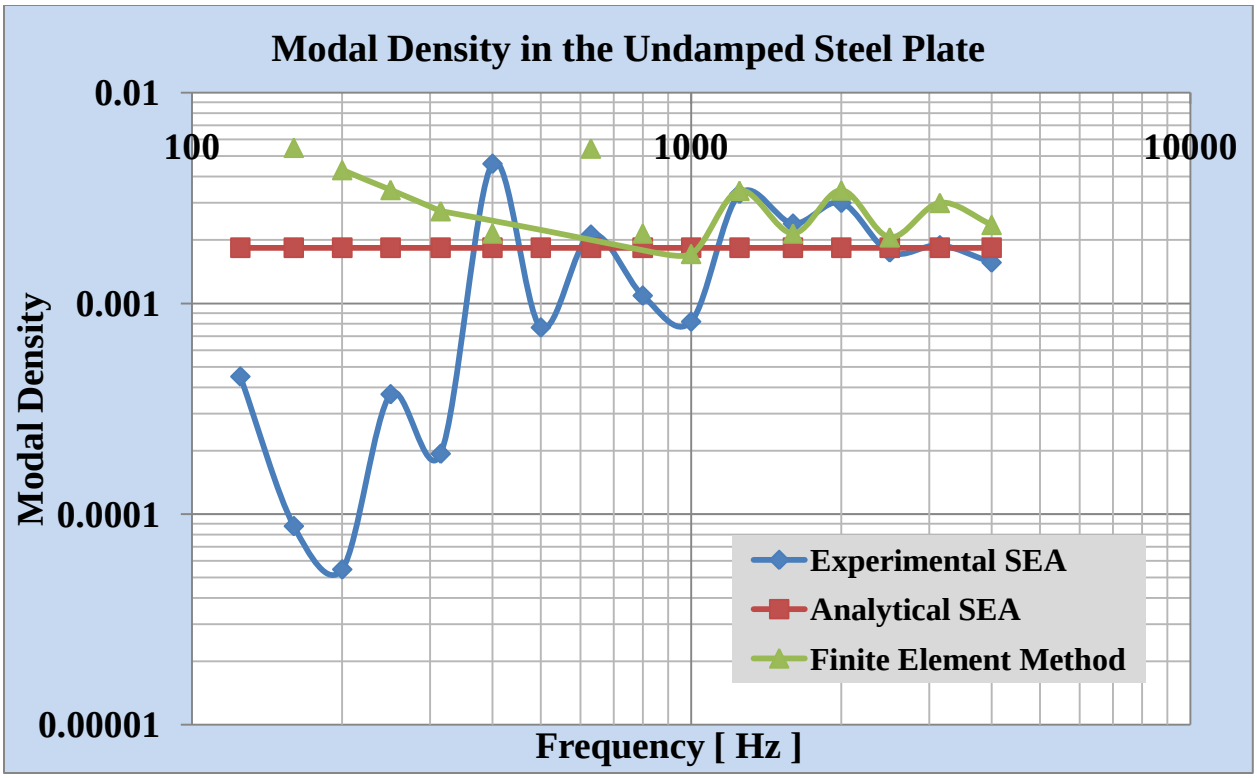

FIGURE 4-1 MODAL DENSITY IN THE UNDAMPED STEEL PLATE

The mode count is a very important parameter in S.E.A. because it represents the number of resonant modes available to receive and store energy in a subsystem. The theoretical mode count for distributed systems is based on combining geometric information about the allowed mode shapes of the system with the dispersion relation for free waves in the system. Figure 4-2 shows the modes in band for the same undamped steel plate and as it can be observed the modes in band have some agreement (30% mean variation) in the 500 Hz – 2500 Hz frequency range but the modes in band are not really accurate in the low frequency i.e., below 500 Hz where the number of modes is less than one – but S.E.A. is based on the assumption that the number of modes in band approach infinity. The modes in band are directly proportional to the modal density according to Lyon and Dejong and are related by the frequency bandwidth. The current analysis was done at one-third octave frequencies with a full octave band width.

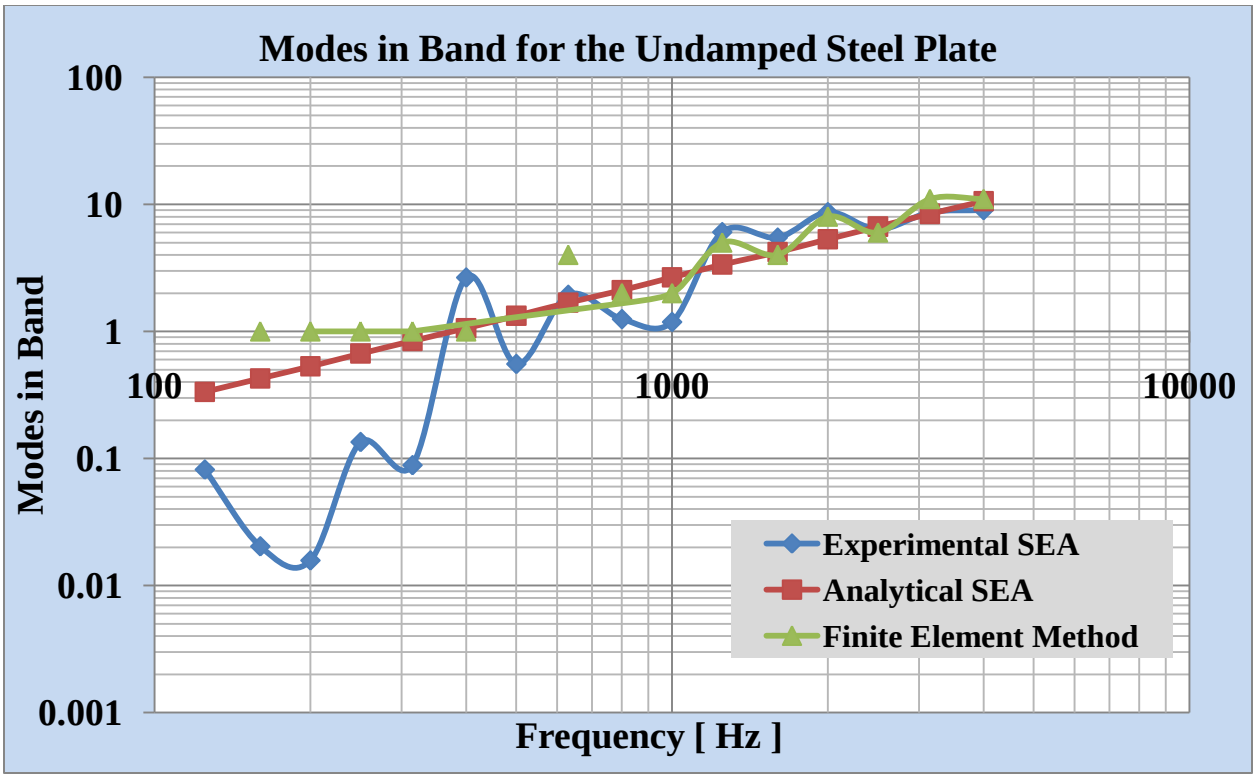

FIGURE 4-2 MODES PER BAND OF THE UNDAMPED STEEL PLATE

4.1.2 STEEL PLATE WITH PARTIAL CONSTRAINED LAYER DAMPING

The modal density of the steel plate with partial constrained layer damping treatment, which has a damping level of approximately 2%, is shown in Figure 4-3. Since this plate has more damping than the other steel plate [which has a 1% damping] the estimated modal density and the modes in band are better compared to the undamped case, but are not in total agreement with the analytical and F.E. results and have the same 30% variation. The estimated modes in band are shown in Figure 4-4. The results are as expected for lightly damped plates, that is, fairly well.

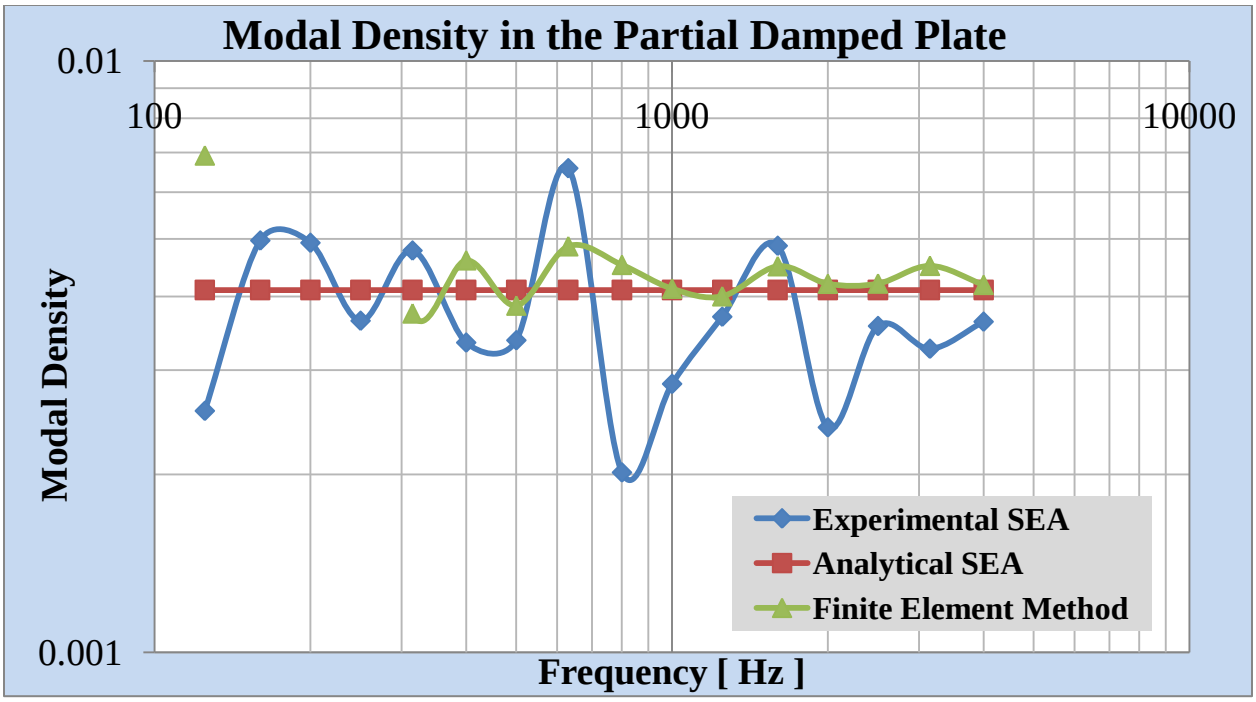

FIGURE 4-3 MODAL DENSITY IN THE PARTIAL DAMPED STEEL PLATE

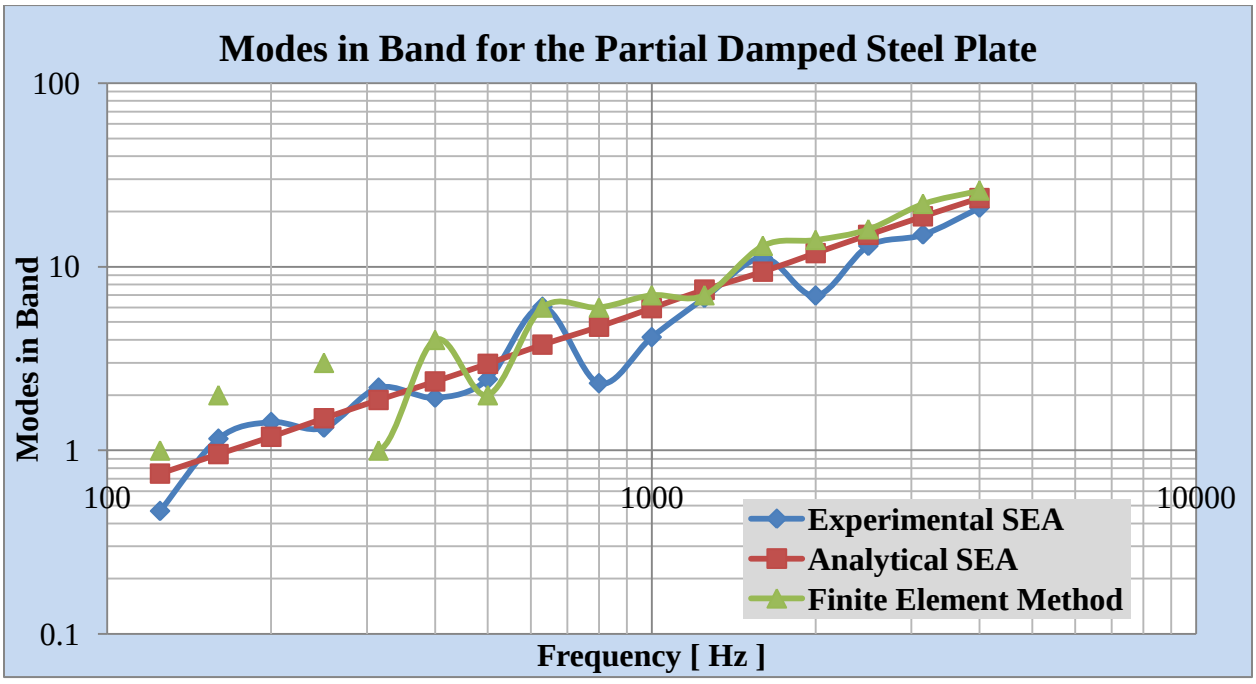

FIGURE 4-4 MODES IN BAND FOR THE PARTIAL DAMPED STEEL PLATE

4.1.3 UNDAMPED ALUMINUM PLATE

The estimated modal densities and the modes in band for the undamped aluminum plates shown in Figure 1-16 are shown in Figure 4-5 and Figure 4-6 respectively. These plates have no damping and the material damping is estimated to be about 0.5 %. As expected, as was the case with the undamped steel plate the estimated results are inaccurate in lower frequencies but are shown to have some agreement (30% variation) with the analytical and F.E. results.

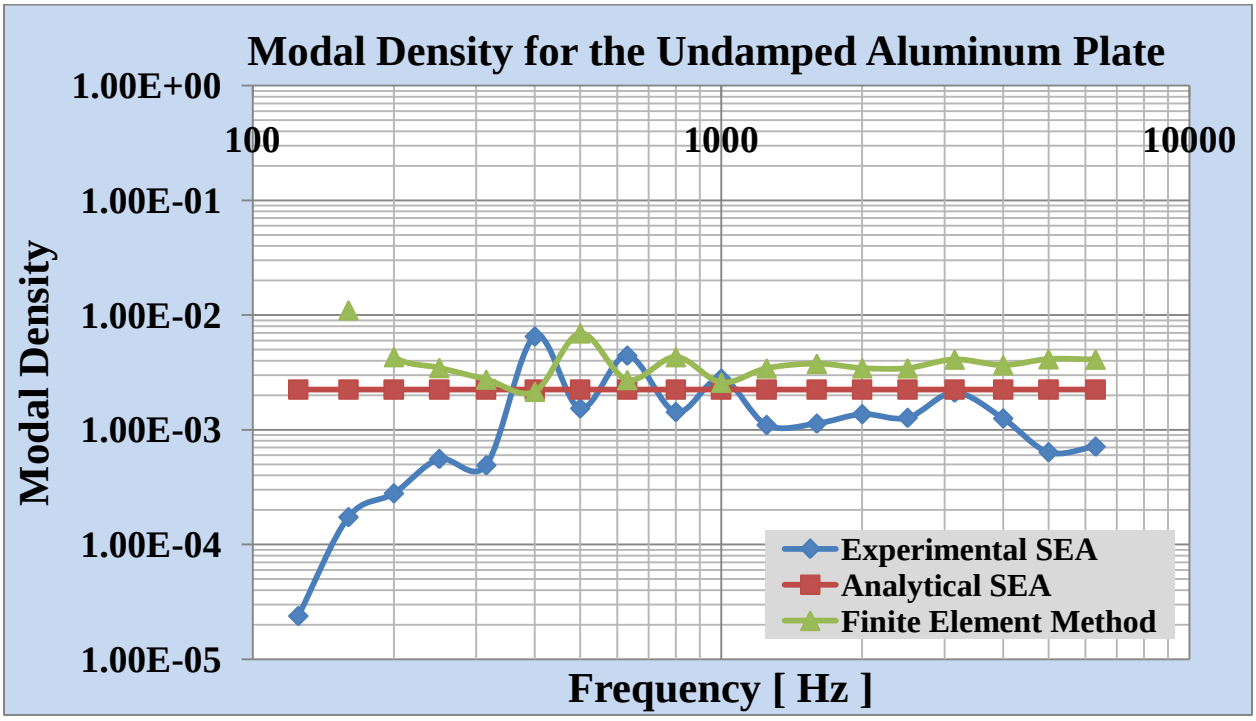

FIGURE 4-5 MODAL DENSITY IN UNDAMPED ALUMINUM PLATE

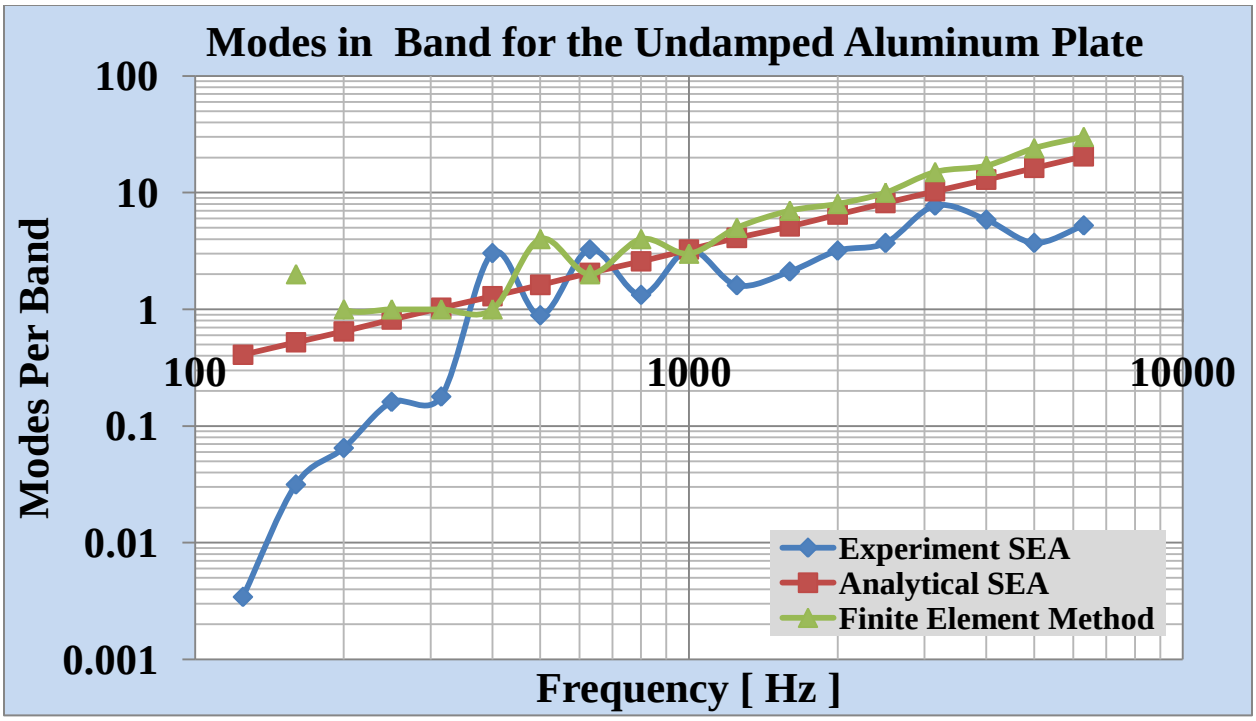

FIGURE 4-6 MODES IN BAND IN THE UNDAMPED ALUMINUM PLATE

4.2 LOSS FACTOR ESTIMATION

For a single plate, the energy input to the plate in a band $\Delta\omega_c$ centered at ω_c must, eventually be dissipated by damping. i.e., $E^{in}(\infty,\omega_c) = E^{diss}(\infty,\omega_c)$.Using the theory of the power input method, the loss factor η of the plate in the band $\Delta\omega_c$ centered at ω_c can be evaluated as

$$\eta\ (\omega_c) = \frac{E^{in}(\omega_c)}{2\omega_c \varepsilon^k(\omega_c)}$$

Here ε^k is the time-integrated kinetic energy of the system. For simplicity $t = \infty$ is dropped.

Using Parseval's theorem, the input energy can be calculated as [22]

$$E^{in} = \int_{-\infty}^{\infty} f(t)v(t)dt = \frac{1}{\pi}\int_0^{\infty} \mathrm{Re}\{F(\omega)V^*(\omega)\}d\omega = \frac{1}{\pi}\int_0^{\infty} \mathrm{Im}\{F(\omega)A^*(\omega)/\omega\}d\omega$$

Note that $f(t)$ and $v(t)$ are the driving force and the driving point velocity, respectively. $F(\omega)$ and $v(\omega)$ are their Fourier transforms. $A(\omega)$ is the Fourier transform of the driving point acceleration and * denotes the complex conjugate. The input energy in the band $\Delta\omega_c$ centered at ω_c is then

$$E^{in}(\omega_c) = \frac{1}{\pi} \int_{\omega_c - \Delta\omega/2}^{\omega_c + \Delta\omega/2} \mathrm{Re}\{F(\omega)V^*(\omega)\} d\omega$$

$$E^{in}(\omega_c) = \frac{1}{\pi} \int_{\omega_c - \Delta\omega/2}^{\omega_c + \Delta\omega/2} \mathrm{Re}\{F(\omega)A^*(\omega)/\omega\} d\omega$$

Similarly the time integrated kinetic energy in the band can be written as

$$\varepsilon^k(\omega_c) = \frac{M}{2\pi} \int_{\omega_c - \Delta\omega/2}^{\omega_c + \Delta\omega/2} |V(\omega)|^2 d\omega = \frac{M}{2\pi} \int_{\omega_c - \Delta\omega/2}^{\omega_c + \Delta\omega/2} |A(\omega)/\omega|^2 d\omega$$

4.3 COUPLING LOSS FACTORS

4.3.1 TWO PLATES JOINED ALONG A LINE

Coupling loss factors for two steel plates joined at a line (a 90-degree bend), but otherwise free to respond in lateral vibration, have been studied both analytically and experimentally. Two cases have been studied: one with no added damping and one in which one of the plates has a small amount of damping provided by a constrained layer treatment. Statistical Energy Analysis (using VA One) and the finite element method have been used to predict the coupling loss factors. The finite element predictions are based on the averaged responses, essentially a "pseudo-statistical" approach.

Equating the power transmitted across the junction between two subsystems to the power dissipated in the receiver subsystem gives [9]:

$$\eta_{12} = \frac{\eta_2 E_2}{E_1 - \frac{\overline{\delta f_2}}{\overline{\delta f_1}} E_2}$$

where η_{12} is the coupling loss factor for plate 1 to plate 2 , η_{21} is the coupling loss factor for plate 2 to plate 1, E_1, E_2 are the energies in plate 1 and plate 2 respectively and $\overline{\delta f_1}, \overline{\delta f_2}$ are the frequency spacing for plate 1 and plate 2.

The total energies of the subsystems are calculated by averaging a number of point response measurements according to $E = M < \upsilon^2 >$ for a structural subsystem.

The frequency spacing is difficult to measure directly in a modally dense frequency range, but can be predicted statistically as [9]:

$$\overline{\delta f_1} = \frac{1}{2\pi \eta_1(\omega_c)}$$

Finally, based on theoretical considerations:

$$\eta(\omega_c)_1 \eta_{12}(\omega_c) = \eta(\omega)_2 \eta_{21}(\omega_c)$$

This relationship may be used to eliminate the need to conduct an experiment wherein a damped system is excited and the coupling loss factor from the damped system to a lightly damped subsystem is estimated.

Alternatively the subsystem loss factors and coupling loss factors can be found by balancing the power input to subsystems in two separate tests to the energies stored in the subsystems at steady state:

$$\begin{pmatrix} \eta_1+\eta_{12} & -\eta_{21} \\ -\eta_{12} & \eta_2+\eta_{21} \end{pmatrix}\begin{pmatrix} E^k_{1,I} & E^k_{1,II} \\ E^k_{2,I} & E^k_{2,II} \end{pmatrix}=\frac{1}{2\omega}\begin{pmatrix} \Pi^{in}_{1,I} & 0 \\ 0 & \Pi^{in}_{2,II} \end{pmatrix}$$

$\eta_2, \eta_1, \eta_{12}, \eta_{21}$ have the same meaning as described above and

$E^k_{i,j}$ is the response energy of plate *i* due to the injection of power in plate *j*, where j takes on values I and II.

$\Pi^{in}_{1,I}, \Pi^{in}_{2,II}$ are the power injected in plate 1 and plate 2 respectively.

The power-energy relationship can be re written more conveniently as:

$$\begin{pmatrix} \eta_1 & \eta_{21} \\ \eta_{12} & \eta_2 \end{pmatrix}=\frac{1}{2D\omega_c}\begin{pmatrix} \Pi^{in}_{1,I}E^k_{2,II}-\Pi^{in}_{2,II}E^k_{2,I} & \Pi^{in}_{1,I}E^k_{1,II} \\ \Pi^{in}_{2,II}E^k_{2,I} & \Pi^{in}_{2,II}E^k_{1,I}-\Pi^{in}_{1,I}E^k_{1,II} \end{pmatrix}$$

where,

$$D=E^k_{1,I}E^k_{2,II}-E^k_{2,I}E^k_{1,II}$$

Coupling loss factors may also be computed using Statistical Energy Analysis software such as VA One. This software package uses traditional S.E.A. plate modeling as well as a finite-element-based technique based on the energy flow method (E.F.M) [22]:

Loss factors for the individual plates were estimated using the power input method (P.I.M.), described in Chapter 2, and the impulse response decay method (I.R.D.M.), described in Chapter 3. For these loss factor estimations, the same data that is used to calculate modal densities is used, and a number of excitation points are averaged thereby avoiding problems

associated with using only one driving point excitation [4] [23]. As has been reported elsewhere [23], the I.R.D.M. appears to be more "believable" considering the widely-varying loss factor estimates from P.I.M. [24].

Finally, the coupling loss factors were estimated using the several hundred response point velocities measured on the two faces of the joined plate. As in the earlier experiments, 4 different excitation points were used. The coupling loss factors were also estimated using both the analytical S.E.A. and E.F.M. processes in VA One. Figure 4-7 and Figure 4-8 show the estimated coupling loss factors based on analytical S.E.A., experimental and finite element techniques. The agreement is excellent (< 10% variation) between the analytical and experimental estimations. The estimations from the E.F.M. are also very good except in the very low frequency range where modal densities are low, as expected [25].

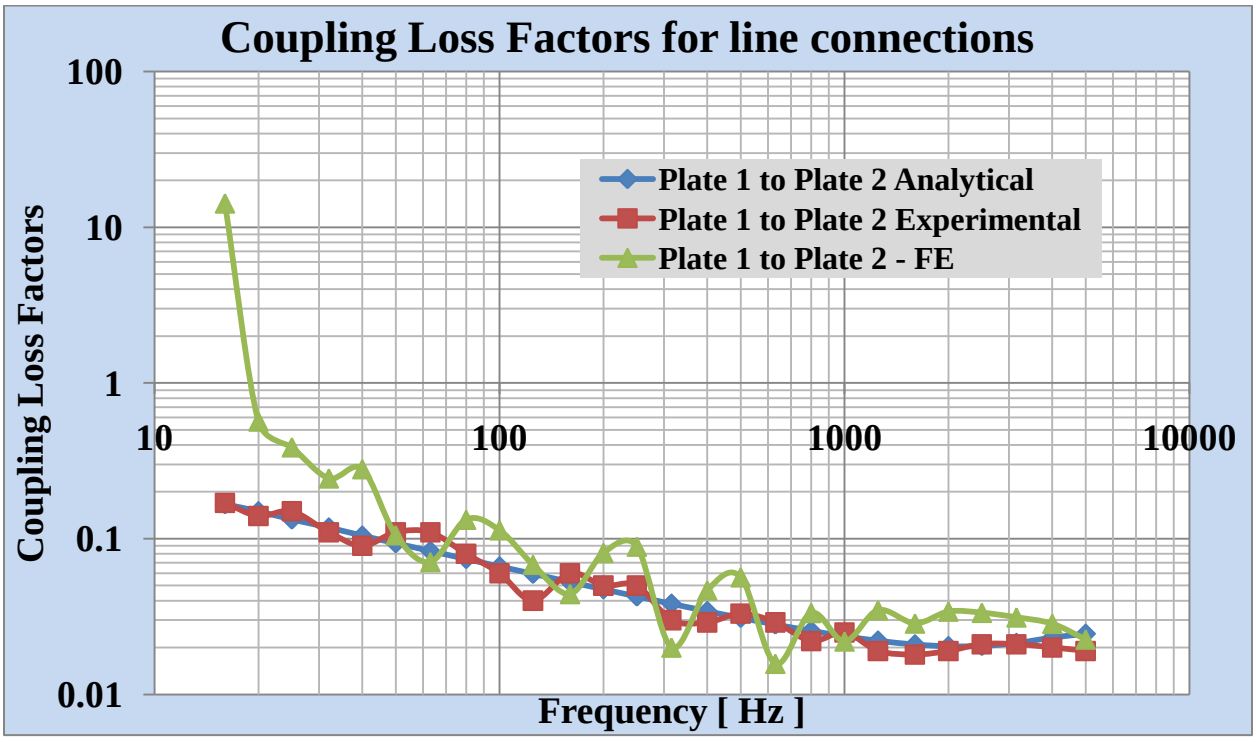

FIGURE 4-7 COUPLING LOSS FACTORS ALONG A LINE (BIG PLATE TO SMALL PLATE)

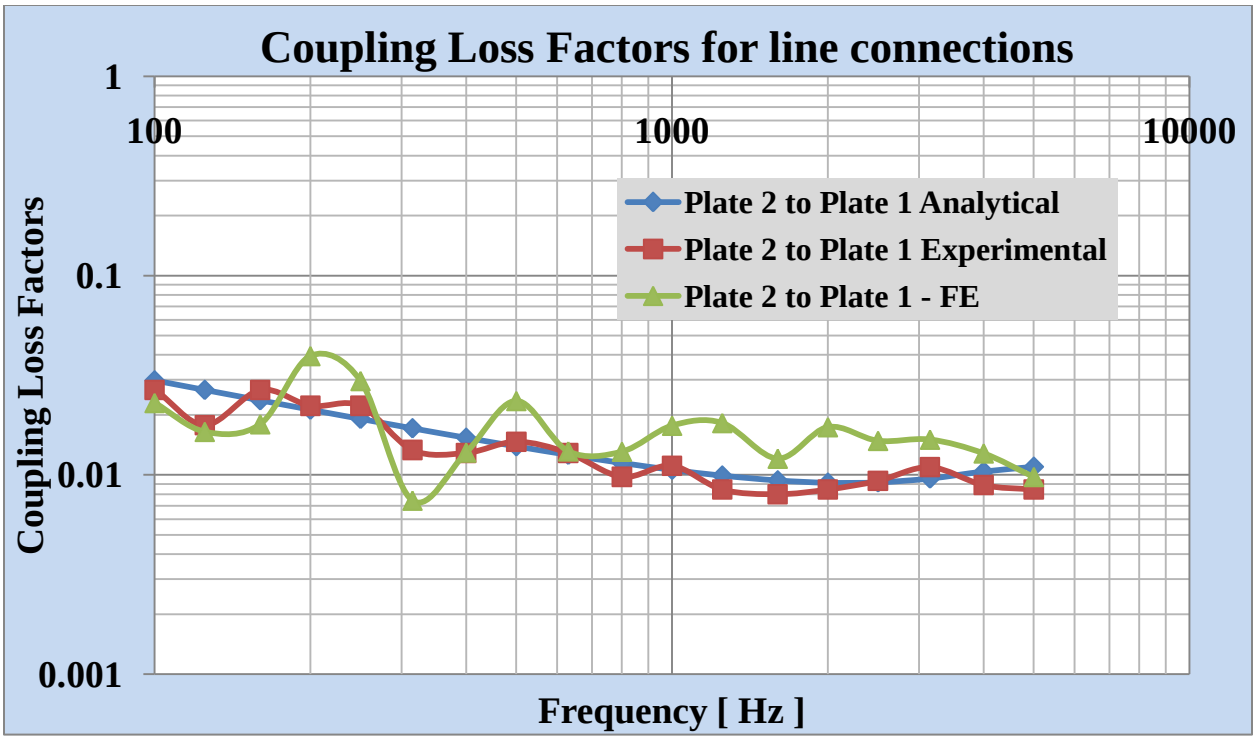

FIGURE 4-8 COUPLING LOSS FACTORS ALONG A LINE (SMALL PLATE TO BIG PLATE)

4.3.2 TWO PLATES JOINED AT A POINT

Coupling loss factors for two lightly damped plates joined at a point, but otherwise free to respond in lateral vibration, have been studied both analytically and experimentally. This study forms the basis for on-going estimations of the transient coupling loss factors of the same system.

Statistical Energy Analysis (using VA One) and the finite element method (using VA One's Energy Flow Method) have been used to predict the coupling loss factors. The finite element predictions are based on the averaged responses, essentially a "pseudo-statistical" approach.

Experimentally, using the technique used by Lai and Soom, a force transducer has been used to measure the force *between the plates* as it is used to attach them. Simultaneously, the kinetic energies in the two plates are measured by 4 accelerometers attached to each plate during both transient and persistent excitation of the plates, one at a time. The coupling loss factors are estimated by balancing the transmitted energies with the kinetic energies in the two plates. The coupling loss factors can also be assessed by a more "traditional" experimental approach, namely balancing the power input to a plate with the energies of the plates. This approach will be presented at the conference. The coupling loss factors are also estimated using two techniques available in VA One, namely the traditional S.E.A. and the energy flow method. The estimations from the three approaches reported here compare as well as may be expected for these lightly damped plates.

Consider now the power input method applied to the calculation of coupling loss factors. If we consider two tests, one where an external force is applied to plate 1, and another with the force applied to plate 2, the energy transferred between the coupled plates can be represented by the individual plate loss factors and the coupling loss factors [26]

$$\begin{pmatrix} \eta_1+\eta_{12} & -\eta_{21} \\ -\eta_{12} & \eta_2+\eta_{21} \end{pmatrix} \begin{pmatrix} E_{1,I}^k & E_{1,II}^k \\ E_{2,I}^k & E_{2,II}^k \end{pmatrix} = \frac{1}{2\omega} \begin{pmatrix} \Pi_{1,I}^{in} & 0 \\ 0 & \Pi_{2,II}^{in} \end{pmatrix}$$

η_1, η_2 are the individual loss factors for the plates 1 and 2 respectively.

η_{12}, η_{21} are the coupling loss factors for plate 1 to plate 2 and plate 2 to plate 1, respectively.

$E_{i,j}^k$ is the kinetic energy of plate *i* due to the injection of power in plate *j*, where in this case *j* takes on the values *I* and *II*.

$\Pi_{1,I}^{in}, \Pi_{2,II}^{in}$ are the power injected in plate 1 and plate 2 respectively.

The above Equation can be re written as follows

$$\begin{pmatrix} \eta_1 & \eta_{21} \\ \eta_{12} & \eta_2 \end{pmatrix} = \frac{1}{2D\omega_c} \begin{pmatrix} \Pi_{1,I}^{in} E_{2,II}^k - \Pi_{2,II}^{in} E_{2,I}^k & \Pi_{1,I}^{in} E_{1,II}^k \\ \Pi_{2,II}^{in} E_{2,I}^k & \Pi_{2,II}^{in} E_{1,I}^k - \Pi_{1,I}^{in} E_{1,II}^k \end{pmatrix}$$

Where, $D = E_{1,I}^k E_{2,II}^k - E_{2,I}^k E_{1,II}^k$

As an alternative, Lai and Soom [21][25] have developed expressions for the *time-varying* coupling loss factors, in terms of the time-integrated kinetic energies, ε^k, and the measured (or computed) energy transferred between plates.

$$2\omega_c \begin{pmatrix} \varepsilon_{1,I}^k(t,\omega_c) & \varepsilon_{1,II}^k(t,\omega_c) \\ \varepsilon_{2,I}^k(t,\omega_c) & \varepsilon_{2,II}^k(t,\omega_c) \end{pmatrix} \begin{bmatrix} \eta_{21}(t,\omega_c) \\ \eta_{12}(t,\omega_c) \end{bmatrix} = \begin{bmatrix} E_{21,I}^{tr}(t,\omega_c) \\ E_{21,II}^{tr}(t,\omega_c) \end{bmatrix}$$

Here I and II represent the plate on which the excitation is applied. The subscripts *12* and *21* indicate energy transferred from plate 1 to 2 and 2 to 1, respectively. Note that this formulation requires a force transducer between the plates.

Using the power input method (P.I.M.), described in Chapter 2, and the impulse response decay method (I.R.D.M.), loss factors for the individual plates were estimated. For these experiments, both hammer and electrodynamic shaker excitation were used (separately). All responses were captured with 8 accelerometers distributed about the plates, 6 at the same locations as Lai and Soom [21] [25] and one extra location per plate. Two sets of hammer excitation were used, one with a hard (metal) tip and the other with a softer (plastic) tip. Hammer excitation results are for 50 hits with each tip type, with roughly equal numbers of hits

applied in the near vicinity of the accelerometers. Therefore, these estimations are based only on driving point measurements.

The loss factors estimated for plates 1 and 2 were used in the analytical S.E.A. and E.F.M. estimations of coupling loss factor. For the experimental study, since the transmitted energy was measured, the individual plate loss factors were not needed. Excitation was applied to plate 1 half the time and to plate 2 otherwise. Figure 4-9 and Figure 4-10 show the estimated coupling loss factors for all 4 cases of excitation: hammer and shaker experiments, analytical S.E.A. and the finite element method. The agreement is as good as can be expected: wide variation of 10% at higher frequencies and more than 100% in lower frequencies) for lightly-damped plate [26].

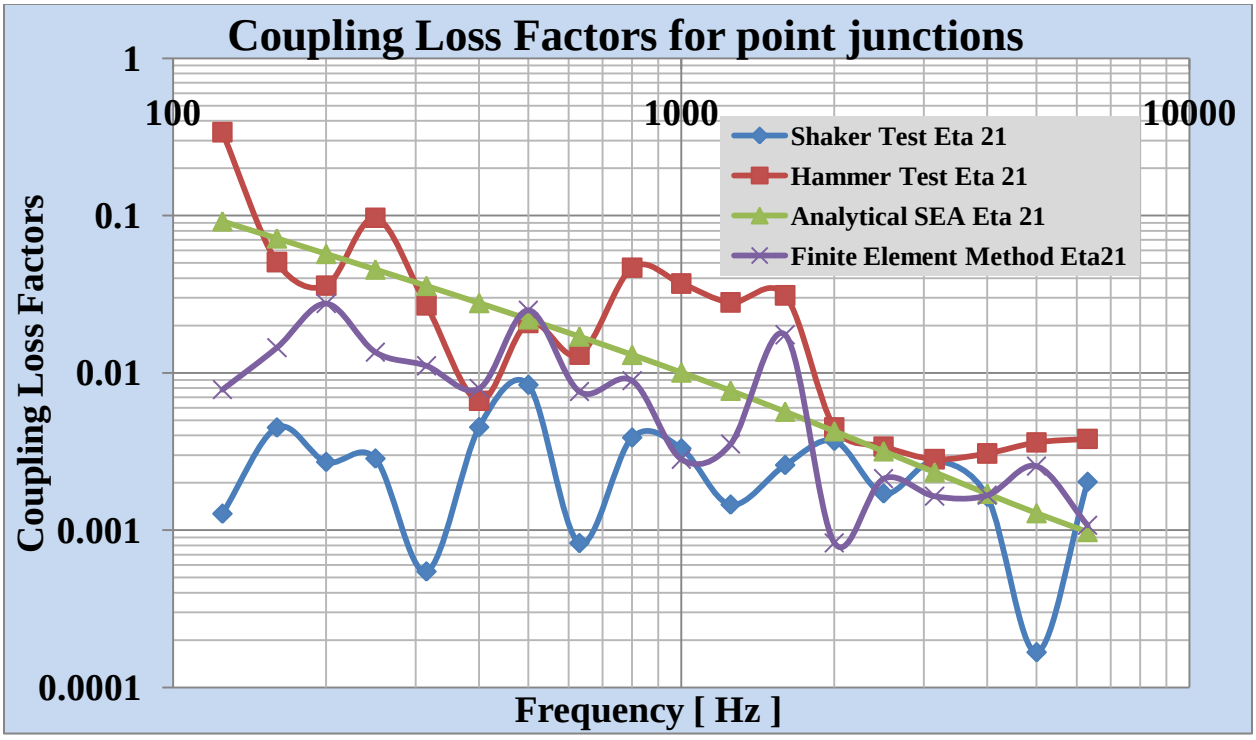

FIGURE 4-9 COUPLING LOSS FACTORS ALONG A POINT (BOTTOM PLATE TO TOP PLATE)

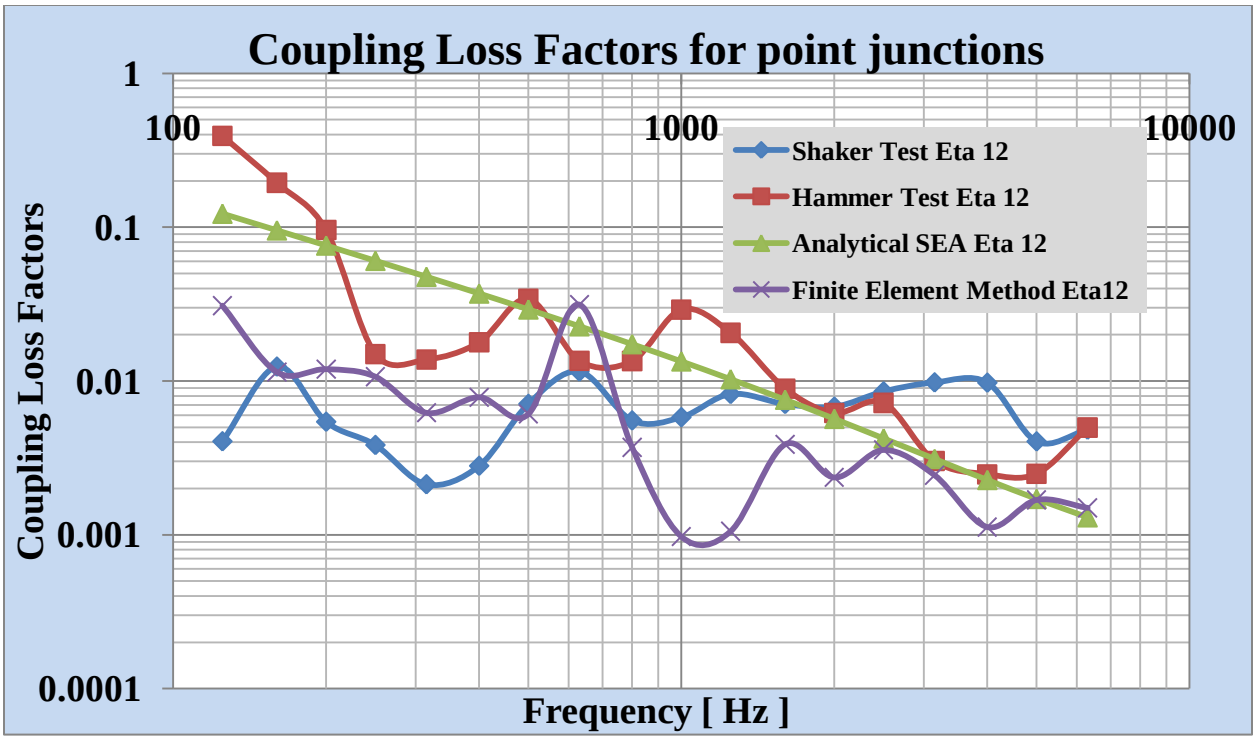

FIGURE 4-10 COUPLING LOSS FACTORS ALONG A POINT (TOP PLATE TO BOTTOM PLATE)

5 CONCLUSIONS AND FUTURE WORK

5.1 CONCLUSIONS

5.1.1 POWER INPUT METHOD

1. The analytical power input method is validated with a single degree of freedom with a random excitation and a sinusoidal excitation. P.I.M. works very well for these S.D.O.F. systems for all levels of damping.
2. Experiments show that for lightly damped plates [$\eta \approx 0.001$] the method fails. For highly damped plates [$\eta \approx 0.1$] the P.I.M. estimates loss factors well i.e., the estimates are within 10% of the I.R.D.M. prediction in the range of 100 Hz – 4000 Hz.
3. For moderately damped plates [$\eta \approx 0.01$] the loss factors estimated with high resolution (i.e., 1Hz and 2 Hz resolution) performed essentially the same but as the resolution is decreased beyond 2 Hz [4 Hz and 8 Hz] the loss factor estimation fails.

5.1.2 IMPULSE RESPONSE DECAY METHOD

1. The analytical impulse response decay method is validated with a single degree of freedom system with a true impulse and a half sine impulse excitation. For these S.D.O.F. systems the estimated loss factors are accurate for a wide range of loss factors.
2. The method is also validated by a computational plate model, for three damping levels of 10 %, 1%, and 0.1%. The loss factors estimated are accurate for low and moderate damping levels in the range 100 Hz – 8000 Hz but for highly damped plates the loss factors are under estimated at high frequency because the responses from the near field are used in the computational process. The method fails for all three analyzed levels of damping below 100 Hz, where modal density is low and the method is expected to fail.
3. There was no effect on the estimated loss factor by employing either full octave, $1/3^{rd}$, $1/6^{th}$ or $1/12^{th}$ octave filters. The $1/3^{rd}$, $1/6^{th}$ and $1/12^{th}$ octave are computationally-intensive making them less attractive. It is recommended to use full octave filters, centered at $1/3^{rd}$ octave frequencies.
4. The accuracy of the estimated loss factors is greatly affected if the frequency resolution is increased for lightly damped and moderately damped plates. For highly damped plates there is no such effect.
5. By increasing the number of measurement points the loss factor estimation is more accurate. However more response points are computationally-intensive and require more resources to measure and hence it is recommended that only 4 response points are needed to get reasonable estimation.

5.1.3 STATISTICAL ENERGY ANALYSIS

1. The modal densities and the mode count are evaluated for lightly damped and moderately damped plates and compared with theoretical values. The estimation fails for lightly damped plates but for moderately damped plates, the estimation is fairly accurate.
2. The coupling loss factors of two sets of plates are estimated experimentally. When the loss factors are computed individually for the plates joined along a line, the coupling loss factor estimation is fairly accurate. When the loss factor is evaluated for the coupled plates there is moderate agreement of the experimental solution with the analytical solution.

5.2 FUTURE WORK

1. Further work on the PIM should focus on experimental methods to eliminate phase errors which cause negative damping estimation.
2. For validating the impulse response decay method the computational analysis was done with uniformly spaced excitation and response points. This method needs to be validated with randomly selected excitation and response points.
3. Further experimental studies on I.R.D.M. are needed to evaluate the effects of measurement noise on the estimated loss factors.
4. Experimental studies of S.E.A. considering various different boundary conditions and damping levels are needed to expand the understanding of this method.

REFERENCES:

[1] Rao S. S, *Mechanical Vibrations*. Addison-Wesley Publishing Company, 1984.

[2] Valette C, and Cacracciolo A., "*Damping mechanisms governing plate vibration*," Molecular and Quantum Acoustics, Acta Acoustica, vol. 7 pp. 393-404, 1995.

[3] Iwaniwec Mark, "*Damping Loss factor Estimation in Plates*," Molecular and Quantum Acoustics, Acta Acoustica, vol. 24, pp. 276-287, 2003.

[4] Liu Wanbo, "*Experimental and Analytical Estimation of Damping in beams and plates with damping treatments*", PhD Dissertation ,University of Kansas, Lawrence, November 2008.

[5] Norton M and Karczub D., *Fundamentals of Noise and Vibration Analysis for Engineers*. Cambridge, UK: Cambridge University Press, 2003.

[6] Bloss B. and Rao M.D., "*Estimation of frequency-averaged loss factors by the power input method and the impulse response decay method* ," Journal of Acoustical Society of America, vol. 117, no. 1, pp. 240-249, 2004.

[7] Nuno Manuel Mendes Maia and Montalvao Julio, *Theoretical and Experimental Modal Analysis*. New York, USA: John Wiley & Sons Inc..

[8] Wolf Jr., J.A. "*The influence of mounting stiffness on frequencies measured in a vibration test*.," vol. SAE Paper 840480, Society of Automotive Engineers, 1984.

[9] DeJong R.H. and, Lyon R.G., *Theory and Application of Statistical Energy Analysis*, 2nd ed. Newton, MA,USA: Butterworth-Heinmann, 1995.

[10] Lyon R.H., *Statistical Energy Analysis of dynamic systems: theory and applications*. cambridge: M.I.T. Press, 1975.

[11] Bies D.A. and Hamid S., "*In situ determination of loss and coupling loss factors by the power injection method*," Journal of Sound and Vibration, vol. 70, no. 2, pp 187-204, 1980.

[12] Bloss B. and Rao M.D., "*Measurement of Damping In Structures by the Power Input Method*," Journal of Sound and Vibration, Vol 26(3) pp. 234-238, 1986.

[13] Carfangi M. and Pierini M., "*Determining the Loss Factors by the Power Input Method. I. Nemerical Investigation*,", Journal of Vibrations and Acoustics, vol.121(2), pp 417- 422, 1997.

[14] Citti P., Pierini M. and Carfangi M., "*Determining loss factors using the power input method with shaker excitation*," , 1998 Proceedings of the XVIth IMAC,CA, 585-590,1998.

[15] Fujimoto J and Okada T., "*Radiation noise reduction by applying vibration damping material*," Inter Noise 94, Yokohama, 1994.

[16] Liu W and Ewing M.S, "Predicting Damping Loss Factors for Beams and Plates with

Constrained Layer Damping," in *AIAA Structures, Structural Dynamics and Materials Conference*, Shaumberg, IL, April 2008.

[17] Ewing S. Mark and Wanbo Liu, "Experimental and Analytical Estimation of Loss factors by the Power Input Method," AIAA Journal, vol. 45, no. 2, pp. 477-484, 2007.

[18] Rife D. D., and Vanderkooy J., "*Transfer-function measurement with maximum length sequences*," *Journal of Audio Engineering Society*, vol. 37, no. 6, pp. 419-443, 1989.

[19] Vorlander M. and Kob M., "*Practical aspects of MLS measurements in building acoustics*," Applied Acoustics, vol. 52, no. 3/4, pp. 239-258, 1997.

[20] Agren A., Soundback U., and Wu L., "*A study of initial decay rate of two-dimensional vibrating structures in relation to estimates of loss factor*," Journal of Sound and Vibration, vol. 206, no. 5, pp. 663-684, 1997.

[21] Lai M.L and Soom A., "*Prediction of transient envelopes using statistical energy analysis techniques*," Journal of Vibration and Acoustics, vol. 112, pp. 127-137, January 1990.

[22] Mace B and Shoter P, "*Energy Flow Models from the finite element analysis*," Journal of sound and vibration, vol. 233, no. 3, pp. 369-389, January 2000.

[23] Ewing, M. S., Dande H., and Vatti, K., "*Validation of Panel Damping Loss factors Estimation Algorithms using a Computational Model*," Proceedings of 50th AIAA/ASME/ASCE/AHS/ASC Structures, Structural Dynamics and Materials Conference, Palm Springs, CA, 2009.

[24] Ewing M. S., Vatti K., and Vaz I., "*Coupling Loss Factor Estimation for Plates Joined Along a Line: Analysis and Experiment*," Journal of Acoustical Society of America, Volume 127, Issue 3, PP 1769 - 1769, March 2010

[25] Lai M.L, "*Modelling of Transient Vibrations with Statistical Energy Analysis*,", PhD Dissertation., State university of New York, Buffalo, September 1988.

[26] Ewing M. S., Vatti K., and Vaz I., "*Coupling Loss Factor Estimation for Plates Joined Along a Point: Analysis and Experiment*," Journal of Acoustical Society of America, Volume 127, Issue 3, PP 1769 - 1769, March 2010

APPENDIX A MATLAB CODES

A.1. GENERATE A TRUE RANDOM SIGNAL

```
%%%%%%%%%%%%%%%%%%%%%%%%%%%%%%%%%%%%%%%%%%%%%%%%%%%%%%%%%%%%%%%%%%%%%%%%%%%%%%%%
%%%%%------------GENERATE A TRUE RANDOM SIGNAL---------------------%%%%%
%%%%%%%%%%%%%%%%%%%%%%%%%%%%%%%%%%%%%%%%%%%%%%%%%%%%%%%%%%%%%%%%%%%%%%%%%%%%%%%%
clear all
close all
clc
Fms=1; %what is the mean square value of the force you want
fs=100;  %set the sample rate
npts=10*fs; %set the number of points in this case 10secs worth
deltaf=fs/npts; %what is the deltaf for the prescribed spectrum
f_low=1;  %we are doing the flat sprctrum with a low frequency cut off
f_high=10;  %and ahigh frequency cutoff
band=f_high-f_low;  % what is the band width
f_cutoff_low=round(f_low/deltaf)+1; % find the low bin of the spectrum
f_cutoff_high=round(f_high/deltaf)+1; % find the high bin of the spectrum
So=Fms/band;  % the spectrum level
P=zeros(npts/2+1,1);  % zero all bins
%specify the level in the meaning full bins
P(f_cutoff_low:f_cutoff_high,1)=So*ones(f_cutoff_high-f_cutoff_low+1,1);
N=length(P);
%scale P
level=P/2;  % single sided to double sided
level=npts*(npts*deltaf)*level;  %scale for ifft
level=sqrt(level);
phase=2*pi*rand(N,1);  %make random phase
H=level.*(cos(phase)+i*sin(phase));  % positive side of fft
H(N+1:2*(N-1))=conj(flipud(H(2:N-1)));  %build the other side
F=real(ifft(H));
```

A.2. IMPULSE RESPONSE FUNCTION

```
%%%%%%%%%%%%%%%%%%%%%%%%%%%%%%%%%%%%%%%%%%%%%%%%%%%%%%%%%%%%%%%%%%%%%%%%%%%%%%%%
%%%%%-------------IMPULSE RESPONSE FUNCTION-------------%%%%%
%%%%%%%%%%%%%%%%%%%%%%%%%%%%%%%%%%%%%%%%%%%%%%%%%%%%%%%%%%%%%%%%%%%%%%%%%%%%%%%%
function [hir]=impresp(t,mass,Wn,Zeta)
Wd=Wn*sqrt(1-Zeta^2);
hir=1/Wd/mass*exp(-Zeta*Wn*t)*sin(Wd*t);
```

A.3. Loss Factor Estimation By Power Input Method: Synthetic, 1 DOF, Random Excitation

```
%%%%%%%%%%%%%%%%%%%%%%%%%%%%%%%%%%%%%%%%%%%%%%%%%%%%%%%%%%%%%%%%%%%%%%%%%%%%
%%%%---LOSS FACTOR ESTIMATION OF A SDOF BY THE POWER INPUT METHOD----%%%%
%%%%%%%%%%%%%%%%%%%%%%%%%%%%%%%%%%%%%%%%%%%%%%%%%%%%%%%%%%%%%%%%%%%%%%%%%%%%
clear all
close all
clc

%SYSTEM PROPERTIES
mass=0.5;
k=1000;
c=0.5;
Wn=sqrt(k/mass);%Natural Frequency
Zeta=c/(2*mass*Wn);%Damping Coefficient
Wd=sqrt(1-Zeta^2)*Wn;% Damped Natural Frequency
%response is set to zero
resp=zeros(1000,1);
figure(1)
subplot(2,1,1)
plot(F,'r')% the true random force
xlabel('Number of Samples','FontSize',14,'FontWeight','b')
ylabel('Magnitude','FontSize',14,'FontWeight','b')
title('Random Force','FontSize',16,'FontWeight','b')
RF=F(500:1000);
RRF=F.*(hanning(1000));
subplot(2,1,2)
plot(RRF)
xlabel('Number of Samples','FontSize',14,'FontWeight','b')
ylabel('Magnitude','FontSize',14,'FontWeight','b')
title('Force with a Hanning Window','FontSize',16,'FontWeight','b')
dt=1/100;
for n=1:1000
for j=1:n
        h=impresp((n-j)*dt,mass,Wn,Zeta);% calculation of the impulse
response function
        resp(n)=resp(n)+F(j)*h*dt;% the response of the system to the random
force
end
if n>1
        velocity(n)=(resp(n)-resp(n-1))/dt;    % calculation of the velocity
using the respone
end
end
figure(2)
plot(resp(1:1000),'m')
xlabel('Number of Samples','FontSize',14,'FontWeight','b')
ylabel('Magnitude','FontSize',14,'FontWeight','b')
title('Displacement Response to the Applied
Force','FontSize',14,'FontWeight','b')
VVelocity=velocity.*transpose(hanning(1000));
figure(3)
subplot(2,1,1)
plot(velocity,'k')
```

```
xlabel('Number of Samples','FontSize',14,'FontWeight','b')
ylabel('Magnitude','FontSize',14,'FontWeight','b')
title('Velocity Response to the Applied
Force','FontSize',16,'FontWeight','b')
Velocity=velocity(500:1000);
subplot(2,1,2)
plot(VVelocity)
xlabel('Number of Samples','FontSize',14,'FontWeight','b')
ylabel('Magnitude','FontSize',14,'FontWeight','b')
title('Velocity Response with a Hanning
Window','FontSize',16,'FontWeight','b')


Energydissipated=VVelocity*RRF;% calculation of the total energy that is
dissipated in the system
KE=(mass/2)*VVelocity*transpose(VVelocity);% the total kinetic energy in the
system
lossfactor(i)=Energydissipated/(2*Wn*KE);% loss factor
```

A.4. POWER INPUT METHOD: SYNTHETIC, 1 DOF, SINUSOIDAL EXCITATION

```
%%%%%%%%%%%%%%%%%%%%%%%%%%%%%%%%%%%%%%%%%%%%%%%%%%%%%%%%%%%%%%%%%%%%%%%%%%%%
%%%%---LOSS FACTOR ESTIMATION OF A SDOF BY THE POWER INPUT METHOD----%%%%
%%%%%%%%%%%%%%%%%%%%%%%%%%%%%%%%%%%%%%%%%%%%%%%%%%%%%%%%%%%%%%%%%%%%%%%%%%%%
clear all
close all
clc
for ii=1:1:10

mass=0.5;
k=[600 1800 3000 4200 5400 6800 9000 12000 18000 25000]*100;
k=k(ii);
c=0.5;
%All the above values are given
%computed as per the formula,Natural frequency
Wn=sqrt(k/mass);
freq(ii)=Wn;
%damping coefficient
Zeta=c/(2*mass*Wn)
zeta(ii)=Zeta;
% damping frequency
Wd=sqrt(1-Zeta^2)*Wn;
%Accelaration due to gravity
a=9.8;
%this for loop computes the values of the impulse function for 200
%intervals of time
Impulse(1999)=0;
for i=1:1:1999
    t=i/100;
    Impulse(i+1)=sin(Wd*t);
end
%response is set to zero
resp=zeros(2000,1);
dt=1/100;
for n=1:2000
for i=1:n
        h=impresp((n-i)*dt,mass,Wn,Zeta);
        resp(n)=resp(n)+Impulse(i)*h*dt;
end
if n>1
        velocity(n)=(resp(n)-resp(n-1))/dt;
end
end
fontname='Times New Roman';
figure(1)
subplot(2,1,1)
plot(Impulse,'r')
xlabel('Number of Samples','FontSize',14,'FontWeight','b','FontName','Times')
ylabel('Magnitude','FontSize',14,'FontWeight','b')
title('Sinusoidal Force','FontSize',16,'FontWeight','b')
subplot(2,1,2)
plot(velocity,'k')
xlabel('Number of Samples','FontSize',14,'FontWeight','b')
ylabel('Magnitude','FontSize',14,'FontWeight','b')
```

```
title('Velocity Response to the Applied
Force','FontSize',16,'FontWeight','b')
%calculates the sum of the energyloss summed over time
Energyloss=(velocity)*transpose(Impulse);
% calculates the total kinetic energy summed over time
KE=(mass/2)*velocity*transpose(velocity);
%calculates the lossfactor for this system
lossfactor=abs(Energyloss)/(2*Wn*KE);
Avg=mean(lossfactor);
Eta(ii)=mean(lossfactor)
end
figure(2)
semilogy(freq,Eta,'--rs','LineWidth',2,...
'MarkerEdgeColor','k',...
'MarkerFaceColor','g',...
'MarkerSize',10)
hold on
semilogy(freq,zeta,'-gd','LineWidth',2,...
'MarkerEdgeColor','c',...
'MarkerFaceColor','r',...
'MarkerSize',10)
            grid on
xlabel('Frequency','FontSize',14,'FontWeight','b')
ylabel('Loss Factor [No Units]','FontSize',14,'FontWeight','b')
title('Damping Loss Factor by the PIM when the Force is
Sinusoidal','FontSize',16,'FontWeight','b')
```

A.5. IMPULSE RESPONSE DECAY METHOD: SYNTHETIC, 1 DOF, IMPULSE FUNCTION

```
%%%%%%%%%%%%%%%%%%%%%%%%%%%%%%%%%%%%%%%%%%%%%%%%%%%%%%%%%%%%%%%%%%%%%%%%%%%%
%-LOSS FACTOR ESTIMATION OF A SDOF BY THE IMPULSE REDPONSE DECAY METHOD-%
%%%%%%%%%%%%%%%%%%%%%%%%%%%%%%%%%%%%%%%%%%%%%%%%%%%%%%%%%%%%%%%%%%%%%%%%%%%%
clear all
close all
clc

%SYSTEM PROPERTIES

m=0.5;
k=1000;
c=0.5;
%All the above values are given
%computed as per the formula,Natural frequencuy
Wn=sqrt(k/m);
%damping coefficient
Zeta=c/(2*m*Wn);
% damping frequency
Wd=sqrt(1-Zeta^2)*Wn;

%TOTAL NUMBER OF ITERATIONS

npts=8192;
dt=0.001;

%CALCULATION OF IMPULSE USING THE IMPULSE RESPONSE FUNCTION

h(npts+1)=0;
for i=0:1:npts
    t=i*dt;
    h(i+1)=1/(Wd*m).*exp(-Zeta*Wn.*t)*sin(Wd.*t);
end
t=(0:1:npts)/100;
time =t./80;
figure(1)
plot(time,h)
xlabel('Time [ Seconds ]','FontSize',14,'FontWeight','b')
ylabel('H(t)','FontSize',14,'FontWeight','b')
title('Plot of Impulse function','FontSize',16,'FontWeight','b')

%hilbert command takes the impulse function and puts a hilbert transform on
%it to have the hilbert transform

%Hilbert function has a real part and an imaginary part the real part is
%computed here and the imaginary part is computed in the next statement

H=hilbert(h);
figure(2)
subplot(2,1,1)
plot(time,real(H)),hold on
plot(time,imag(H),':'),hold off
xlabel('Time [ Seconds ]','FontSize',14,'FontWeight','b')
```

```
ylabel('Hilbert Transform','FontSize',14,'FontWeight','b')
title('Real and Imaginary Hilbert Transform of the Impulse
Function','FontSize',16,'FontWeight','b')
subplot(2,1,2)
plot(time,abs(H))
xlabel('Time [ Seconds ]','FontSize',14,'FontWeight','b')
ylabel('Hilbert Transform','FontSize',14,'FontWeight','b')
title('Absolute Value of the Hilbert
Transform','FontSize',16,'FontWeight','b')

z=log10(abs(H));
figure(3)
plot(time,z)
xlabel('Time [ Seconds ]','FontSize',14,'FontWeight','b')
ylabel('Decibels [ dB ]','FontSize',14,'FontWeight','b')
title('Logrithmic Decrement of the Hilbert
Transform','FontSize',16,'FontWeight','b')
%the loss factor is calculated for a particular interval of time in the
%graph and the average of this loss factor is calculated subsequently

for i=1:1:10
    skip=i*10;
for j=1:1:10
delay=j*10;
for n=delay+1:delay+10
Eta(n-10)=-(z(n+skip)-z(n))/(skip*dt) *2/Wn/0.4343;
Avg(i,j)=mean(Eta)/0.0224;
end

end

end

Skip=zeros(10,1);
for k=1:10
    Skip(k)=k*10;
end
Delay=zeros(10,1);
for l=1:10
    Delay(l)=l*10;
end
figure(4)
mesh(Delay,Skip,Avg)
xlabel('Delay','FontSize',14,'FontWeight','b')
ylabel('Skip','FontSize',14,'FontWeight','b')
zlabel('Lossfactor','FontSize',16,'FontWeight','b')
title('Loss Factor as a Function of Skip and
Delay','FontSize',16,'FontWeight','b')
```

A.6. IMPULSE RESPONSE DECAY METHOD: SYNTHETIC, 1 DOF, HALF SINE PULSE

```
%%%%%%%%%%%%%%%%%%%%%%%%%%%%%%%%%%%%%%%%%%%%%%%%%%%%%%%%%%%%%%%%%%%%%%%%%%%%
%-LOSS FACTOR ESTIMATION OF A SDOF BY THE IMPULSE REDPONSE DECAY METHOD-%
%%%%%%%%%%%%%%%%%%%%%%%%%%%%%%%%%%%%%%%%%%%%%%%%%%%%%%%%%%%%%%%%%%%%%%%%%%%%
clear all
close all
clc
%SYSTEM PROPERTIES
mass=0.5;
k=1000;
c=0.5;
Wn=sqrt(k/mass);
Zeta=c/(2*mass*Wn)
Wd=Wn*(sqrt(1-Zeta^2));
tpts=4096*8;
dt=0.005;
npts=tpts/4;
Wnf=0.1*Wn;
dt=0.005;
for i=1:1:tpts
    t=i*dt-dt;
    f1(i)=1-cos(Wnf*t);
end

for i=282:1:tpts
    t=i*dt-dt;
    f2(i)=-1+cos(Wnf*t);
end
f=f1+f2;
for i=1:1:npts
    t=i-1;
    F1(i)=f(4*t+1);
end
for i=1:1:npts/4
    t=i-1;
    F(i)=F1(4*t+1);
end
time=linspace(0,1,2048);
figure(1)
subplot(3,1,1)
plot(time(1:25),F(1:25),'*')
xlabel('Time [ Seconds ]','FontSize',14,'FontWeight','b')
ylabel('Magnitude','FontSize',14,'FontWeight','b')
title('Simulated Half Sine Impulse','FontSize',16,'FontWeight','b')
subplot(3,1,2)
plot(time,F)
xlabel('Time [ Seconds ]','FontSize',14,'FontWeight','b')
ylabel('Magnitude','FontSize',14,'FontWeight','b')
title('Simulated Half Sine Impulse','FontSize',16,'FontWeight','b')
%%RESPONSE USING THE CONVOLUTION INTEGRAL
R1=zeros(1,npts/4);
for n=1:npts/4
for i=1:n
```

```
        h=impresp((n-i)*dt,mass,Wn,Zeta);% calculation of the impulse
response function
        R1(n)=R1(n)+F(i)*h*dt;% the response of the system to the random
force
end

end

subplot(3,1,3)
plot(time,R1)
xlabel('Time [ Seconds ]','FontSize',14,'FontWeight','b')
ylabel('Magnitude','FontSize',14,'FontWeight','b')
title('Response due to Half Sine Impulse','FontSize',16,'FontWeight','b')
%%%FOURIER TRANSFORM OF THE FORCE AND THE RESPONSE TO CONVERT FROM TIME
DOMAIN TO THE FREQUENCY DOMAIN

Fw11=fft(F);
Rw11=fft(R1);
hw=Rw11./Fw11;

%%%%INVERSE FOURIER TRANSFORM ON THE FREQUENCY AVERAGED IMPULSE RESPONSE
FUNCTION

hhh=ifft(hw);
figure(2)
subplot(3,1,1)
plot(abs(Fw11))
xlabel('Frequency [ Hz ]','FontSize',14,'FontWeight','b')
ylabel('Magnitude','FontSize',14,'FontWeight','b')
title('Fourier Tansform of the Half Sine
Impulse','FontSize',16,'FontWeight','b')
subplot(3,1,2)
plot(abs(Rw11))
xlabel('Frequency [ Hz ]','FontSize',14,'FontWeight','b')
ylabel('Magnitude','FontSize',14,'FontWeight','b')
title('Fourier transform of the Response to Half Sine
Impulse','FontSize',16,'FontWeight','b')
subplot(3,1,3)
plot(abs(hw))
xlabel('Frequency [ Hz ]','FontSize',14,'FontWeight','b')
ylabel('Magnitude','FontSize',14,'FontWeight','b')
title('Fourier transform of the Impulse
Function','FontSize',16,'FontWeight','b')

figure(3)
subplot(3,1,1)
plot(time,hhh)
xlabel('Time [ Seconds ]','FontSize',14,'FontWeight','b')
ylabel('Magnitude','FontSize',14,'FontWeight','b')
title('Impulse Response Function','FontSize',16,'FontWeight','b')
H=hilbert(hhh);
subplot(3,1,2)
plot(time,real(H));hold on
plot(time,imag(H))
xlabel('Time [ Seconds ]','FontSize',14,'FontWeight','b')
ylabel('Magnitude','FontSize',14,'FontWeight','b')
```

```
title('Real and Imaginary parts of the Hilbert
Transform','FontSize',16,'FontWeight','b')
subplot(3,1,3)
plot(time,abs(H))
xlabel('Time [ Seconds ]','FontSize',14,'FontWeight','b')
ylabel('Magnitude','FontSize',14,'FontWeight','b')
title('Absolute value of the Hilbert
Transform','FontSize',16,'FontWeight','b')
figure(4)
z=log(abs(H));
plot(time,z)
xlabel('Time [ Seconds ]','FontSize',14,'FontWeight','b')
ylabel('Magnitude [ dB ]','FontSize',14,'FontWeight','b')
title('Logrithmic Decrement of the Hilbert
Transform','FontSize',16,'FontWeight','b')

for i=1:1:20
    skip=10*i;
for j=1:1:30
delay=10*j;

for n=delay+1:delay+10
 Eta(n-10)=-(z(n+skip)-z(n))/(skip*dt) *2/(Wn);
 avg(i,j)=mean(Eta);
end
end

end

Skip=zeros(20,1);
for k=1:20
    Skip(k)=k*10;
end
Delay=zeros(30,1);
for l=1:30
    Delay(l)=l*10;
end
figure(5)
mesh(Delay,Skip,avg)
xlabel('Delay','FontSize',14,'FontWeight','b')
ylabel('Skip','FontSize',14,'FontWeight','b')
zlabel('Loss factor','FontSize',16,'FontWeight','b')
title('Loss Factor as a Function of Skip and
Delay','FontSize',16,'FontWeight','b')
```

A.7. EXPERIMENTAL POWER INPUT METHOD

```
%%%%%%%%%%%%%%%%%%%%%%%%%%%%%%%%%%%%%%%%%%%%%%%%%%%%%%%%%%%%%%%%%%%%%%%%%%%%
%--LOSS FACTOR ESTIMATION OF A MDOF BY EXPERIMENTAL POWER INPUT METHOD--%
%%%%%%%%%%%%%%%%%%%%%%%%%%%%%%%%%%%%%%%%%%%%%%%%%%%%%%%%%%%%%%%%%%%%%%%%%%%%
clear all;
close all;
clc
Mass=1.25;% Mass of the structure
fin=fopen('DampedAluminum225_31.asc');  %input from asc file
N=225;  %number of total scanning points
f=31;  %reference point
df=1; %resolution
f1=0;  %starting freq
f2=6400;    %ending freq
Nfft=6400;  %number of FFT line
for n=1:Nfft
    freq(n)=f1+(n-1)*df;
end
mass=Mass/N;
line=fgetl(fin);
n=0;    %index of point number
%
while feof(fin)==0
if line(1:2)=='Tr'
        n=n+1;
        q=0;    %index of current fft line
for p=1:9   %continue to read and write 9 more lines
           line=fgetl(fin);
end
        line=fgetl(fin);
for p=1:(Nfft-1)/3  %Nfft-1: 2 reading at the end of each frf, 3 fft lines
per row
            line=fgetl(fin);
            q=q+1;
            h(n,q)=str2num(line(1:13))+i*str2num(line(14:26));
            q=q+1;
            h(n,q)=str2num(line(27:39))+i*str2num(line(40:52));
            q=q+1;
            h(n,q)=str2num(line(53:65))+i*str2num(line(66:78));
end
        line=fgetl(fin);
        q=q+1;
        h(n,q)=str2num(line(1:13))+i*str2num(line(14:26));
end
    line=fgetl(fin);
end
fclose(fin);
num=real(h(f,:));
s=0;    %summation
for n=1:N
    s=mass*abs(h(n,:)).^2+s;
end
for n=1:Nfft
    den(n)=2*pi*freq(n)*s(n);
```

```
end
eta=num./den;

fid = fopen('DampedAluminum225_31_Eta.txt','w');
for n=1:Nfft
    fprintf(fid,'%12.8f %12.8f\n',freq(n),eta(n));
end
fclose(fid)


for n=1:Nfft
    rms(n)=norm(h(:,n))/length(h(:,n));    %1884.7 hz
end
fid = fopen('DampedAluminum225_31_Rms.txt','w');
for n=1:Nfft
    fprintf(fid,'%12.8f %12.8f\n',freq(n),rms(n));
end
fclose(fid);

save DampedAluminum225_31h


f_c=[16 20 25 32 40 50 63 80 100 125 160 200 250 315 400 500 630 800 1000
1250 1600 2000 2500 3150 4000 5000 6300 8000].';
f_l=f_c*2^(-1/6);
f_u=f_c*2^(1/6);
f=linspace(f1,f2,Nfft);
for i=1:1:length(f_c)
        I=find(f>=f_l(i)& f<f_u(i));
        DD(i)=length(I);
        LF(i)=sum(eta(I))/(DD(i));
end
LF=abs(LF);
figure(1)
loglog(f_c,LF,'d',f_c,LF)
xlabel('Frequency [ Hz ]','FontSize',14)
ylabel('Loss Factor','FontSize',14)
title('The Loss factor of the Plate In Bands','FontSize',16);grid on
figure(2)
plot(freq,eta)
xlabel('Frequency [ Hz ]','FontSize',14)
ylabel('Loss Factor','FontSize',14)
title('The Loss factor of the Plate','FontSize',16);grid on
```

A.8. EXPERIMENTAL IMPULSE RESPONSE DECAY METHOD

```
%%%%%%%%%%%%%%%%%%%%%%%%%%%%%%%%%%%%%%%%%%%%%%%%%%%%%%%%%%%%%%%%%%%%%%%%%%%%
%---LOSS FACTOR ESTIMATION OF A MDOF BY IMPULSE RESPONSE DECAY METHOD---%
%%%%%%%%%%%%%%%%%%%%%%%%%%%%%%%%%%%%%%%%%%%%%%%%%%%%%%%%%%%%%%%%%%%%%%%%%%%%
clear all
close all
clc

load input_1_quadrant_1_2.mat
load input_1_quadrant_2_3.mat
load input_1_quadrant_3_2.mat
load input_1_quadrant_4_1.mat

Fs=20000;
N=20002;
f=linspace(0,20001,20001);
Frf1=zeros(1,10001);
Frf2=zeros(1,10001);
Frf3=zeros(1,10001);
Frf4=zeros(1,10001);
for k=1:1:10001
Frf1(k)=input_1_quadrant_1_2(k);
Frf2(k)=input_1_quadrant_2_3(k);
Frf3(k)=input_1_quadrant_3_2(k);
Frf4(k)=input_1_quadrant_4_1(k);
end
Frf1(10002:20002)=fliplr(conj(Frf1(1:10001)));
Frf2(10002:20002)=fliplr(conj(Frf2(1:10001)));
Frf3(10002:20002)=fliplr(conj(Frf3(1:10001)));
Frf4(10002:20002)=fliplr(conj(Frf4(1:10001)));

f_c =[16 20 25 32 40 50 63 80 100 125 160 200 250 315 400 500 630 800 1000
1250 1600 2000 2500 3150 4000 5000 6300 8000].';
f_l = f_c*2^(-1/2); %full octave bandwidths
f_u = f_c*2^(1/2);

TwoH1stack=zeros(4,20002);
TwoH1stack(1,:)=Frf1;
TwoH1stack(2,:)=Frf2;
TwoH1stack(3,:)=Frf3;
TwoH1stack(4,:)=Frf4;

analsum = zeros(length(f_c),N);
```

```
for acc=1:1:4
for i=1:1:length(f_c)

    temp = zeros(N,1)*(eps + 1j*eps);

        I = find(f >= f_l(i) & f < f_u(i));
        temp(I+2) = TwoH1stack(acc,I); %I added the +2 to make temp
'conjugate symmetric', but i think it may be spuriously shifting the
frequencies.  Probably has negligable effect.
        temp(N-I+2) = conj((TwoH1stack(acc,I)));
        decay = ifft(temp,N,'symmetric');
        anal = hilbert(real(decay)).'; %calculating the analytical signal
        anal = abs(anal)./max(abs(anal)); %normalizing for easy visualization
later
        analsum(i,:) = anal + analsum(i,:);
end
end
analAVG = analsum/4;
dbdecay_full = 20*log10(analAVG.');  %dB decays for exporting out to excel
save dbdecay_fulldbdecay_full
```

A.9. FREQUENCY RESPONSE FUNCTION EXTRACTION FROM NASTRAN FO6 FILES

```
%%%%%%%%%%%%%%%%%%%%%%%%%%%%%%%%%%%%%%%%%%%%%%%%%%%%%%%%%%%%%%%%%%%%%%%%%%%%%%%%
%%%%-------------DATA EXTRACTION FROM NASTRAN FO6 FILES-------------%%%%
%%%%%%%%%%%%%%%%%%%%%%%%%%%%%%%%%%%%%%%%%%%%%%%%%%%%%%%%%%%%%%%%%%%%%%%%%%%%%%%%
close all
clear all
clc

fin=fopen('steady_state_less.f06'); %input from asc file
ff=1;  %reference point number in patran/nastran
f1=0;  %starting freq
f2=10000;    %ending freq
Ndf=10000+1; %number of frequency increments
df=(f2-f1)/(Ndf-1); %frequency resolution

n1=0;
n2=0;
n3=0;

line=fgetl(fin);
while feof(fin)==0
    temp=size(line);
if temp(1,2)==26 & line(23 :26)=='7033'
        line=fgetl(fin);
        temp=size(line);
if temp(1,2)==88 & line(44:88)=='C O M P L E X   A C C E L E R A T I O N   V
E C T O R'
          line=fgetl(fin);
          line=fgetl(fin);
          line=fgetl(fin);
          temp=size(line);
if temp(1,2)== 109& line(7:15)=='FREQUENCY'
for i=1:1:16
               n1=n1+1;
              liner=fgetl(fin);
              freq(n1)=str2num(liner(4:15));
              linei=fgetl(fin);
              h4(n1)=str2num(liner(57:69));
              h5(n1)=str2num(linei(57:69));
end
end

end
end
    line=fgetl(fin);

end
fclose(fin);
```

A.10. MANUAL DECAY MEASUREMENT

```
%%%%%%%%%%%%%%%%%%%%%%%%%%%%%%%%%%%%%%%%%%%%%%%%%%%%%%%%%%%%%%%%%%%%%%%%%%%%
%%%%---------------MANUAL DECAY MEASUREMENT ALGORITHM----------------%%%%
%%%%%%%%%%%%%%%%%%%%%%%%%%%%%%%%%%%%%%%%%%%%%%%%%%%%%%%%%%%%%%%%%%%%%%%%%%%%
clear all
clc
close all

f_c =[16 20 25 32 40 50 63 80 100 125 160 200 250 315 400 500 630 800 1000
1250 1600 2000 2500 3150 4000 5000 6300 8000 ].';

for j=1:1:length(f_c)

while(1<2)
    calculate(j)
    choice1=input('Do you wish to Proceed(y/n):','s')
if (choice1=='y')
        display('Will Go to Next Graph')
break
elseif (choice1=='n')
        display('Will Exit From The Program')
        plot(dbdecay)
       calculate(55)
break

end
end
end
```

```
%%%%%%%%%%%%%%%%%%%%%%%%%%%%%%%%%%%%%%%%%%%%%%%%%%%%%%%%%%%%%%%%%%%%%%%%%%%%
%%%%---------------MANUAL DECAY MEASUREMENT ALGORITHM----------------%%%%
%%%%%%%%%%%%%%%%%%%%%%%%%%%%%%%%%%%%%%%%%%%%%%%%%%%%%%%%%%%%%%%%%%%%%%%%%%%%
function Calculate(j)

clear dbdecay_full.mat
load dbdecay_full.mat


dbdecay=dbdecay_full;
f2=linspace(0,1,20002);

f_c =[16 20 25 32 40 50 63 80 100 125 160 200 250 315 400 500 630 800 1000
1250 1600 2000 2500 3150 4000 5000 6300 8000].';


close all
figure(1)
F=dbdecay(:,j);
    plot(f2,F)
    xlabel('Time')
    title('Log Decrement')
```

```
    keyboard
    H=ginput(2);
    K=H(:,1);
K2=H(:,2);
    frequency=f_c(j)

        N=H(2,1)-H(1,1);

        D=H(2,2)-H(1,2);


%%%%%%%%%%%%

         Eta=-D/N/f_c(j)/27.3
         figure(2)

    plot(f2,dbdecay(:,j)),hold on
    plot(K,K2,'r','LineWidth',3),hold off

    xlabel('Time')
    title('Log Decrement')
        choice=input('Are You Satisfied(y/n):','s')
if (choice=='n')
            Eta(j)=-D/N/f_c(j)/27.3;
            calculate(j)
elseif (choice=='y')
            display('The Loss Factor is')
            Eta=-D/N/f_c(j)/27.3

return
end
end
```

A.11. MODAL DENSITY AND MODES IN BAND MEASUREMENT

```
%%%%%%%%%%%%%%%%%%%%%%%%%%%%%%%%%%%%%%%%%%%%%%%%%%%%%%%%%%%%%%%%%%%%%%%%%%%%
%%%%---------MODAL DENSITY AND MODES IN BAND MEASUREMENT ------------%%%%
%%%%%%%%%%%%%%%%%%%%%%%%%%%%%%%%%%%%%%%%%%%%%%%%%%%%%%%%%%%%%%%%%%%%%%%%%%%%
close all
clear all
clc
load DampedAluminum225_31.mat
Mass=1.25;% Mass of the total system
N=225; % Total number of scanning Points
f=31; % The Drive point
L=6400; % Total number of FFT lines
df=3.125; % Frequency resolution
Mobility=h;
f_c=[125 160 200 250 315 400 500 630 800 1000 1250 1600 2000 2500 3150 4000
5000 6300 8000 ].';
f_l=f_c*2^(-1/6);
f_u=f_c*2^(1/6);
f1=linspace(1,20000,L);
HH=zeros(1,length(f_c));
mass=Mass/N;
    M=zeros(1,L);
    M(1:L)=real(Mobility(f,1:L));
for i=1:1:length(f_c)
        I=find(f1>=f_l(i)& f1<f_u(i));
        DD(i)=length(I);
        HH(i)=sum(M(I))*2*Mass/(pi*DD(i));
end

figure(1)
semilogx(f_c,HH,'^',f_c,HH,'LineWidth',2,'Color',[1 0 0]);grid on;
xlabel('Frequency(Hz)--1/3 Octave','FontSize',14)
ylabel('Modal Density','FontSize',14)
title('Modal Density of the Plate','FontSize',16)
HHH=(HH).*DD;
figure(2)
loglog(f_c,HHH,'^',f_c,HHH,'LineWidth',2,'Color',[1 0 0]);grid on;
xlabel('Frequency(Hz)--1/3 Octave','FontSize',14)
ylabel('Modes Per Band','FontSize',14)
title('Modes per band in the plate','FontSize',16)
```

A.12. ALTERNATIVE EXPERIMENTAL POWER INPUT METHOD

```
%%%%%%%%%%%%%%%%%%%%%%%%%%%%%%%%%%%%%%%%%%%%%%%%%%%%%%%%%%%%%%%%%%%%%%%%%%%%%%%
%%%%---------LOSS FACTORS BY THE LAI AND SOOM METHOD-----------------%%%%
%%%%%%%%%%%%%%%%%%%%%%%%%%%%%%%%%%%%%%%%%%%%%%%%%%%%%%%%%%%%%%%%%%%%%%%%%%%%%%%

% The mass of the plates is M1=4.82; M2=3.628;

clear all
close all
clc

% load the data set; This is extracted from the file and saved as
% plastictipdata

load Plate2Hammer65536.mat
M=3.628; % mass of the plate
H=P2_data;
[U,V]=size(H);
%pre allocating memory for the six accelerations and the two force data
hits=20;
u1=U/hits;
P1_Acc=zeros(3,U);
P2_Acc=zeros(3,U);
H=transpose(H);
for i=1:1:3
    P1_Acc(i,:)=H(i+2,:);
    P2_Acc(i,:)=H(i+5,:);
end
Force1=H(2,:);
Force2=H(9,:);

% Each force data above has ten individual data sets and each of them is
% taken seperately and stored in respective arrays
Acc1=zeros(hits,u1);
Acc2=zeros(hits,u1);
Acc3=zeros(hits,u1);
Acc4=zeros(hits,u1);
Acc5=zeros(hits,u1);
Acc6=zeros(hits,u1);
P1_Force=zeros(hits,u1);
P2_Force=zeros(hits,u1);

% each of the Accelerometers has a sensitivity and so the sensitivity is
% therefore accounted for in this section

for i=1:1:hits
for j=1:1:u1
        k=(i-1)*u1+j;
        Acc1(i,j)=P1_Acc(1,k)/0.984;
        Acc2(i,j)=P1_Acc(2,k)/0.931;
        Acc3(i,j)=P1_Acc(3,k)/1.036;
        Acc4(i,j)=P2_Acc(1,k)/0.974;
        Acc5(i,j)=P2_Acc(2,k)/1.012;
```

```
        Acc6(i,j)=P2_Acc(3,k)/1.021;
        P1_Force(i,j)=Force1(1,k)*77.39;
        P2_Force(i,j)=Force2(1,k)*77.39;
end
end

clear H
% Since we are dealing in the frequency domain we convert all the time data
% to frequency domain data by doing a fourier transform on the data

for i=1:1:hits
    Acc1(i,:)=fft(Acc1(i,:));
    Acc2(i,:)=fft(Acc2(i,:));
    Acc3(i,:)=fft(Acc3(i,:));
    Acc4(i,:)=fft(Acc4(i,:));
    Acc5(i,:)=fft(Acc5(i,:));
    Acc6(i,:)=fft(Acc6(i,:));
    P1_Force(i,:)=fft(P1_Force(i,:));
    P2_Force(i,:)=fft(P2_Force(i,:));
end

% defining the frequency; Sampling frequency is 65536 Hz

freq=linspace(0,65536,u1);

% Taking the complex conjugate of the drive point acceleration

for i=1:1:hits
    Acc7(i,:)=conj(Acc6(i,:));
end

% Defining the centers frequencies for the different  Octave bands

f_c =[16 20 25 32 40 50 63 80 100 125 160 200 250 315 400 500 630 800 1000
1250 1600 2000 2500 3150 4000 5000 6300 8000 10000 ].';
f_l=f_c/sqrt(2);
f_u=f_c*sqrt(2);
N=u1;

% This loop calculates the Internal energy and Kinetic energy for all the
% different 10 force sets.

for i=1:1:hits
for j=1:1:length(f_c)
        temp1 = zeros(N,1)*(eps + 1j*eps);
        temp2 = zeros(N,1)*(eps + 1j*eps);
        temp3 = zeros(N,1);
        temp4 = zeros(N,1)*(eps + 1j*eps);
        temp5 = zeros(N,1);
        I = find(freq >= f_l(j) & freq < f_u(j));
        temp1(I)=P1_Force(i,I);
        temp2(I)=Acc7(i,I);
        temp3(I)=freq(I);
        temp4(I)=Acc6(i,I);
        A1=temp1.*temp2;
```

```
        A2=A1./temp3;
        IE(i,j)=sum(imag(A2))*(1/pi);
        IE=abs(IE);
        temp5(I)=(temp4(I)./temp3(I));
        KE(i,j)=sum(abs(temp5(I)).*abs(temp5(I)))*(M/2/pi);

end
end

% initialize the size of loss factor array for easy computing.

Eta=zeros(hits,29);

% calculates loss factors for each frequency band and for all the ten
% different sets of data

for i=1:1:hits
for j=1:1:29
        Eta(i,j)=IE(i,j)/2/f_c(j)/abs(KE(i,j));
end
end

% The loss factors are averaged to get a averaged coupling loss factor

LF=zeros(1,29);
for i=1:1:hits
    LF=LF+Eta(i,:);
end
LF=LF/hits;

% the results are plotted

figure(1)
loglog(f_c,LF,'d',f_c,LF,'r','LineWidth',2)
xlabel('Frequency [ Hz ]','FontSize',16)
ylabel('Loss Factor [ No Units ]','FontSize',20)
title('The Loss Factor Plate 1 In Bands','FontSize',16);grid on
```

A.13. COUPLING LOSS FACTORS ALGORITHM

```
%%%%%%%%%%%%%%%%%%%%%%%%%%%%%%%%%%%%%%%%%%%%%%%%%%%%%%%%%%%%%%%%%%%%%%%%%%%%
%%%%----------COUPLING LOSS FACTOR MEASUREMENT ALGORITHM-------------%%%%
%%%%%%%%%%%%%%%%%%%%%%%%%%%%%%%%%%%%%%%%%%%%%%%%%%%%%%%%%%%%%%%%%%%%%%%%%%%%
clear all
close all
clc

% internalenergy11 is the internal energy of plate 1 when plate 1 is
% excited

load internalenergy11.mat
e11=IE;
clear IE

% internalenergy12 is the internal energy of plate 2 when plate 1 is
% excited

load internalenergy12.mat
e12=IE;
clear IE

% internalenergy21 is the internal energy of plate 1 when plate 2 is
% excited

load internalenergy21.mat
e21=IE;
clear IE

% internalenergy22 is the internal energy of plate 2 when plate 2 is
% excited

load internalenergy22.mat
e22=IE;
clear IE

% kineticenergy11 is the kinetic energy due to excitation at plate 1

load kineticenergy11.mat
E1=KE;
clear KE

% kineticenergy22 is the kinetic energy due to excitation at plate 2

load kineticenergy22.mat
E2=KE;
clear KE

f_c =[16 20 25 32 40 50 63 80 100 125 160 200 250 315 400 500 630 800 1000
1250 1600 2000 2500 3150 4000 5000 6300 8000 10000 ].';

for i=1:1:hits
```

```
for j=1:1:length(f_c)
        D1=[e21(i,j) -e11(i,j)];
        D2=[e22(i,j) -e12(i,j)];
        C=[D1;D2]*2*f_c(j);
        K=inv(C)*[E1(i,j);E2(i,j)];
        LF21(i,j)=K(1);
        LF12(i,j)=K(2);
end
end

Eta12=zeros(1,29);
Eta21=zeros(1,29);
for i=1:1:hits
    Eta12=Eta12+LF12(i,:);
    Eta21=Eta21+LF21(i,:);
end
Eta12=Eta12/hits;
Eta21=Eta21/hits;

figure(1)
loglog(f_c,Eta12,'d',f_c,Eta12,'r','LineWidth',2);hold on;
loglog(f_c,Eta21,'*',f_c,Eta21,'b','LineWidth',2)
legend('Eta12','Eta21')
xlabel('Frequency [ Hz ]','FontSize',14)
ylabel('Loss Factor [ No Units ]','FontSize',14)
title('The Coupling Loss Factors for the Plates','FontSize',18);grid on
```